2011

An automated nozzle controller for self-propelled sprayers

John Phillip Kruckeberg
Iowa State University

An automated nozzle controller for self-propelled sprayers

by

John Phillip Kruckeberg

A thesis submitted to the graduate faculty
in partial fulfillment of the requirements for the degree of
MASTER OF SCIENCE

Major: Agricultural Engineering (Advanced Machinery Engineering)

Program of Study Committee:
Brian Steward, Major Professor
Mark Hanna
Matt Darr
Joel Coats

Iowa State University
Ames, Iowa
2011

Dedication

This thesis is dedicated in memory of my grandfather, the late Roy Lee Thomas.

Table of Contents

List of Figures

List of Tables

List of Equations

Acknowledgements

As I conclude my master's research, I am reminded of the many people who have not only been involved with this project, but also with my education and development over the past few years. I would like to thank Dr. Mark Hanna for his continued support and encouragement through each and every step of my project. I would also like to thank Dr. Matt Darr, Dr. Brian Steward, and Dr. Joel Coats for their leadership and expertise.

Although I am uncertain whether they added to, subtracted from, or were neutral in regards to the content of my project, my officemates, colleagues, and most importantly friends Jeff Zimmerman, Curt Thoreson, Keith Webster, and Robert McNaull at least deserve mentioning. As I went through the continual highs and lows of the master's experience, it was good to know that I was there with others fighting the same fight.

Most importantly, I would like to thank my parents, Drs. John and Linda Kruckeberg. I can travel far from home, learn from professors of great universities, and age in both body and mind, but I will always be a product of your instruction and love, and for that I am truly grateful.

Abstract

Pesticide application is a vital, integrated component of 21st century agriculture. Pesticides allow more produce to be generated from fewer acres, increasing the world's capacity and improving quality of life. Pesticide use however, is not independent of concerns. Pesticides by nature are destroyers. When applied to target pests, their destructive nature can be advantageously utilized, however when misapplication unites pesticides and susceptible non-target organisms, resulting effects can be catastrophic.

The airborne movement of pesticides, spray drift, can result in up to 36.6% of the applied pesticide volume transporting outside of the intended swath to non-target organisms under high drift potential conditions (Grover et al., 1997). Studies have shown that through the implementation of best management principles, namely spraying with large droplet sizes, drift is reduced to less than 1% of the applied volume (SDTF, 1997; Grover et al., 1997). State-of-the-art drift reduction technologies inform applicators of real-time, site-specific dangers of drift, prompting applicators to implement best management practices. These technologies rely on the applicator for the decision making and implementation processes, adding subjectivity to the system and consequently, suboptimal performance. Objective, scientific decision making avenues are required for the future development of automated nozzle selection controllers to reduce spray drift.

A basis for automated nozzle control was developed, implemented, and tested in the form of a tier 1 nozzle controller. Decision making processes rely on an on-board, real-time risk assessment; the comparison of mapped predicted depositions to established acceptable levels of depositions in sensitive areas. In-field testing results indicated the critical roles of a high-resolution representation of the nozzle spectrum (specifically for droplets < 150 μm), and a regression model maintaining specificity within overall predictive accuracy. The nozzle controller was found to theoretically protect sensitive areas from excessive drift however significant differences between the predicted and actual drift phenomenon led to depositions measured in sensitive areas exceeding acceptable levels. Attempting to account for real-time operating conditions was found to significantly reduce the predictive accuracy of the controller, largely due to insufficient representation of highly variable wind speeds and

direction vectors acting on droplets after release. Further development of predictive capabilities in representing wind speed and direction for durations up to 30 seconds after a droplet is released are required for micro-scale nozzle control.

Chapter 1. Introduction

Spray drift, the off-target movement of pesticides, reduces application rates, damages non-target organisms, and creates environmental concerns. Each year thousands of spray drift violations are reported in the United States, with many more going unrecognized (EPA, 1999). An Environmental Protection Agency (EPA) sponsored spray drift research organization, the Spray Drift Task Force (SDTF), has determined that the single most influential factor affecting the magnitude of drift is droplet size (SDTF, 1997). In the past decade, the agriculture industry has been working to develop nozzles which produce larger droplet sizes in order to combat drift.

Recently the US EPA, which governs the use of pesticides in the United States, began revising their approach to mitigating drift (EPA, 2009a). Proposed revisions would require specific wording on pesticide labels concerning required application techniques to reduce drift, increasing the EPA's ability to identify and enforce drift infractions. With these increasing regulatory measures comes a heightened motivation to apply pesticides at low boom heights, under low wind speeds, and most importantly, with large droplets. Reducing drift however does not come without a cost. Research has shown that increasing droplet size often reduces efficacy (depending on the type of pesticide and pest), resulting in a negative economic impact on farmers and applicators.

The state-of-the-art in drift reduction technology systems aims to optimize the balance between drift and efficacy. These systems formulate a site specific real-time drift assessment, informing the applicator of the potential for drift. Reduction technologies can then be implemented on an "as-needed" basis rather than being broadcasted for a field as a whole. Sprayer position and weather conditions, which are constantly changing for a spraying event, drive the need for implementation of drift reduction techniques. When drift is not a concern, spraying techniques can be shifted to increase efficacy.

Currently, the decision maker and instigator for balancing drift and efficacy is the applicator himself. While computer programs have been developed to aid in this decision making process, ultimately changes in application are left in the subjective mind and hands of the applicator. With highly variable in-field conditions and the complex nature of drift, few applicators are able to judge the potential for drift, let alone modify application

techniques on the go. This project aims to develop a scientific basis for automated, real-time nozzle selection to optimize the balance between drift and efficacy. Accompanying this development is the design, implementation, and testing of a prototype nozzle selection controller founded upon the derived scientific principles.

Chapter 2. Literature Review

2.1. Pesticide and Spray Drift Regulation

In the first century, the Romans doused captured enemy cities and fields with salt to both symbolically and literally curse the inhabitants and prevent future agricultural endeavors. From these humble beginnings, the pesticide industry has grown into a highly specialized, multi-billion dollar production, with a reported $4 billion of pesticides sold annually in the United States alone (Cooper and Dobson, 2007). The widespread use of pesticides in the United States began shortly after World War II, both a cause and effect of a post-war agricultural boom. In 1959, one farmer could feed 50 persons, in 2000, 120 people could be fed by a single farmer, partly due to the increased use of pesticides (Stone, 2008). Today more than 550,000 tons of pesticides are used each year as they have become a vital component of agriculture, with benefits ranging from economic returns when used in crops, as much as four-fold or $16 billion (Pimentel et al., 1992), to increased aesthetic appeal in lawns and gardens (Cooper and Dobson, 2007).

While the use of pesticides is vital to modern agriculture, their use does not come without concern. The agriculture industry fights a constant battle in working to maintain a balance between the benefits and risks of pesticides. Pesticide regulation has played a critical role in the development of pesticides, and the way in which they are applied, over time. Early regulation can be traced back to the founding of the Federal Insecticide Act in 1910. This act was administered by the United States Department of Agriculture (USDA) to establish standardized pesticides which would protect farmers from purchasing a fraudulent or altered pesticide. At this time very little was known concerning the impact of pesticide on humans or the environment, largely due to an inability to detect trace levels of residue and to link these levels back to the effects. Not until 1938 did the USDA first issue an act (The Federal Food Drug and Cosmetic Act) to protect humans from pesticides. The installment of this act came on the eve of the development of the first synthetic, organic pesticide which greatly increased pesticide production and use. In 1947, the Federal Insecticide, Fungicide, and Rodenticide Act (FIFRA) was established, creating a new, specific federal law to oversee pesticide regulation. Most notably, FIFRA initiated and controlled the labeling process of pesticides which includes everything from registering a pesticide to required methods of application.

After the development of synthetic alternatives, pesticide use continued to increase without much concern until in 1962, Rachel Carson, a scientist, published *Silent Spring* which began an anti-pesticide environmentalist movement. Carson's book laid out the dangers of pesticide misuse and the potentially dire outlook if current trends continued, and called for a reform in the methods used to regulate pesticides (Delaplane, 1996). In 1964 FIFRA was amended requiring more extensive testing of pesticides prior to registration as well as increased pesticide manufacturer responsibilities to prove the safety of their products.

In 1970, the United States Environmental Protection Agency (US EPA) was created by President Nixon as a single agency to handle all environmental related regulatory topics. Control of FIFRA was handed over from the USDA to the EPA, bringing about more revisions and stricter regulations. During this time, the EPA changed the control of pesticides from being a more reactive stance to more proactive in reduction of unreasonable risks. Labeling became more specific in regards to methods used for pesticide application. Applicator education programs were also established to train farmers how to safely apply pesticides. The most recent major revision in pesticide regulation was in 1996 to make the registration process include proof that pesticides do not harm vulnerable organisms (Collins, 2005).

Spray drift regulation falls under the methods of proper use of a pesticide contained within FIFRA which is today managed and enforced by the EPA. The methods of proper use for each specific pesticide are determined by the manufacturer, approved by the EPA, and stated on the labeling of the pesticide. Methods are established to prevent "unreasonable adverse effects on the environment" (EPA, 1999) resulting from application. Specific spray drift labeling for each pesticide is handled on a case by case basis. Pesticide toxicity (risk assessment), potential benefits, driftability, typical application methods, and environmental fate are all taken into account in determining the drift specific labeling. Applying pesticide in a way inconsistent with its labeling is a violation of federal law and is the means by which the EPA enforces the implementation of drift reduction methods. An example of specific drift labeling is "do not apply when wind speeds exceed 10 mi/hr", or "only apply using a coarse droplet size". Many labels include the general language "off-target drift is to be avoided or prohibited". The EPA recognizes that with any application some drift will occur, however

applicators are responsible for implementing all available drift prevention measures to maintain “unreasonable risks” in consistency with the labeling. The EPA handles drift violations on a case by case basis taking into account its magnitude, effect, and the measures employed by the applicator in controlling drift.

In 2005, in response to a request from the EPA, the Pesticide Program Dialog Committee (PPDC), a Federal Advisory Committee made up of pesticide stakeholders, reviewed EPA’s current methods for mitigating drift. The PPDC found the currently used labeling methods “wordy, unenforceable, confusing, impractical, and/or contradictory” (Spray Drift Workgroup, 2007). In response to these negative reviews, the EPA initiated a proposed revision to their current labeling methods in 2009. The revision aimed to create more standardized, concise, and enforceable statements directly related to reducing drift (example of revised drift label in Figure 1). In addition to providing more pesticide specific drift reduction language, the EPA has proposed adding the statement:

> “Do not apply this product in a manner that will contact workers or other persons, either directly or through drift. In addition, do not apply this product in a manner that results in spray [or dust] drift that could cause an adverse effect to people or any other non-target organism or site”. (EPA, 2009a)

It is anticipated that the addition of this language to pesticide labels will give the EPA greater jurisdiction over pesticide drift infractions.

Ground Boom Sprayer Drift Requirements:

Nozzle height, droplet size, wind speed, and buffer zones between application sites and specified sensitive areas must be consistent with the following table:

Wind Speed	Nozzle Height	Droplet Size (ASAE Standard 572)	Buffer Zone
Less than ***X*** mph	Up to ***A*** feet	Medium or coarser	***D*** feet
	A to ***B*** feet	Coarse or coarser	***E*** feet
	B to ***C*** feet	Very Coarse or coarser	***F*** feet
X to *Y* mph	Up to ***A*** feet	Coarse or coarser	***G*** feet
	A to ***B*** feet	Very Coarse or coarser	***H*** feet
	B to ***C*** feet	Extremely Coarse or coarser	***I*** feet
DRT *			***J*** feet
DRT **			***K*** feet
DRT *** or higher			***L*** feet

The applicator must consider equipment speed, nozzle angle, and pressure in determining droplet size.
Do not apply when the wind speed exceeds *Y* miles per hour.
Do not apply with a nozzle height of greater than ***C*** feet above the ground or crop canopy.
Do not apply within the buffer zone distance of the following sites: **[specify sensitive site(s) of concern specific to product]**.

Figure 1. EPA proposed drift-specific label displaying required buffer zones based on weather and application conditions.

2.2. Prevalence of Drift

2.2.1. Drift Statistics

The Association of American Pesticide Control Officials (AAPCO) conducted a survey in 2005 to access the extent of drift violations and their handling. State pesticide bureaus are the first line of investigation and enforcement in drift infraction cases, therefore the subjects of the survey were members of State Pesticide Regulatory Lead Agencies. Results of the survey show 1,705 drift complaints were reported in 2004. Figure 2 displays the distributions of parties cited as responsible, methods of application causing drift, and the repercussions in the reported drift cases.

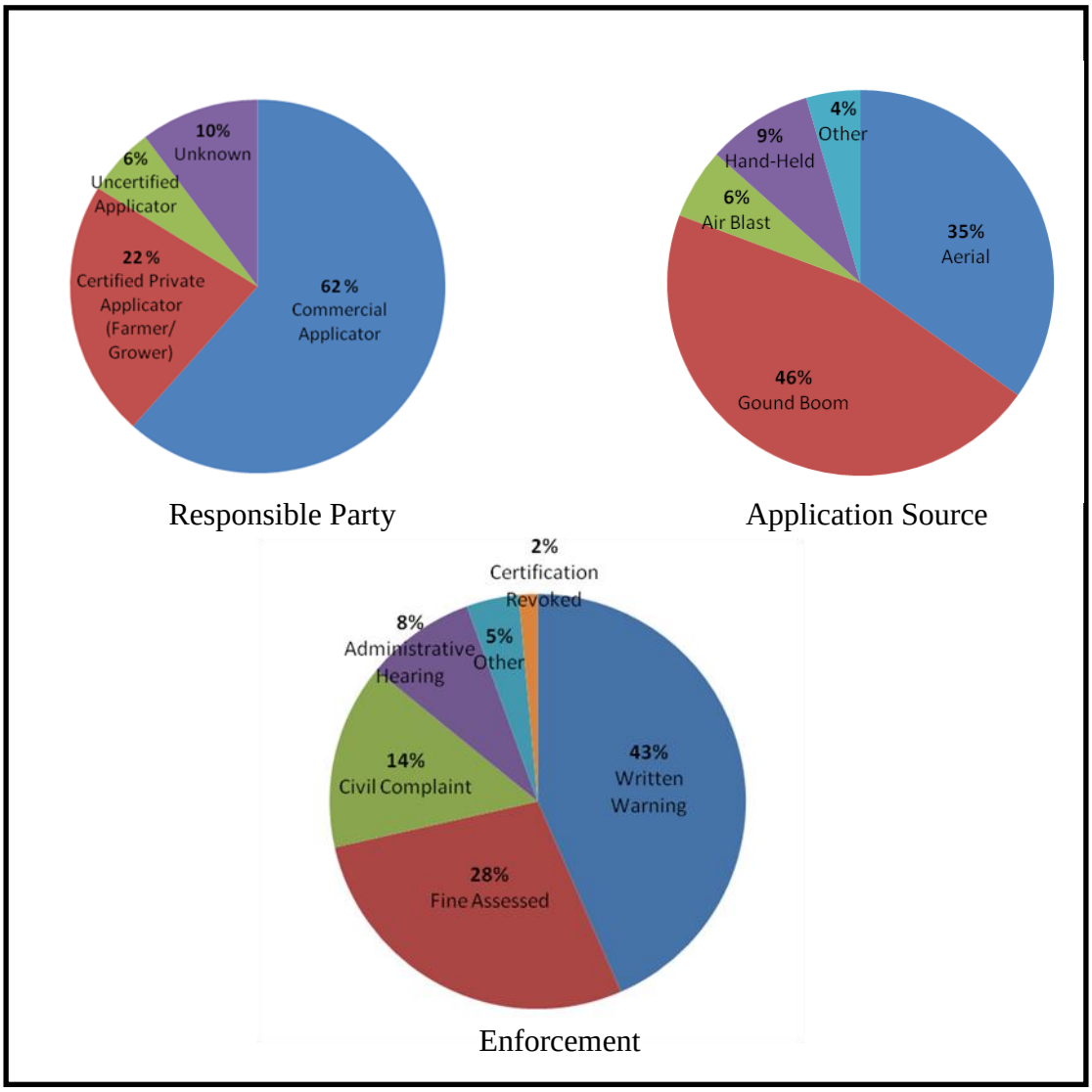

Figure 2. Responsible party, source of drift, and enforcement of drift complaints distributions (AAPCO, 2005)

A summary of the determined causes of drift in insurance claims, compiled by Farmland Insurance (Shaw, 1996) is shown in Figure 3. As can be seen within this figure, the majority of drift damage instances are due to applicators neglecting to sufficiently implement measures to reduce drift. Poor or improper nozzle selection caused drift damage in 26% of the cases. Physical causes of drift pertain to weather conditions such as high wind speeds.

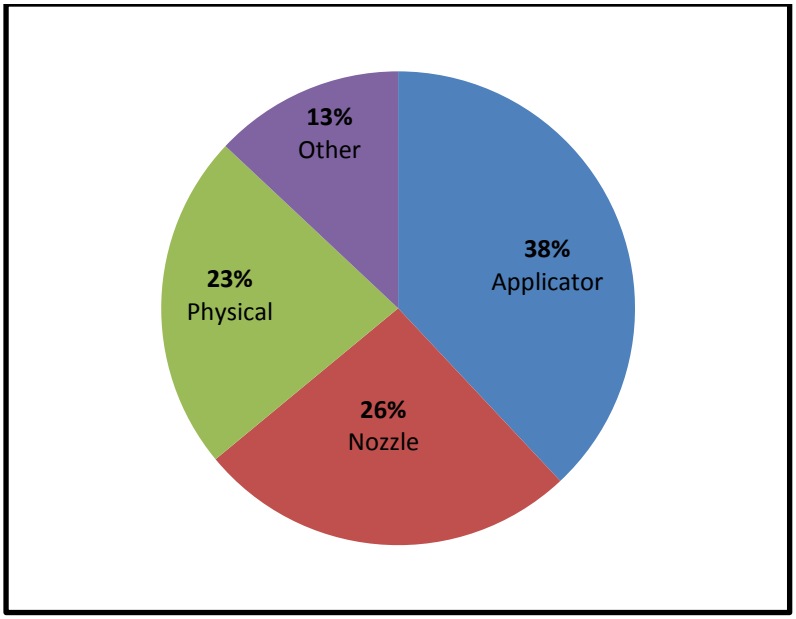

Figure 3. Causes of drift cited in insurance claims (Shaw, 1996)

2.2.2. Magnitude of Drift

In an effort to better understand and quantify the amount of spray drift occurring in everyday ground-spraying applications, the EPA formed the Spray Drift Task Force (SDTF) in 1990 to perform extensive in-field testing. The SDTF is made up of a variety of chemical companies with interests in determining the impacts of their products on the environment. Ten field studies with over 300 applications were made in developing a large, experimentally determined drift database. Results of the testing show the high impact of weather conditions, droplet size, and field configuration on the amount of drift which leaves the boundaries of the field. Drift leaving the boundary of test fields was found to be around 0.5% of the applied volume when best management principles (low boom height, large droplet size, and low wind speeds) were maintained throughout testing. As expected, increasing field size decreased the percentage of the volume leaving the field, as the perimeter to area ratio decreased causing a greater percentage of the drift to deposit within the field. While drift which deposits within the field is also of concern to applicators in terms of its impact on efficacy, the off-field drift is generally thought of as having the greatest negative impact on the environment and is the subject of most regulatory action.

Many independent researchers have also studied the magnitude of drift occurring for typical in-field spraying events. Grover et al. (1997) performed in-field trials using a SpraCoupe® (AGCO, Duluth, GA) sprayer with three different tips under varying wind speeds to determine the impact of droplet sizes and wind speed on drift. Drift was quantified as the percent of the applied volume drifting beyond the boom edge for a single swath, with a perpendicular wind direction thus giving one an idea of drift within a field as well as beyond the edge of a field. For an extended range flat fan nozzle (Teejet XR 11002, Spraying Systems, Wheaton, IL) at low wind speeds (7.7 km/hr), 8.23% of the applied volume drifted beyond the boom edge. Intermediate wind speeds (14.9 km/hr) using the same nozzle increased drift to 12.7%. High wind speed (28 km/hr) resulted in 35.6% of the applied volume drifting beyond the edge of the boom.

Bateans et al. (2007) measured drift at varying distances from the boom edge with wind directions perpendicular to the sprayer path, to derive a profile of drift deposition. Depositions expressed as a percentage of the application rate were found to be 10%, 1.8%, and 1% at distances of 0.5, 5, and 10 m from the boom edge respectively under low wind speeds (2.2 m/sec). In terms of applied volume, under the same conditions 10.45% of the applied volume drifted outside of the swath, while under high wind speeds (3.9 m/sec), 31.4% of the applied volume left the swath.

2.3. Drift Reduction Technologies

Ever increasing regulation of spray drift has created a large market for drift reduction technologies. The fundamental approach of most reduction techniques is to modify variables which influence a droplet's travel path as it leaves the nozzle until it deposits on the ground. Droplet size, wind speed, and release height each have a high impact on drift distances and are thus common targets of alteration.

A study by the SDTF showed that droplet size is the single most influential variable effecting drift (SDTF, 1997); therefore it is no surprise that the droplet generation process is the target of many drift reduction technologies. Drift reduction nozzles aim to decrease the percentage of volume made up of droplets smaller than 150 μm (i.e. high drift prone droplets). Nearly every nozzle manufacturer now has a form of drift reducing nozzle, which utilize either a pre-orifice or method for drawing in air to increase droplet sizes. Pre-orifice

nozzles increase droplet size by decreasing turbulence at the nozzle exit through a reduction in exit velocity. Air induction nozzles draw in air which is mixed with the liquid, producing droplets with air-liquid volume ratios from 0.22 to 0.29 (Lafferty, 2001) which in turn have larger diameters than non-filled droplets. Derksen et al. (1999) found that two of the most popular drift reduction nozzles, the Turbo Teejet produced by Spraying Systems and the TurboDrop nozzle produced by Greenleaf Technologies (Covington, La), reduced the percentage of volume dispensed as droplets classified as very fine (<150 µm) from 52% (in a standard flat fan nozzle) to 31.15% and 8.63% respectively for the same nozzle size and flow rate. The larger droplet sizes for both drift reduction nozzles resulted in significantly less downwind deposition.

A less direct method to alter droplet size than changing nozzles is through the use of drift retardant surfactants. Shear stresses generated at the exit of the nozzle are responsible for droplet production. Greater fluid viscosities result in less shearing of the liquid thus a more continuous fluid and overall larger droplets. Ozkan et al. (1995) evaluated the ability of five different drift surfactants to increase droplet sizes and reduce drift when compared to water. Droplet sizes for the five commercially available products: Nalco-trol, Target, Direct, Driftgard, and Formula 358, reduced the portion of droplets sizes in the very fine category by 62.6%, 61.4%, 55.8%, 34.5%, and 23.1% respectively. A reduction in downwind drift depositions was seen for four of the five drift retardants as well when compared to that of water (shown in Figure 4.)

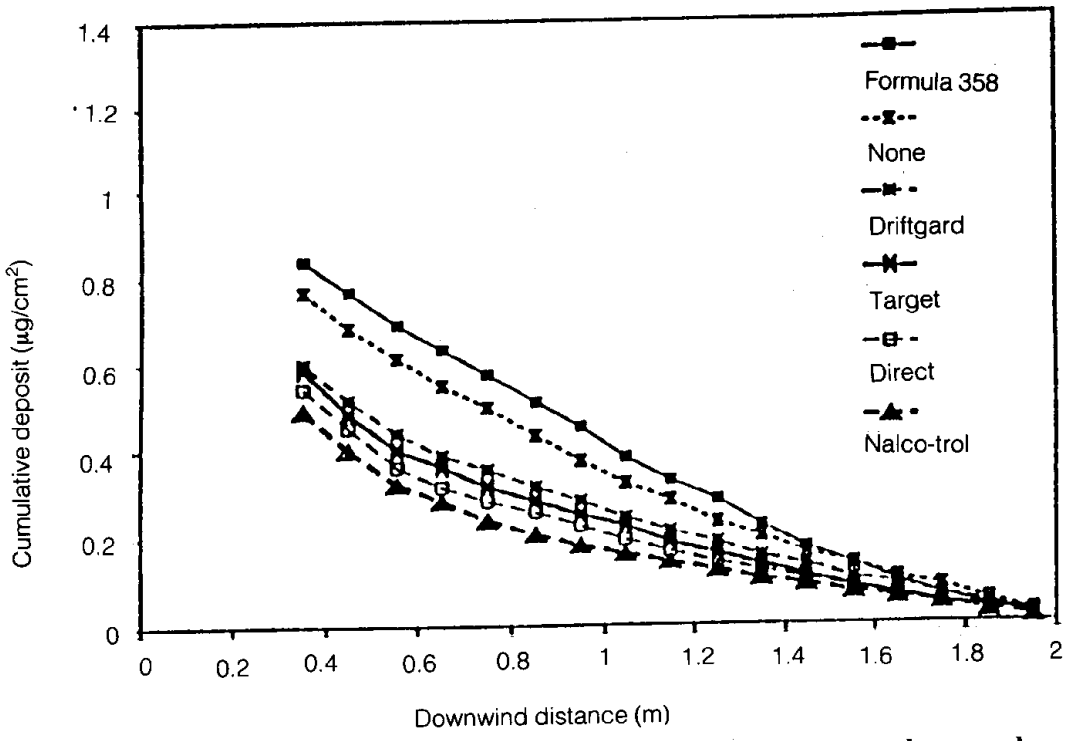

Figure 4. Comparison of downwind drift depositions for 5 drift retardants compared to water (Ozkan et al., 1995)

While drift retardants have performed well in lab testing, their impact on increasing droplets sizes and reducing drift in the field is still relatively uncertain. Zhu et al. (1997) found that subjecting liquids containing drift retardants to stress magnitudes which would be seen in a typical field-sprayer pump reduces the impact of the retardant on the droplet size. After several circulations within a pump most of the 12 polymers observed provided little difference in droplet size when compared to water (see Figure 5 for four of the polymers tested).

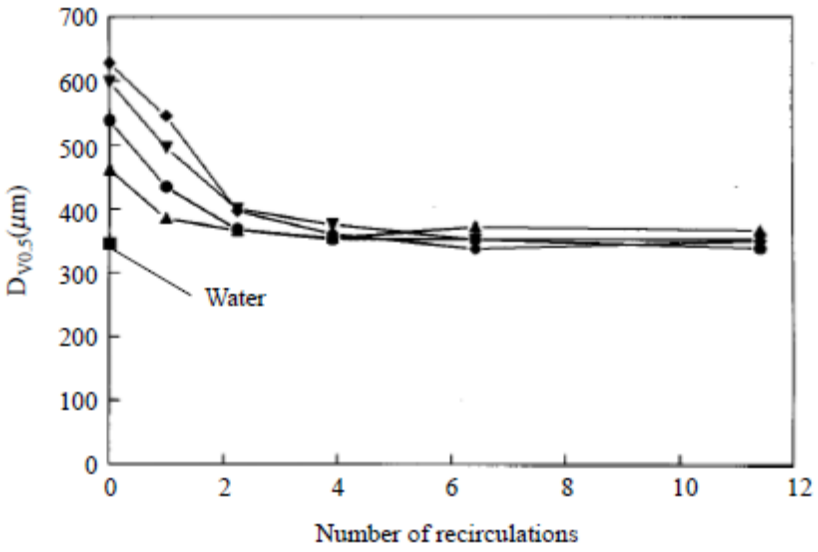

Figure 5. Median droplet sizes of four surfactant laden mixtures compared to water after subjection to shearing

Spray shields attempt to reduce the impact of wind speed on droplets thereby reducing drift. This shielding technique can be performed for a sprayer boom as a whole or individual nozzle shields. Wolf et al. (1993) found both methods of shielding to be significantly beneficial in reducing drift. Individual nozzle shields reduced drift (percentage of sprayed volume leaving the swath boundary) by 33% while using a sheet metal shield to cover the full boom and lowering the boom reduced drift by 85%. Additionally, increasing wind speeds were found to have less of an impact on drift from the shielded boom applications than the unshielded instances.

Air assist and electrostatic spraying systems have become increasingly popular for applicators desiring to reduce drift while producing better leaf coverage for increased efficacy. Air assist systems introduce a generated air stream into the spray liquid stream at the outlet of the nozzle to create a controlled region of air entrained with droplets between the nozzle and plant canopy. The entrained region is made up of high speed airflows perpendicular to the ground which reduce the influence of wind acting on the droplets. Electrostatic sprayers apply a positive charge to the liquid exiting the nozzle so that it is attracted to negatively charged plants. It is commonly believed that each of these systems

also reduce drift however little testing has been performed to quantify such impacts. A limited study performed by Storozynsky (1997) found electrostatic sprayers to reduce airborne drift (compared to a standard system) by 50% whereas a tested air-assist system actually increased drift by 5%.

2.4. Advanced Drift Controllers

Increased drift regulations combined with an influx of new technologies to agriculture has led to the recent development of intelligent drift management systems. These systems are founded on implementing drift reduction methods only when needed and not for a spraying event as a whole. Such systems are becoming increasingly popular in Europe where buffer zone requirements can be reduced if applicators implore drift reduction technologies (Rautmann, 2003).

Hewitt et al. (2002) describe a drift management system under development in New Zealand for orchard spraying which accounts for real-time site specific conditions in presenting an applicator with necessary information to determine the effects of spraying. Meteorological conditions are monitored by an on-site weather station and input into a drift model to predict real-time drift. GIS information concerning the sensitivity of surrounding sensitive areas is overlaid with the predicted deposition allowing the operator to gauge the impact of spraying under current conditions.

A more complex 2-D mapping prediction model was developed by Lebeau et al. (2009) in Belgium. A sprayer was equipped with a GPS unit and sensors to measure real-time operating condition including wind speed, direction, temperature, humidity, and boom height and store operating conditions with field position in a data acquisition system programmed in LabVIEW. Operating conditions recorded during spraying can then be uploaded by the operator into a Matlab program which produces a 2-D map of the predicted drift for the application. The motivation for the development of Lebeau et al.'s system is to evaluate the ability of a prediction model to be later used as the basis of real-time prediction in a drift controller.

2.5. Conclusion

Drift regulations in the United States are becoming more restrictive, with proposals in place which once passed will implement regulations similar to those seen in Europe.

Increased regulatory control will bring with it new challenges to create advanced drift reduction systems similar to those beginning to be developed in New Zealand and Europe. The most popular, straightforward approach to drift reduction is through the selection of larger droplet producing nozzles. State-of-the-art in spray drift reduction systems monitor real-time weather conditions and present predicted drift levels to the operator allowing for adjustment of operating parameters or to determine go/no- go decisions. While these systems are excellent management tools, their endpoints are merely raw decision making inputs, thus their desired goal is left in the pre-occupied, subjective minds of applicators. A logical next step in drift control is the development of an automated system which predicts drift real-time and changes nozzles according to scientifically based criteria. For the development of such a system, research is needed to generate a basis for the nozzle selection process, specifically the underlying real-time prediction model and method of protecting sensitive areas. Research into the basis for such decision making processes would provide a significant step in drift control methods in the United States in preparation of inevitable, increased regulation.

2.6. Research Questions

The following questions form the motivation for this work:

1. What modifications to existing drift prediction models are necessary for real-time nozzle control?
2. How can sensitive areas be protected by a nozzle controller?
3. How does droplet size influence efficacy? Can this relationship be incorporated within a controller to increase efficacy during instances of low drift potential?
4. Is controller based real-time drift prediction sufficiently accurate for protecting sensitive areas?

2.7. Research Objectives

The overall goal of this research is to develop the required critical information requirements for automated nozzle selection control on self-propelled sprayers, specifically a real-time prediction model and logic for nozzle selection to protect sensitive areas. The scope of this research includes the design of a controller based on these generated nozzle selection procedures and in-field testing to provide proof-of-concept and to quantify the predictive

abilities of the system. This research will further the development of innovative technologies to reduce spray drift though the application of state-of-the-art technologies. Specific objectives to be met in achieving the overall goal are as follows:

1. Determine required modifications to existing drift prediction models for application to real-time nozzle control.
2. Conclude criteria and measures for protecting sensitive areas from drift.
3. Establish a relationship between droplet size and efficacy for herbicides, insecticides, and fungicides.
4. Evaluate the feasibility of a nozzle control system employed to protect sensitive areas.
5. Statistically evaluate the ability of a developed model to predict drift through in-field testing.

The open ended nature of the preceding objectives requires a multi-dimensional approach to fully satisfy each of the defined learning-based objectives. Literature review, conceptual development, system development, and testing are all components necessary for crafting a basis for real-time nozzle control and understanding its potential use in agricultural production.

Chapter 3. Development of a Real-time Spray Drift Prediction and Mapping System

Real-time drift prediction is the basis for decision making within Lebeau et al.'s (2009) drift reduction system. Outputs from this model are analyzed by the applicator in determining whether to adjust nozzle selection, boom height, or abstain from spraying altogether. In the same manner, drift prediction is the heart of an automated drift reduction system with nozzle selection being the single object of control.

The use of drift prediction for real-time nozzle control presents new challenges nonexistent in static drift prediction. With the overall goal to protect sensitive areas from drift, the decision making process, in addition to being based on an accurate relationship between application and weather conditions and drift, takes on both spatial and temporal aspects absent within present drift prediction techniques. The development of a real-time prediction and mapping algorithm is the first step in forming a basis for real-time nozzle selection. Specific objectives within this development are as follows:

- Selection of a verified ground based drift prediction model based on findings from an in-depth literature review.
- Formulate an algorithm for prediction of drift from a ground sprayer.
- Establishment of an algorithm to map real-time predicted drift based on simulated in-field spraying events.
- Verify algorithm performance through simulations of influential drift variables.

3.1. Drift Prediction Literature Review

3.1.1. Variables Influencing Drift

The search for a model which accurately predicts drift is a quest with a long history influenced by researchers around the world. Understanding the complex physical phenomenon of drift is the first step in developing methods to reduce it. Drift prediction research includes determining the factors which influence drift, the degree of influence of each factor, and the development of techniques to represent the relationships between these influences and the magnitude of drift. While each have a different motivation, regulatory agencies, agricultural equipment companies, pesticide manufacturers, and environmentalists all share a common goal in continuously working to develop a better understanding of drift.

The sheer number of variables which influence drift is one of the largest hurdles to overcome in generating methods for prediction. In-field and wind tunnel testing have both sought to reduce the scope of the drift phenomenon to include only the more influential factors. Smith et al. (2000b) found that distance downwind, wind speed, and boom height have the greatest impact on drift depositions through in-field testing. Surprisingly droplet size was found to be insignificant in describing the drift depositions. Through in-field testing Nuttyens et al. (2007) also found drift depositions to be highly correlated to distance downwind and boom height, however concluded droplet size, nozzle pressure, temperature, and humidity were also significant variables impacting drift. The SDTF (1997) conducted a large study over two years to determine what factors greatest impact drift, concluding that droplet size was overall the most influential, with wind speed and boom height also having a significant impact on deposition downwind. Wind tunnel testing by Taylor et al. (2004) showed increases in droplet size to result in a non-linear decrease in downwind depositions. Wind speed and boom height were also found to have a high impact on drift depositions.

The time and cost inputs required for extensive experimental testing to evaluate a wide range of values for each variable are limited, thus in-field tests are often conducted with reduced scope. Additionally, weather conditions cannot be controlled or held constant during in-field testing therefore it is difficult to determine cause-and-effect relationships. These complexities are largely responsible for the various conclusions drawn concerning what factors greatest influence drift. As a whole, the drift research community sees distance as a

spatial measure of drift, therefore it is not mentioned as an independent variable affecting drift. Droplet size is generally thought to be the most influential independent variable, followed by boom height and wind speed. Temperature and humidity are considered to have significant influence; however their impact is a tier below the previously mentioned variables, therefore they are often excluded from drift studies.

3.1.2. Drift Prediction Models

Both regression and analytical models have been proposed by researchers to represent the relationships between drift and the variables which greatest influence it. Variability between models is derived from variables of expression, datasets serving as the basis for regression (within regression models), scope of the model, representation of drift, and mode of prediction (within analytical models).

3.1.2.1. Regression Models

Regression models are generated through data collected during wind tunnel or in-field testing. Statistical methods establish the numerical relationships seen in the data typically through a regression type analysis.

Smith et al. (1982) conducted 99 in-field tests over three years with a goal to derive an accurate regression equation to predict drift. In this study, 18 independent variables were recorded (nine weather-related variables and nine application method variables) while drift deposits were collected up to 27.5 m (90 ft) from the boom edge. Eight multiple regression equations were developed relating the most significant three input variables to an output drift characteristic variable. The eight different equations each contained a different output variable characterizing drift. Output variables ranged from the absolute drift at a given distance (for example, 2 meters from the boom edge) to the distance at which 95% of the total measured drift had been collected from the edge of the boom. Smith et al.'s derived regression models had high coefficients of determination (R^2) in relation to his collected dataset, ranging from 65.6% to 90.2%. A related discovery based on Smith's data is that 68%-90% of drift is directly influenced by applicator controlled variables (such as droplet size, pressure, etc.).

Threadgill and Smith (1975) performed in-field testing in order to develop a single regression equation for use in predicting drift. Drift deposits were collected up to 8 m (26 ft) downwind of a sprayer and multiple linear regression was used to relate total collected drift to weather, spray, and application variables. Specifically, the air stability ratio (calculated based on temperature variability over height and wind velocity), droplet size, wind speed, and the coefficient of variation of droplet size (for a nozzle) were used in developing the regression model which had a correlation coefficient of 0.58.

Bode et al. (1976) similarly generated a regression model based on in-field data collections. Nine independent variables were measured through testing to relate to total spray drift deposition measured (out to 312 m, or 1,023 ft), deposits beyond 2.4 m (8 ft), and total spray lost as drift (calculated from a mass balance analysis). Wind speed, temperature, atmospheric pressure, relative humidity, Richardson's number (a measure of atmospheric instability), boom height, application rate, nozzle pressure, and the concentration of drift retardant comprised the monitored independent variables. Statistical regression produced a maximum coefficient of determination of 0.53 with significant independent variables of application rate, wind speed, Richardson's number, temperature, and relative humidity, as well as combinations of these variables (as linear regression was used).

3.1.2.2. Mechanistic Analytical Models

Analytical drift prediction models differ from regression models in that the relationships between variables describe mechanistic, physical phenomenon rather than numerical relationships. The complex nature of drift can lead analytical models to become quite extensive. Typically only the more important variables, determined from past in-field testing, are used in developing analytical models in order to reduce their complexity. Most analytically derived models can be classified as either plume or random-walk, which differ in the mode of action for tracking liquid volume leaving the sprayer.

Plume models treat the volume of liquid leaving the sprayer as a single cloud, of which portions settle out as deposition based on Gaussian diffusion principles. Plume models for drift prediction originated out of the modeling of chimney smoke and air pollutants from factories which were first developed in the 1930's (Bosanquet, 1936). Concentration differences between the cloud and surrounding air, atmospheric turbulence, and statistical

parameters combine in determining the dispersion of the cloud. Gaussian dispersion models describe movement from tall stacks and point sources, therefore in parallel application to describing spay drift, such models perform well for aerial applications where spray is released from a high, concentrated sources (which can be treated as a point source). The diffusion principles accounted for by the Gaussian dispersion models tend to predict drift better for long distances (up to 10 km), however since they are not focused on initial release conditions, their short range drift prediction accuracy is limited.

While plume models are generally more applicable to aerial applications, they are still occasionally used for ground-application drift prediction. A recent real-time prediction method relied on a Gaussian dispersion model due to its computational simplicity and thus attractiveness for continuously updating predictions (Lebeau et al., 2009). The model was found to overpredict near distance drift as expected, while underpredicting far-field drift. Lebeau et al. concluded that the model produced "realistic" visual descriptions of drift however further research is needed to develop more representative wind speeds which act on the cloud.

Random-walk prediction models are much more commonly used in ground application situations. These models track individual droplets from the point at which they exit the nozzle until the water within the droplet completely evaporates or the droplet deposits within the field. Air drag and gravity comprise the simplified force profile acting on the droplets. The "random" nature of the model is derived from a random number pulled from a Gaussian, or normal, distribution which is factored into determining the trajectory of each individual droplet. Droplet trajectories are tracked in a numerical, Lagrangian fashion, meaning the change of the droplets position and velocity is tracked during small time steps during which the droplet is acted upon by the wind drag, gravity, and statistical parameter influences. The change in velocity and change in position are added incrementally to the initial conditions to determine absolute droplet velocity and position at an instance in time.

Like plume prediction models, random-walk models were not initially derived to describe spray drift. Fluid flow in a channel and wind fluctuations were two of the earliest phenomenon modeled by random-walk models (Sullivan, 1971; Daniels and Jones, 1970). Hall (1975) proposed the first application of random-walk models for drift prediction and

performed experiments to determine if observed behavior of a spray agreed with the model. Under stable atmospheric conditions, the random-walk model performed well in predicting the heights of droplets at distances downwind from their release point. There were large discrepancies however between the model and observations when a large time step was used and when there was high atmospheric turbulence.

Thompson and Lay (1983) built upon Hall's random-walk model by adding the effects of evaporation on drift. Evaporation reduces a droplet's diameter throughout its travel trajectory. This effect is taken into account during each time step of the random-walk process. Under high evaporation conditions (low humidity, high temperature, high wind speeds), liquid within initially small diameter droplets can completely evaporate before deposition, leaving the particulate (solid pesticide component) highly susceptible to in-air suspension. Particulate pesticides do not impact evaporation rates (Elliott and Wilson, 1983), therefore only the properties of water need to be considered in the evaporation process. Drift retardants however do impact the liquid properties and can greatly reduce evaporation and overall drift by maintaining a larger droplet size. According to Elliott, in the evaporation process droplets smaller than 50 microns can completely evaporate leaving only their particulate core suspended in the air. The core, which is not retained in the modeling process, remains suspended in the air during turbulent conditions, depositing typically at night when the atmosphere stabilizes.

Miller and Hadfield (1989) further improved the predictive capabilities of the random-walk model by adding in effects of air-entrainment near the nozzle, which is generated from the vertical exit velocities of droplets. Droplet trajectories are modeled in two distinct phases, near the nozzle where the droplets initial conditions and generated air-entrainment have the greatest influence on the trajectory, and at a distance from the nozzle where the trajectory is dominated by atmospheric conditions. In-lab testing was performed to determine the predictive ability of the modified model with air-entrainment, specifically in comparison to Thompson and Lay's more simplified approach. In-air drift was measured and compared to the predicted in-air spray volumes from both models. Results showed that the air-entrainment model qualitatively improved predictive ability when compared to the more simplified model.

Holtermann et al. (1997) and Baetens et al. (2007) incorporated 3-dimensional (3-D) analysis into the random-walk model approach to drift prediction. Holtermann's IDEFICS (IMAG Program for Drift Evaluation for Field Sprayers by Computer Simulation) uses a 3-D analysis of the more complex air-entrainment region then converts to a 2-D approach for the atmospheric dominated region to reduce computing requirements. Baetens et al. modeled drift entirely in 3-D in an effort to describe the high variability seen in field testing, which is believed to be caused by complex wind turbulences which cannot be fully described by 2-D analysis. In-field testing was performed to compare Baetens et al.'s model, evaluated using ANSYS, to experimental data. Simulations in ANSYS required 18 hours each to establish predicted drift levels for comparison. Figure 6 shows a physical representation of the trajectory of each droplet as it leaves the boom. The model was found to accurately predict drift for distances less than 5 m (where there was only a 13% difference between the average predicted and experimental depositions for a wind speed of 3.1 m/sec) however at greater distances the model under-predicted by around 60%. This reduction in accuracy was attributed to additional complexities related to wind speed and wind direction variability.

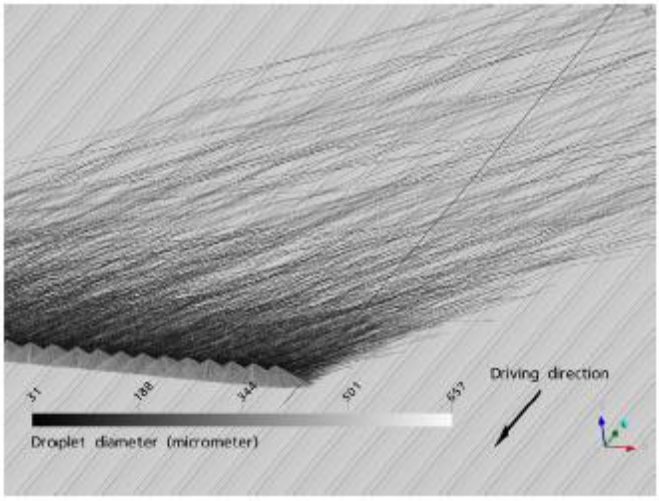

Figure 6. Physical representation of predicted drift from Baetens et al.'s (2007) model displaying trajectories of each individual droplet

For regulatory purposes and to aid in management decisions, several software programs have been developed which provide easy interfacing with the inputs and outputs of prediction models. AgDRIFT®, developed through the joint effort of the US EPA, USDA,

and SDTF, primarily predicts drift for aerial applications. The US EPA currently uses AgDRIFT® within their risk assessment process for product registration and establishing drift specific labeling. Within this program, both plume and random-walk drift modeling techniques are incorporated into the drift prediction process. Unique to AgDRIFT® is the inclusion of aircraft wake influences on drift (Bilanin et al., 1989). AgDRIFT® contains a tier 1 (a developed regression model) model for ground applications; however Woodward et al. (2008) found through in-field testing that AgDRIFT® overpredicted out-of-swath deposition by a factor from 3.5-100. Developments to revise the tier 1 prediction model with a more analytical approach to provide greater accuracy are ongoing (Teske et al. 2001, Teske et al., 2004).

Zhu et al. (1995) developed DRIFTSIM specifically for ground application drift prediction based on a random-walk model. DRIFTSIM has become a highly recognized and applied tool for the management of drift by extension personnel and regulatory agencies (White, 2006). The model accounts for the impact of evaporation on drift however takes a more simplified approach to handling near-nozzle conditions when compared to Bateans et al.'s random-walk model. Trajectories of droplets are tracked in 2-D and the entrainment effects near the nozzle are ignored. The specific random-walk model used for drift prediction was developed by Fluent Inc., now ANSYS Fluent (Canonsburg, PA), for use within their computational fluid dynamics (CFD) program, which models the movement of droplets within a gas under the influence of evaporation. Independent model variables within DRIFTSIM are temperature, humidity, wind speed, droplet size, and boom height. To reduce DRIFTSIM's computing time requirements, over 2 million simulations within Fluent were performed using a wide range in each independent variable. The output dependent variable within these simulations was the drift distance of a single droplet. Drift distances, along with the independent variables producing each distance, were stored within text files which are used as lookup tables within DRIFTSIM for reduced computational and time requirements (Zhu et al., 1995).

Reichard et al. (1992) performed wind tunnel testing to evaluate the accuracy of Fluent, which contains the underlying random-walk model used by DRIFTSIM, in predicting the drift distances of droplets. Fluent was found to be highly accurate for drift distances

tested, with correlations between the measured and calculated data above 0.95. The greatest difference between the experimental and predicted drift distances of a single droplet was found to be only 5.4%, however the furthest distance evaluated within this testing was slightly less than 2 m. Reichard et al. concluded that while additional testing is required for long distance drift, Fluent is an excellent tool for predicting short distance spray drift.

3.1.3. Conclusion

Regression and analytical models have both been developed for drift prediction. Regression models provide highly accurate prediction when determining drift under conditions similar to those for which the model was developed. Additionally, regression models are generally simplistic relationships between independent variables and drift, reducing time and computing requirements for a prediction. The limitation in regression models is the overly specific relationship which results from limited datasets used to derive the model. The complexities of in-field testing and data collection reduce the ranges in operating and weather conditions for which data are collected. Relationships derived are then only representative of the collected dataset and not for drift as a whole. It is then difficult to obtain a general expression for drift for a wide range in operating conditions, leading to high inaccuracies when trying to predict drift for conditions outside the scope of the model (Thompson and Ley, 1983).

Analytical models for drift prediction have increased in popularity over the last several decades as technology has advanced to the point where simulations can be performed on personal computers. In contrast to regression models, analytical models have a much wider range of application as they are derived from mechanistic relationships. The major limitation of analytical models is the computing time requirements for simulation.

Real-time spray drift prediction requires both minimal computing time as well as accuracy for a wide range in operating and weather conditions. The system in development by Lebeau et al. (2009) attempts to satisfy these requirements using the plume modeling approach to drift prediction. Plume models are not as computationally expensive as random-walk models and are not limited in scope, however such models are much better suited for aerial applications. Developments made within the random-walk model approach to account for evaporation have made such models the frontrunners in ground application drift

prediction. The approach of Zhu et al. (1995) to overcome the computing time hurdle opens the door for the use of random-walk models for real-time spray drift prediction. Further development however is needed to go from the droplet-by-droplet prediction basis of the random-walk model to a system which predicts drift for an entire boom application. Additionally, development of a mapping algorithm is required to satisfy the spatial nature of in-field drift prediction.

3.2. Methods and Materials

3.2.1. Drift Prediction Model

DRIFTSIM was selected as the base drift model for nozzle control due to its highly recognized practical use, high predictive accuracy at short drift distances, and pre-compiled data tables. An obvious uncertainty of DRIFTSIM is its unevaluated long-distance predictive accuracy. The basis of prediction within DRIFTSIM is similar to that of Thompson and Ley's model; therefore it is assumed that the models produce similar predictive accuracies. More complex models considering air-entrainment effects have been shown to produce greater predictive accuracy for the tested conditions. In selecting the more simplistic approach to prediction of DRIFTSIM when compared to models such as Bateans et al.'s, an expected tradeoff between accuracy and computing time was made. The intended use of DRIFTSIM within the nozzle selection controller was approved by its original developer, Dr. Heping Zhu.

DRIFTSIM's method of prediction is through the use of an extensive set of lookup tables derived from over 2 million simulations performed in Fluent by Zhu et al. (1995). An average drift distance was determined for each possible combination of temperature, humidity, wind speed, droplet size, boom height, and initial droplet velocity shown in Table 1. The average was calculated from 100 simulated drift distances for each set of conditions, which varied based on the random component within the time steps of each droplets trajectory.

Table 1. DRIFTSIM simulation variables and conditions (Zhu et al., 1995).

Variable	Units	Range	Increment
Temp	°C	10-30	5
Nozzle Height	m	0-2	0.25
Initial Velocity	m/sec	0-20	5
		20-50	10
Relative Humidity	%	10-100	10
Wind Velocity	m/sec	0-10	0.5
Droplet size	µm	10-100	10
		120-300	20
		350-1000	50
		1100-2000	100

The use of lookup tables allows DRIFTSIM to run as a standalone program without Fluent, and significantly reduces computing time requirements. This development makes DRIFTSIM much more appealing as an end user tool, however it is of note that the random component of drift distance introduced through Fluent, a random-walk model, is potentially lost as the drift distance represents an average of 100 simulations.

While the lookup table method is sufficiently fast for the purposes of DRIFTSIM, there are several drawbacks to using the same method within a real-time nozzle selection controller. First, the lookup tables contain over 2 million drift cases, or more than 28 Mb worth of data. Limited hard drive space on in-cab controllers, the target computers for housing the nozzle controller, places a premium on smaller, more memory efficient programs. Secondly, nozzles produce a variety of droplet sizes therefore multiple lookup calls would be required to determine the drift profile from a single nozzle. Running a lookup sequence for each droplet size would require excessive amounts of computing time. Computing time, which is directly related to the system update rate, is critical to the accuracy of drift mapping. Fast update rates allow the system to represent the sprayer path with greater confidence, and thus more accurately map drift depositions. A table of the travel distance between update rates based on a 32 km/hr (20 mi/hr) sprayer speed is shown in Table 2. An

update rate goal of 2 Hz was selected for the nozzle controller as it provides a balance between mapping accuracy and computing time.

Table 2. Travel distance between updates based on 32 km/hr (20 mi/hr) speed emphasizing impact of update rate on positioning accuracy

Update Rate [Hz]	Distance Between Updates [m, (ft)]
0.5	17.8(58.7)
1	8.9 (29.3)
2	4.5 (14.7)
4	2.2 (7.3)

An alternative approach to the lookup table method is a mathematical description of the relationships seen within the data, i.e. the development of a regression model. The purpose of the regression model is to relate the independent weather and application variables accounted for by DRIFTSIM to the predicted drift distances obtained from the random-walk model, as shown by Equation 1. A regression model derived from DRIFTSIM data would possess the computational speed of experimentally derived regression models while having the scope and fidelity of a mechanistic model.

Equation 1. Desired regression model form

$$drift\ distance = f(droplet\ size, wind\ speed, temperature, humidity, initial\ velocity, boom\ height)$$

The complex nature of drift and the high degree of interaction of the independent variables due to the effect of evaporation suggests that this relationship is non-linear in nature. Statistical Analysis Software, SAS (Cary, N.C.), contains a multiple nonlinear regression application which evaluates parameter values given a regression equation structure and a set of initial parameter conditions. An internal algorithm incrementally adjusts each parameter until sum-of-squares error reaches a local minimum. Choosing suggested parameters which are truly representative of the relationships seen in the data is key to deriving an equation which converges to a local minimum sum-of-squares error which is also a global minimum. An analytical analysis was performed in order to gain a general

understanding of the relationships between these variables in the context of the methods used by random-walk models for drift prediction.

A physical representation of the drift process, based on Fluent's predictive approach, and influential variables is shown in Figure 7.

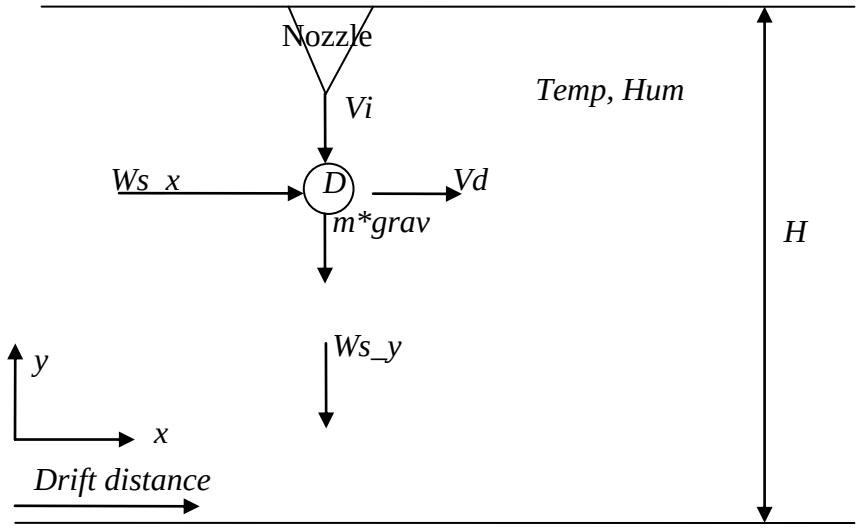

Figure 7. Droplet weight, wind (air drag), evaporation, and inertia in the drift process

where (units listed are specific to regression equations)

D=droplet diameter (µm)

Drift distance=droplet displacement in the x-direction (m)

grav=gravity

H=boom height (m)

Hum=relative humidity (%)

m=droplet mass

Temp=temperature (°C)

Vd=droplet horizontal velocity (m/sec)

Vi=initial vertical nozzle exit velocity (m/sec)

Ws_x=wind speed in *x* direction (m/sec)

Ws_y=wind speed in *y* direction (m/sec)

x=horizontal coordinate

y=vertical coordinate

Applying Newton's second law of motion gives

Equation 2. Forces acting on droplet

$$\vec{F}_{drag} + (m_{droplet} * \vec{g}) = m_{droplet} * \frac{d\vec{V}_{droplet}}{dt}$$

In the *x*-direction only the drag force is present while in the *y*-direction, both the drag force and gravity influence acceleration. The drag force is described by Reichard et al. (1992) as

Equation 3. Drag force acting on droplet

$$\vec{F}_{drag} = \left[\frac{3 * \mu_{air} * K_d * Re}{4 * \rho_{water} * D^2}\right] * (\overrightarrow{Ws} - \vec{V})$$

where

μ_{air}= dynamic viscosity of air

Kd = drag coefficient of the droplet

ρ_{water} =density of water

Re = Reynold's Number (function of drop velocity)

$\vec{V}$=droplet velocity

Drag forces drive droplets to terminal velocities in both the horizontal (*x)* and vertical (*y)* directions. The relationship between terminal velocity in the *y*-direction assuming a vertical wind speed of zero is shown in Equation 4. Small droplets, specifically those smaller than 150 µm, have high surface area to volume ratios making them more vulnerable to air drag forces (Yates, 1985). Although droplets can exit the nozzle at high velocities (~20 m/sec), the high impact of drag forces causes these droplets to reach terminal velocities both in the *x* and *y*-directions, nearly instantaneously (a 50 µm droplet reaches a vertical terminal velocity of 0.538 m/sec in 0.019 seconds). Figure 8 displays a comparison of the time required to reach terminal velocity in the vertical direction and the total time to travel (i.e. fall) the distance of the boom height (*H*, which was assumed 2 m in the analysis) for varying droplet sizes. The intersection of the two series at a droplet diameter of around 4000 µm is representative of the minimum droplet diameter at which deposits occur prior to reaching

terminal velocity. A droplet's terminal velocity in the *x*-direction is equal to the wind speed, therefore horizontal droplet displacement is dominated by atmospheric conditions.

Equation 4. Terminal velocity as a function of droplet diameter

$$terminal\ velocity = \sqrt{\frac{\rho_{water} * D * grav}{3 * \rho_{air} * Kd}}$$

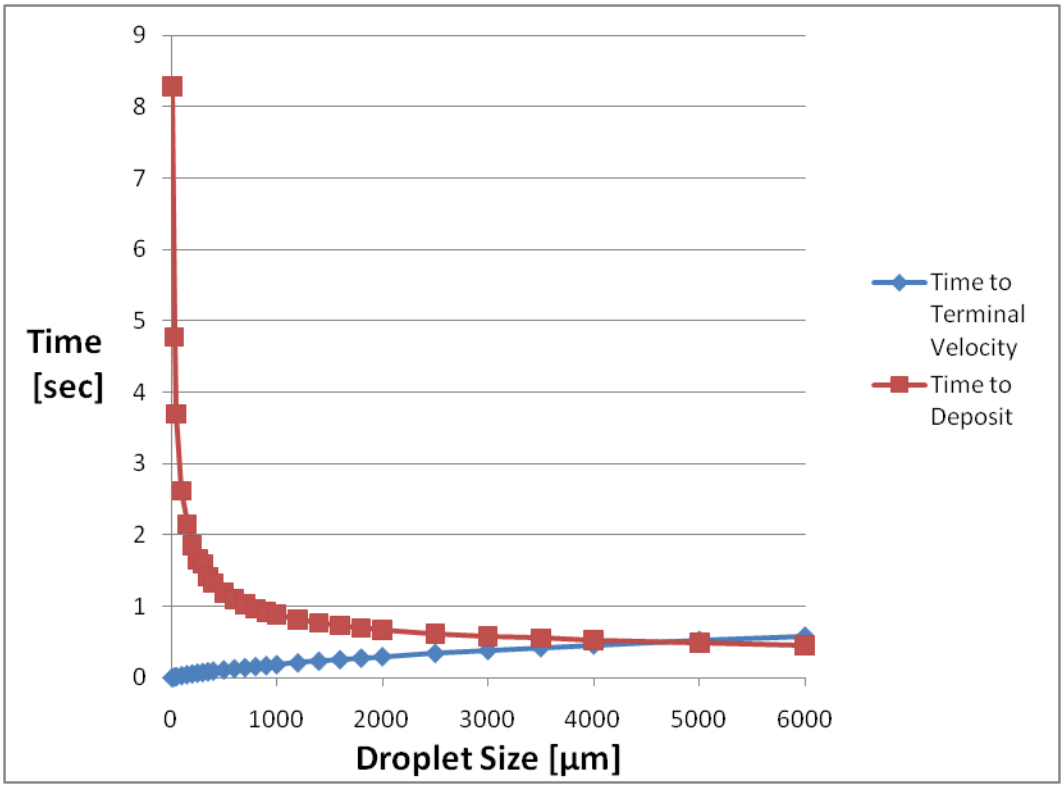

Figure 8. Time required to reach terminal velocity and to travel the boom height (time to deposit) for varying droplet sizes

Evaporation causes the droplet diameter to decrease during flight. Bird et al. (1966) represented this relationship as

Equation 5. Droplet Evaporation

$$\frac{dD}{dt} = \frac{2 * K_{mass} * (P_{airvapor} - P_{air})}{1 - P_{airvapor}}$$

where

K_{mass} = mass transfer coefficient

$P_{airvapor}$ = vapor pressure at the surface of the droplet

P_{air}= atmospheric pressure

Random-walk models track the droplet trajectory over small time steps assuming constant velocities and accelerations over these steps, i.e. through an Euler approach. The random component, derived from a random number generator within Fluent, is added to the wind velocity over each step, both in the *x* and *y* directions. Turbulence in the *y*-direction is responsible for suspending small droplets for long durations, resulting in large horizontal displacements. The trajectory of each droplet is extended until the droplet evaporates, the diameter becomes 0 based on equation 5, or the change in the vertical height is equal to *H*. From the above relationships, and method of calculating the droplet trajectory, it can be seen that drift distance is directly related to the horizontal wind speed (*Ws_x*) and boom height (*H*), and inversely related to the droplet diameter (*D*). When looking at evaporation, the vapor pressure increases with temperature, therefore evaporation rate is directly related to temperature. At a given temperature, increasing the humidity results in an increase in the air pressure, as the added humidity increases the partial vapor pressure of the air, therefore evaporation rate is inversely related to humidity. Evaporation rate is directly related to drift distance, concluding that temperature is directly related to drift distance and humidity is inversely related to drift distance.

A limitation in developing a regression model from the random-walk approach is the inability to directly represent the effects of vertical wind speeds. Wind speeds in the vertical (*y)* direction are introduced entirely as a random component within Fluent. The parameters defining the normal distribution of the vertical wind speed (mean and standard deviation) are a function of turbulence intensity (which was held constant for all Fluent simulations at 20%) and the horizontal wind velocity. Capturing the impacts of the vertical wind speed component is therefore performed entirely by the horizontal wind speed component in a regression model. As the DRIFTSIM data is an average of 100 simulations (for a single set of conditions acting on a droplet), much of the “randomness” inherent within the Fluent model is lost. For this reason, it is anticipated that little of the turbulent influences on drift are included within the regression model.

The drift distances represented in DRIFTSIM's lookup tables are positive if the corresponding droplet deposits before evaporating and negative if the droplet evaporates before depositing, with the negative distance being the distance at evaporation. Prior to regression analysis in SAS, the negative and positive value were separated into two datasets to derive two different regression equations. The first regression equation was derived using the positive dataset and presents the drift distance as a function of weather and application variables. The second regression equation was derived using the absolute values of the negative dataset. Drift distances within the second equation represent the distance a droplet can travel before evaporation as a function of application and weather variables. It is of note that both the first and second regression equations are biased to the non-evaporating and evaporating cases respectively since each were derived for exclusive cases. In application however it is assumed that the relationships derived are representative of each respective phenomenon. From this point of view, the first prediction equation is assumed to accurately predict the drift distance of any droplet regardless of whether it evaporates or not, while still considering the effects of evaporation on drift distance. In the same manner the second regression equation represents the distance any droplet can travel before it evaporates.

The regression procedure was performed using SAS's multi-nonlinear regression application with initial parameter values and structures based on the general relationships previously described. Two different models were explored to provide relative comparison and selection. The first model, shown as Equation 6, represents simplified dynamics of a falling droplet being acted upon by wind drag in the *x*-direction, and wind drag and gravity in the *y*-direction. A derived variable, *T,* is defined as the time duration of a droplet trajectory. Assuming the wind direction in the *y*-direction is zero and that a droplet reaches terminal velocity in the *y*-direction instantaneously after release, *T* can be expressed as the boom height, *H*, divided by the terminal velocity. As noted in the analysis of Equation 4, small droplets reach terminal velocities very quickly, however for large droplets this assumption will induce error. It is anticipated that the multiplication of *T* by the horizontal wind speed, *Ws_x*, within Equation 6 (and the SAS derived parameters) allows the regression equation to account for effects of vertical wind speed (turbulence). The effects of evaporation are ignored in this simplified representation of the droplet travel distance.

Equation 6. Regression structure #1 based on simplified dynamics

$$Drift\ distance = a * [T] * Ws_x - b * D * Ln\left[\frac{c * [T]}{D} + \frac{1}{Ws_x}\right] + e * D * ln\left[\frac{1}{Ws_x}\right]$$

where

$$T = \frac{H}{\sqrt{\frac{p_{water} * D * grav}{3 * p_{air} * Kd}}}$$

a ,*b*, *c*, and *e* are parameters to be estimated by SAS

The goal of the second regression structure was to give SAS more control in deriving the relationships seen within the dataset through the use of flexible exponents on each independent variable. General relationships concluded from the analytical analysis were relied upon to develop the basic structure. Variables are combined for an overall interaction term as shown in Equation 7.

Equation 7. Regression structure #2 with flexible exponents

$$Drift\ distance = a * \frac{H^b * Ws\_x^c * Temp^d}{D^e * Vi^f * Hum^g} + constant$$

Coefficients of determination of each of these equations were calculated to compare the ability of the respective equation to account for the variability seen within the input data sets. The coefficients of determination for Equation 6 and Equation 7 were 0.55 and 0.65 respectively, therefore Equation 7 was chosen as the drift prediction model for use within the real-time nozzle selection controller.

The final prediction equation with parameters determined by SAS is shown as Equation 8.

Equation 8. SAS derived drift prediction equation

$$Drift\ distance = 383.9 * \frac{H^{0.45} * Ws\_x^{0.35} * Temp^{-0.04}}{D^{0.84} * Vi^{0.05} * Hum^{-0.24}} - 3.67$$

Somewhat surprisingly the powers of both temperature and humidity are negative, corresponding to temperature being inversely related to drift distance and humidity being directly related to drift distance which is contrary to what was determined from the analytical analysis. Examination of the dataset used for derivation revealed these relationships to also be contradictory of those within the data concluding they are a product of the regression procedure. The un-exemplary relationships are likely due to correlations between variables both in the dataset and the regression equation which compromises the perceived

independent effect of each variable. Additional forms of regression equations were considered with modified variables, however the coefficient's of determination of these alternatives offered no improvement in representation of the dataset.

A single form of the evaporation model was derived using SAS and is shown in Equation 9. The same flexible regression model form was provided with initial parameters based on the analytical analysis.

Equation 9. SAS derived evaporation drift distance

$$distance_{evap} = 0.1855 * \frac{Ws\_x^{0.82} * H^{0.18} * D^{1.15} * Hum^{0.34}}{Temp^{0.58} * Vi^{.15}} - 2.97$$

The evaporation drift distance regression equation establishes a basis to determine if a droplet evaporates prior to deposition. Evaporated droplets, according to Elliot and Wilson (1983), do not impact drift deposition levels in close proximity to the spraying event, as the liquid completely evaporates and the solid particle can travel great distances in turbulent wind. While this evaporative transport is still an environment concern, it is not included within the scope of the nozzle controller thus fully evaporated droplets are excluded from the prediction procedure.

The coefficient of determination of 0.65 represents the variability in the data which is accounted for by regression model. Use of the regression model rather than the lookup table method trades predictive accuracy for reduced computing time. In an attempt to justify the lost accuracy, a simple program was written within Microsoft Visual Basic Application (VBA) to perform and time a drift prediction using the lookup table method and the regression equation method respectively. The lookup table method took slightly more than five minutes to perform prediction (and mapping described in the following Mapping Algorithm section) of drift for an entire nozzle, while the regression prediction method took two minutes. From this simple exercise several conclusions were drawn. First, the lost accuracy due to the use of the regression method was justified due the savings in computing time. Secondly, it was determined that the high level operation methods (and its dependence on Windows functions) within VBA require excessive computing times, far in access of the desired 2 Hz update rate. An alternative programming language is required for more in depth program development.

3.2.2. Mapping Algorithm

3.2.2.1. Mapping Algorithm Objectives

The overall goal of a nozzle selection controller is to protect sensitive areas from excessive amounts of drift. Deposition, volume per unit area, is the acting physical variable that leads to effects in sensitive areas, thus its magnitude is the fundamental decision making input for nozzle control. Drift deposition prediction for in-field spraying is both a temporal and spatial concept. In the context of nozzle selection control, the required endpoints of drift prediction are then depositions at locations within the field for a given instance in time.

The random-walk drift prediction models of Thompson and Ley (1983), Miller and Hadfield (1989), Holtermann et al. (1998), Teske et al. (2004) and Zhu et al. (1995) approach drift 2-dimensionally (2-D, i.e. along the x and y axes shown in Figure 7). Outputs from these models are either the depositions along a one dimensional axis, or the drift distances of individual drops. The model developed by Bateans et al. (2007) is innovative in its 3-D approach to drift, however the complexity of the model and computing requirements limits its application to merely an in-lab tool. Each of these models requires significant modification for real-time drift prediction and mapping, as desired by a nozzle selection controller.

DRIFTSIM's raw form of prediction, the vertical drift distance of a single droplet, provides an ideal flexible platform on which to build an overall drift prediction and mapping algorithm. Necessary modifications defined as specific objectives for the development of a nozzle selection controller include the following:

- Establishment of an algorithm to determine deposition levels based on drift distances for multiple droplets and nozzles
- Inclusion of the impact of wind direction on deposition location
- Location of drift deposition expressed in absolute coordinates
- Continuous updating of spatial deposition
- Storage of all predicted values for future references

3.2.2.2. Mapping Algorithm Development

Establishment of the drift mapping algorithm was done in the context of the development of a real-time spray drift prediction software program. The program is a tier 1 (i.e. base prediction model which will be further expanded upon for full-scale nozzle control) design in the overall development of an automated nozzle selection controller, as it is merely the drift prediction component in the overall control system. In an effort to simulate in-field operations, assumed inputs to the program are temperature, humidity, wind speed, wind direction, initial droplet velocity, boom height, and vehicle position. C++ was chosen as a programming language for the further development of the spray drift mapping algorithm due to the limitations in processing time experienced through preliminary trials. When compared to Visual Basic, C++ is more independent of Windows with lower level functionality resulting in faster run time.

Predicting drift depositions at locations in the field is a large scale evaluation of the continuous drift prediction equation developed from the DRIFTSIM data. Multiple evaluations of a continuous function are analogous to a discrete representation of a continuous process. Based on the desired end form of drift, deposition levels, a discrete representation of two physical entities, field area and nozzle spectrum, was required.

A gridding approach was taken in discretely representing field area (Figure 9). This approach maps an n x n cell grid onto the field of spraying. Each grid cell corresponds to a cell of memory within the computer processor which stores the level of predicted drift deposition at that in-field grid position. Upon the initiation of a program, C++ requires all variable dimensions to be defined (and hard-coded, i.e. non-variable), therefore the grid dimensions must be pre-established regardless of the field area which is actually sprayed. The algorithm is limited to mapping drift only within the pre-defined field extents, as memory is not allocated to represent locations outside the field grid. Latitudes and longitudes define the absolute position of the lower left hand corner of each of the grid cells. The centermost grid cell is given the initial set of coordinates, read serially into the algorithm program, allowing for travel to be mapped in any initial direction. Absolute locations of all grid cells are calculated using this initial set of coordinates and the grid cell spacing according to the haversine relationship (Equation 10).

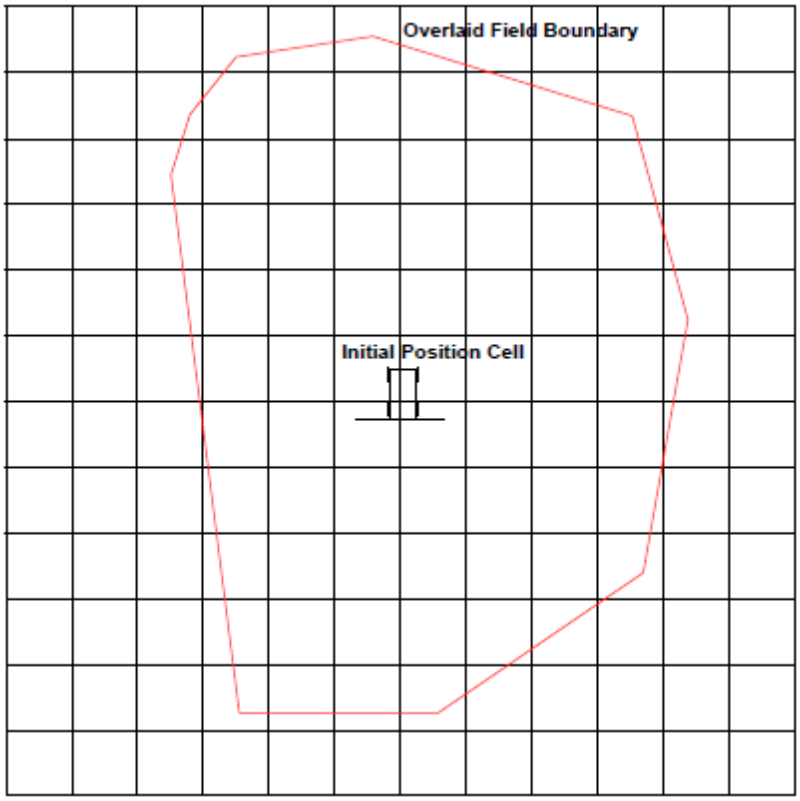

Figure 9. Field boundary (in red) overlaid on drift mapping grid

Equation 10. Haversine equation

$$sin^2\left(\frac{d}{2R}\right) = sin^2\left(\frac{\Delta Latitude}{2}\right) + cos(Lat_1)\,cos(Lat_2)\,sin^2\left(\frac{\Delta Longitude}{2}\right)$$

where

d= distance between two geographical coordinates

R=radius of sphere (average of 6367 km for earth)

The output of the prediction equation (Equation 8) is the drift distance of an individual droplet. Deriving deposition levels, volume per unit area, at positions within the field grid requires an algorithm which adds the volume contribution of each droplet size to the volume of drift at each grid cell. Performing this operation requires information concerning the nozzle droplet spectrum, the application rate, the grid spacing, nozzle spacing, and boom length. Nozzle droplet spectrums characterize the droplet producing capabilities of the nozzle, giving the portion of the volume as a continuous function of the droplet size. For

evaluation of depositions at each distance, conversion from continuous to a discrete representation is necessary. ASABE S.572.1 (2009) specifies using three nozzle spectrum characteristics to classify a nozzle, the 10%, 50%, and 90% threshold diameters of which the respective percentage of the volume produced by the nozzle is contained in smaller droplets. Ten droplet sizes were chosen to characterize the nozzle spectrum within the prediction and mapping algorithm, as the increased spectrum resolution leads to a more continuous drift deposition representation. Droplet producing characteristics of three different size nozzles, classified according to ASABE S.572.1, were hardcoded into the program. Droplet sizes were chosen in 10% cumulative volume increments as shown in Table 3.

Table 3. Fine, medium, and coarse nozzle spectrums defined in 10% cumulative volume increments as hardcoded within the prediction program

Fine	Medium	Coarse
Droplet Size	**Droplet Size**	**Droplet Size**
100	180	250
150	250	320
175	300	380
220	340	425
250	370	475
280	400	525
310	475	610
350	530	700
400	650	800
550	800	900

A drift profile for each nozzle is established by applying the drift prediction equation to each droplet size category defining the nozzle spectrum. Incorporating the percentage of the released volume in each size category gives the percentage of the applied volume drifting to each distance. Deriving the volume deposited within each cell is based on the general drift case seen in Figure 10.

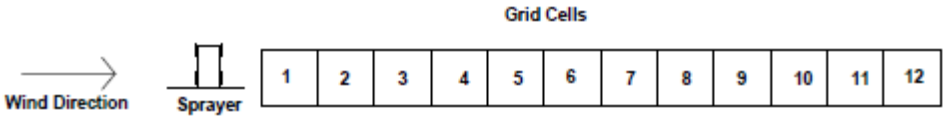

Figure 10. General drift mapping case

The grid cell which contains each category of droplets is determined based on the drift distance. An "if" statement routine, modeled after a successive approximation A/D converter to reduce computing time, selects the specific grid cell which contains the respective drift distance. Deposition within the grid cell based on the singular droplet size is calculated as

Equation 11. Deposition within each grid cell

$$Deposition = \frac{Rate_{application} * \%Volume_{dropletsize} * nozzlespacing}{Width_{grid}}$$

The mapping sequence is iterated for each of the 10 droplet sizes characterizing the volume expelled by the nozzle. Depositions at each grid cell are cumulated by adding each calculated deposition to the previously existing deposition at the respective grid cell.

As noted previously, DRIFTSIM contains only an average drift distance for a certain droplet diameter, thus removing the "randomness" of the random-walk model. Randomness in the drift distance is due to the turbulent nature of wind. Wind turbulence is created by either wind flowing over uneven elements or by a temperature gradient within the atmosphere and is most often described as turbulence intensity. Turbulence intensity is defined as the standard deviation divided by the average of wind speed measurements made over a duration (Leung and Lui, 1995). In the data generation state of DRIFTSIM, a turbulence intensity of 20% was used for the Fluent simulations (Zhu et al., 1995). The specified turbulence intensity defined the distribution from which the random wind velocity component is formulated. In an attempt to reintroduce this random component back into the drift distance predictions, the 20% turbulence intensity was incorporated into the drift mapping algorithm through the use of wind speed statistics. Over short time periods (1 minute), wind speed follows a Gaussian distribution (Cochran, 2002). Based on a 20% turbulence intensity, 16% of wind speeds measured over a duration would be in excess of 1.2

times the average wind speed, while another 16% would be less than 0.8 times the average wind speed. Assuming each droplet to be acted upon by a single wind speed over its entire trajectory and the rate of release of each droplet size category to be constant over time, 16% of the volume released over a duration is acted upon by high wind speed cases and 16% of the volume is acted upon by the low wind speed cases. In the same discrete fashion 68% of the volume is acted upon by the average wind speed over the duration. This logic was applied within the drift prediction algorithm by applying the high, low and assumed average wind speeds to 16%, 16% and 68% of the volume in each droplet size class, thus generating a total of 30 drift predictions for each nozzle. While the motivation of these methods was to incorporate variability into the drift prediction model, increasing the number of discrete predictions also led to a more continuous, intuitive representation of drift deposition.

The drift profile for a single nozzle is represented by a "straight line" vector of elements. Elements are stored within processor memory such that each succeeding element corresponds to an adjacent downwind grid cell (Figure 11). The magnitude of each element is the level of deposition within a corresponding grid cell. Drift vectors are the fundamental method of deriving and mapping drift deposition within the drift prediction program.

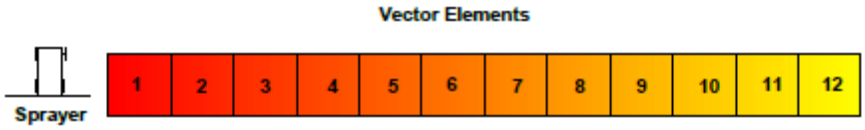

Figure 11. Drift vector elements with colors representing varying deposition levels

Mapping resolution is determined by the grid cell size. Large grid cell sizes mesh the volumes at discrete distances together, generating a smoother drift deposition gradient within the drift vector. Smaller grid cell sizes give better mapping resolution; however with the limited number of deposition levels mapped to the grids (30), it is possible to have intermediate cells which contain zero or counterintuitive depositions due to the limited range in distances contained within the cell. In addition to resolution, grid cell size affects the total mappable area. With a constant sized matrix representing the field (hardcoded at 1000 x 1000 cells), larger grid cells increase mappable area while smaller cells decrease mappable area. A

grid cell size of 2 m by 2 m was selected for use within the mapping algorithm as it provided optimal balance between mapping resolution (2 m length and width) and total mappable area (400 ha or 988 ac).

An overall drift vector is derived to describe drift from all nozzles on the sprayer. The initial element within the total deposition vector corresponds to the furthest upwind grid impacted by drift within the field. Drift distances from each nozzle are offset based on the nozzles position relative to the overall drift vector. Depositions within each grid cell are based on the summation of depositions from each droplet class size and nozzle. Handling drift in this manner results in an overall deposition vector which accounts for the total volume applied by the sprayer, both within and outside of the sprayer swath.

Sprayer position and wind direction determine the placement of the overall deposition vector elements within the grid-represented field. To provide a consistent deposition gradient, wind directions are handled by the algorithm in 45° increments, with 0° corresponding to due east (wind directions out of the west). Incrementing wind directions by 45° maintains wind direction vector slopes of 0, ∞, 1, and -1 (see slope of 1 case in Figure 12). Drift distances are modified based on the wind direction such that placement within the deposition vector corresponds to angular placement in the field.

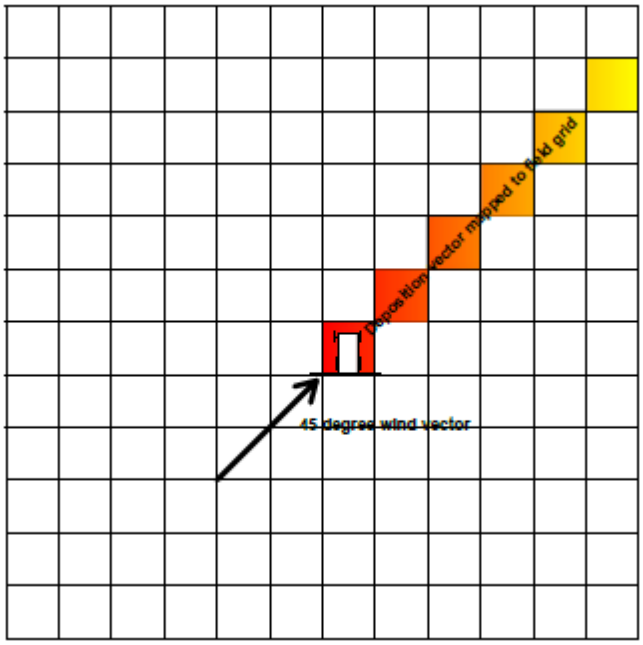

Figure 12. 45° deposition vector mapped to field grid displaying continuous drift vector

Incrementing the wind direction by 45° simplifies the mapping algorithm considerably. Figure 13 considers a mapped deposition vector with a wind direction vector of 63° or a slope of 2 in terms of grid cells. The continuous nature of the drift deposition vector is lost when mapping to the field grid due to the discrete nature of the gridding technique. A more complex mapping algorithm would be required to adjust drift distance and place drift deposition in a continuous fashion for wind directions which are not truncated to 45° increments.

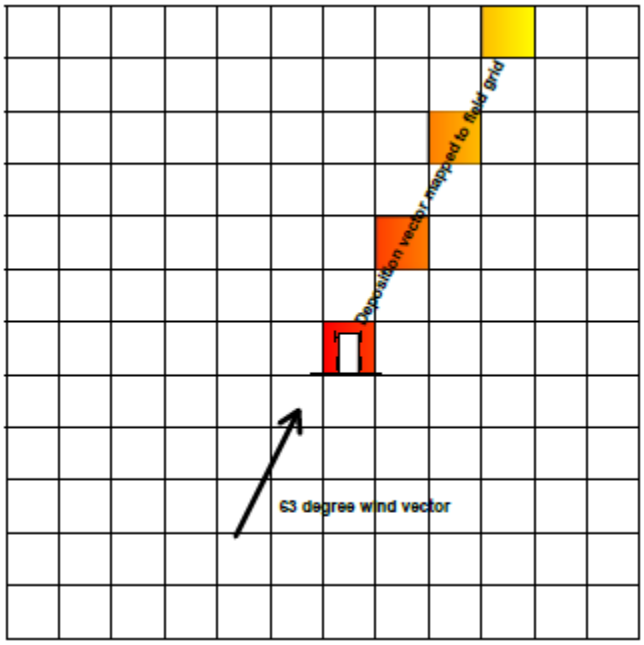

Figure 13. Lost continuity of deposition vector with 63° wind direction displaying discontinuous drift vector

The mapping algorithm thus far described provides a single instantaneous representation of drift. As previously stated, real-time drift prediction and mapping for in-field spraying contains both spatial and temporal aspects. Drift prediction is dynamic in that operating and weather conditions, as well as the sprayer position within the field, are constantly changing. The drift prediction equation accounts for the changing operating and weather conditions; responsibility to account for changing position falls on the mapping algorithm. A continuous looping procedure of the single drift prediction defines the prediction update rate as the computing time required for a single prediction instance.

Location of the mapped deposition vector for each prediction instance is based on both the position of the sprayer in the field at the time of the prediction and the wind direction. Figure 14 displays the mapped drift from these multiple predictions.

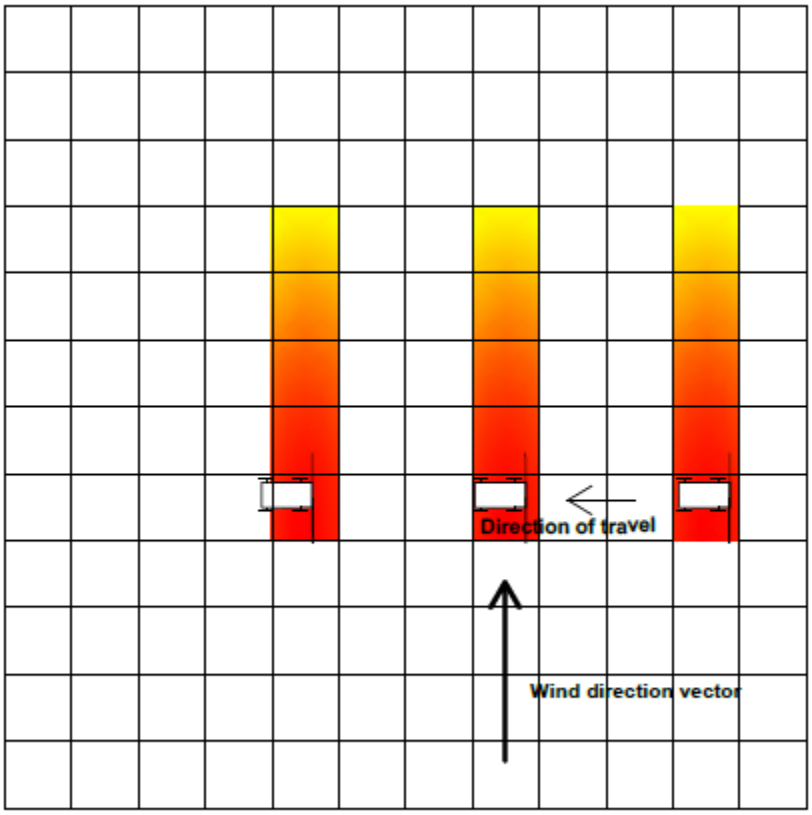

Figure 14. Iteration of single vector predictions with "unknown" gaps between vectors

For real-time nozzle selection control with a goal of protecting sensitive areas from drift, several additional algorithm components are necessary. The high speeds of in-field spraying can result in the distance between predictions being 5-10 m (16 to 32 ft) or more as shown in Table 2. Even with a fast update rate of the program, there always remains an area between predictions which must be accounted for in terms of both predicted drift and locating sensitive areas. The algorithm handles this "unknown" area by assuming straight line travel and constant application and weather conditions between two predications. Deposition levels are then "filled in" between known points as shown in Figure 15.

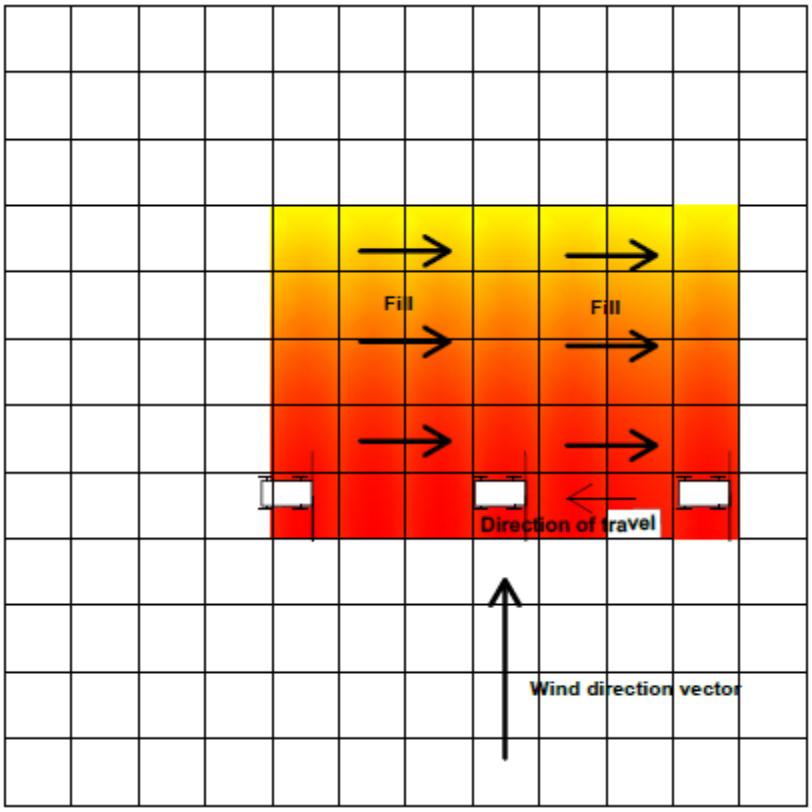

Figure 15. "Filled-in" depositions within unknown regions

The drift prediction and write back scheme described provides a representation of drift *after* it is applied. For nozzle selection to protect sensitive areas, drift must be predicted prior to true application due to inherent system delays both within the prediction algorithm and the electrical and mechanical components of the system. A “look-ahead” or offset distance applied within the algorithm shifts the sprayer location and thus the location of the predicted deposition so that decisions concerning the nozzle can be made prior to actually applying pesticide over an area. The defined “look-ahead” distance within the algorithm is a variable equal to twice the distance traveled by the sprayer within one update cycle. A look-ahead distance of twice the travel distance rather than just one travel distance accounts for the filling in procedure (which is writing drift “back”). This method assumes that the electrical and mechanical actions required to physically change the nozzle are small relative to the computing time. With a 32 km/hr (20 mi/hr) spraying speed and an update rate of 2 Hz, a look-ahead distance of 9 m (29 ft) would be applied by the program. The constant travel

direction assumption (angle of travel) can induce large systematic errors in irregular shaped fields or when spraying along the field boundary. Additionally weather and application conditions are displaced in both time and space with this method, placing upmost importance on fast program update rates to reduce error.

Record keeping capabilities of the controller have potential importance in both the regulatory and educational sectors. For this reason, the mapping algorithm records two text files of the predicted deposition and operating (weather and sprayer application) conditions at positions within the field. An example of the predicted deposition file is shown in Table 4 while the weather conditions are shown in Table 5. It is of note that wind direction is stored as measured by the sensor not in the truncated form used in placing the depositions. Each of these files can be easily uploaded into special imaging software for more in-depth analysis by either the applicator or regulatory personnel.

Table 4. Recorded drift deposition .txt file with geographic location

Predicted Dep. [L/ha]	Latitude [dec. deg.]	Longitude [dec. deg.]
0	42.01931	-93.641667
0	42.01933	-93.641667
0	42.01934	-93.641667
4.19	42.01936	-93.641667
5.59	42.01938	-93.641667
5.59	42.0194	-93.641667
4.19	42.01942	-93.641667
5.59	42.01943	-93.641667
5.59	42.01945	-93.641667
5.59	42.01947	-93.641667
4.19	42.01949	-93.641667
5.59	42.01951	-93.641667
5.59	42.01952	-93.641667
5.59	42.01954	-93.641667
4.19	42.01956	-93.641667
1.39	42.01958	-93.641667

Table 5. Operating conditions .txt file stored with time and position of measurement

Hour	Min.	Sec.	Latitude	Longitude	Temp. [C]	Hum. [%]	Wind speed [m/sec]	Wind direction [deg.]	Boom Height [m]	Pressure [kPa]
10	11	1	42.0226	93.7588	9.85	67.44	5.68	231.85	1.16	222.94
10	11	3	42.0226	93.7588	9.85	67.44	4.33	333.50	1.16	222.94
10	11	5	42.0226	93.7588	9.65	67.44	4.47	190.67	1.16	222.94
10	11	7	42.0226	93.7588	9.65	67.44	5.74	276.52	1.16	222.94
10	11	9	42.0226	93.7588	9.65	67.44	5.74	276.52	1.16	222.94
10	11	11	42.0226	93.7588	9.65	67.44	5.74	276.52	1.16	222.94
10	11	13	42.0226	93.7588	10.25	67.44	3.25	39.59	1.16	222.94
10	11	16	42.0226	93.7588	10.66	67.44	4.34	228.24	1.16	224.09
10	11	18	42.0226	93.7588	8.50	68.46	4.57	150.38	1.16	224.09

3.3. Results

The performance of the drift prediction and mapping algorithm was analyzed in the lab by simulating spaying events under different operating conditions. Application and weather conditions were varied during simulation to verify the ability of the prediction program to account for constantly changing in-field conditions. A GPS simulator provided the sprayer position inputs to the prediction program, while an accompanying user interface was added to the prediction program to allow for soft coded application and operating conditions (Figure 16).

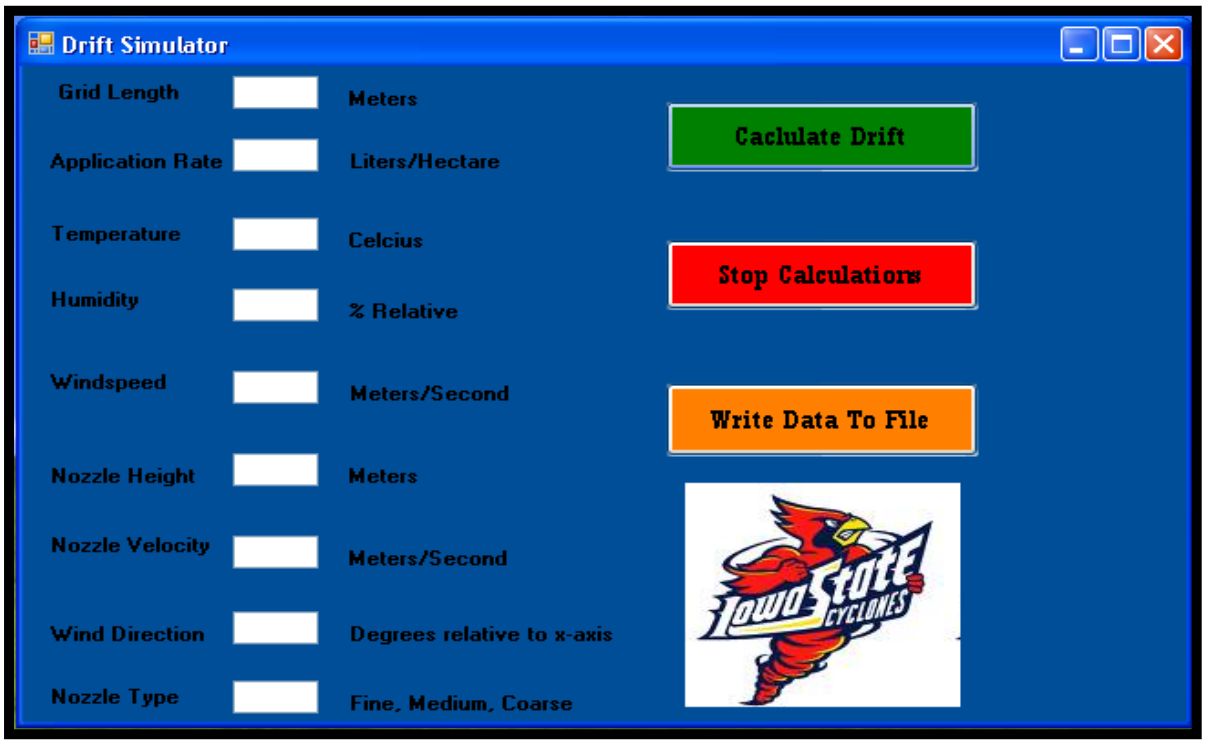

Figure 16. User interface for Tier 1 program with weather and application conditions input through text boxes by user

Wind speed, boom height, nozzle type, and wind direction were each varied individually throughout the test and the resulting drift prediction text file was uploaded into Spatial Management Systems (SMS; Ag Leader, Ames, IA) software for analysis. Application and weather variables, when not the subject of testing, were held constant throughout each of the tests. These parameters were as follows:

- Application rate: 100 L/ha (10.7 gal/ac)
- Temperature: 26 °C (79 °F)
- Relative humidity: 60%
- Wind speed: 4.4 m/sec (9.8 mi/h)
- Nozzle velocity: 20 m/sec (44 mi/hr)
- Wind direction: 0° (Due East from the West)
- Direction of travel: 90° (Due North)
- Nozzle type: Medium
- Nozzle (boom) height: 0.6 m (2 ft)

Predicted deposition maps were generated based on the spatial data within the text files. Although depositions are maintained with a 2 m by 2 m resolution, lumped depositions are displayed within the maps to simplify viewing. Deposition ranges are represented by eleven color bands within the maps. Analysis was also conducted based on the higher resolution data within the text files.

Wind speeds were varied from 0.44 m/sec to 8.8 m/sec in five increments. Figure 17 displays the resulting drift from this application. Depositions are shown from the center of the boom and beyond. A boom width of 30 m was used throughout testing, therefore deposition within the first 15 m is in-swath deposition.

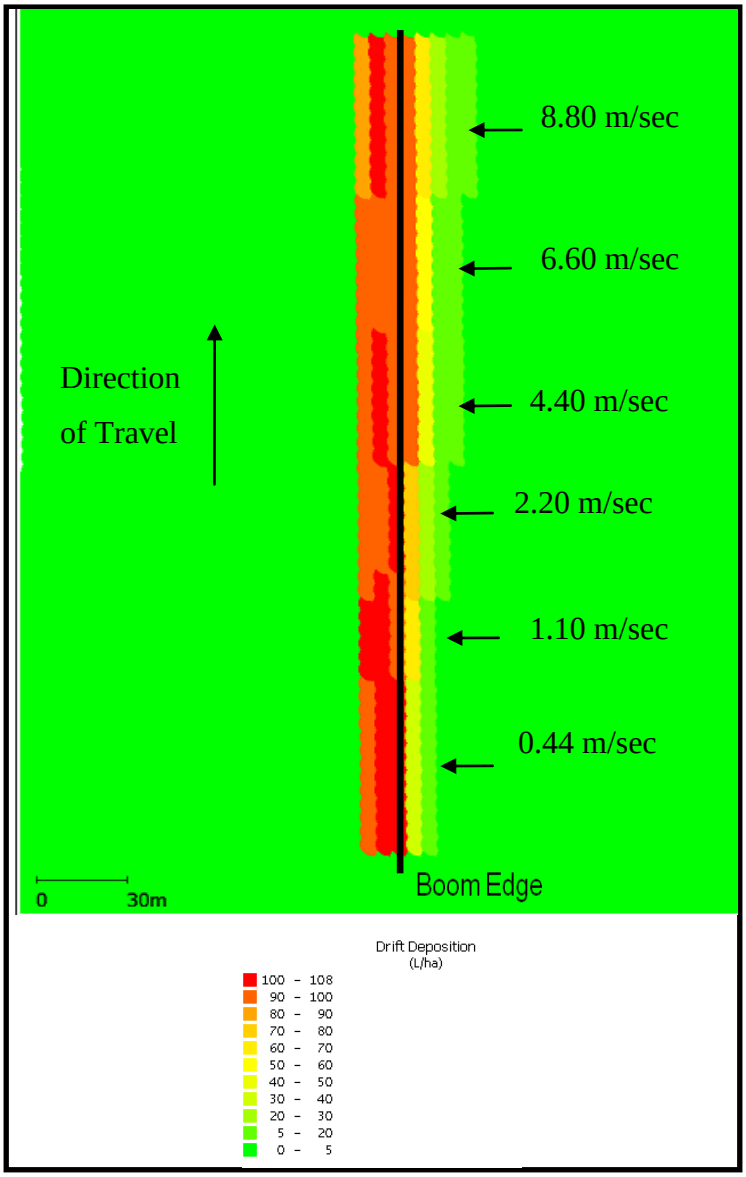

Figure 17. Program predicted depositions for varying wind speeds

For the 0.44 m/sec wind speed, drift occurs up to 10 m, where there is 5 L/ha of deposition. For the 8.80 m/sec wind speed, deposition at 10 m is 40 L/ha and occurs up to 25 m from the boom edge. Deposition near the center of the boom is around 95 L/ha, with the rate increasing to above 100 L/ha as position moves toward the end of the boom. This increasing rate within the boom width is due to the compiling drift levels from each individual nozzle.

The influence of boom height on drift deposition, as determined by the drift prediction algorithm, is shown in Figure 18. Boom heights of 0.30 m, 0.61 m 0.91 m and 1.21 m were tested in this simulation. The 1.21 m boom height results in measurable drift 10 m beyond the furthest extent of drift deposition for the lowest boom height. At a distance of 10 m from the boom edge, 61 L/ha drift depositions are seen for the 1.21 m boom height while for the lowest boom height (0.3 m) depositions at 10 m are only 7 L/ha.

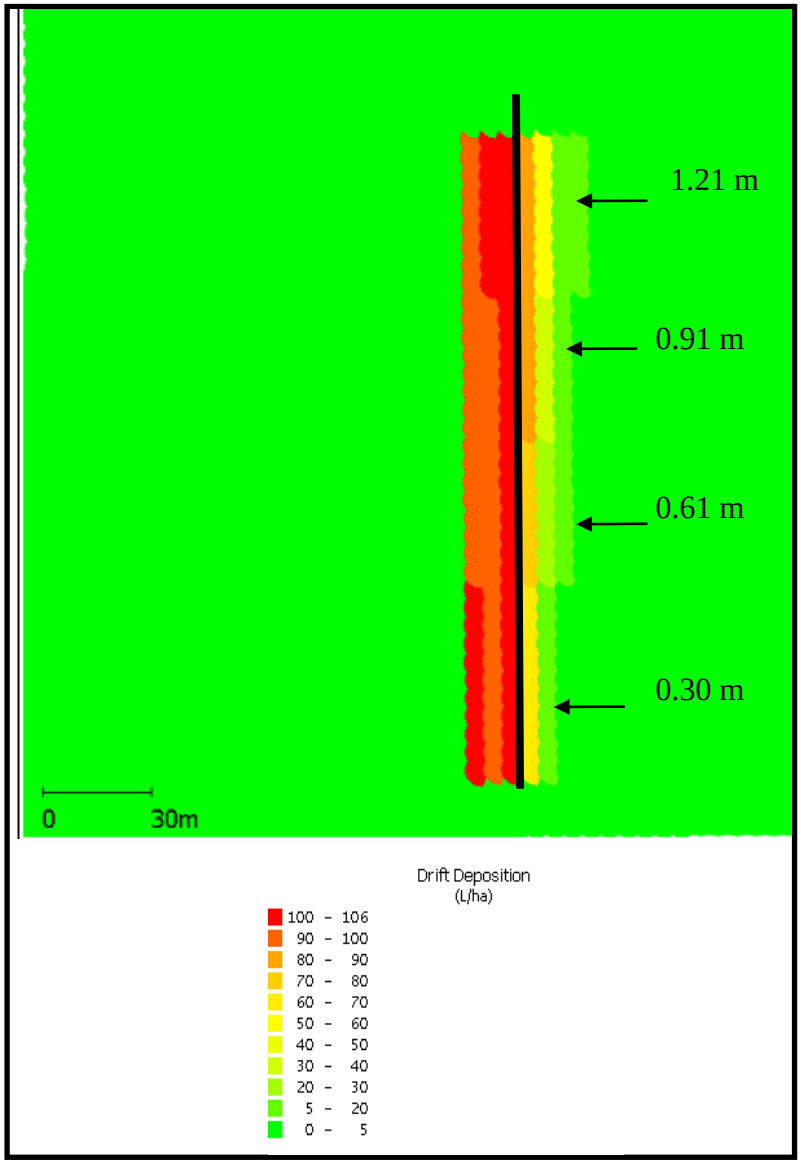

Figure 18. Predicted depositions for varying boom heights

Results for nozzle type testing are shown in Figure 19. Fine, medium, and coarse nozzles droplet spectrums measured according to ASABE S572.1 (2009) were stored within the program allowing for this analysis. At 7 m from the end of the boom, the fine nozzle produces 40 L/ha of deposition, while the medium produces 15 L/ha, and the coarse 6 L/ha. For the deposition as a whole, there is little difference between the coarse and medium nozzles; however there is a large difference for the fine.

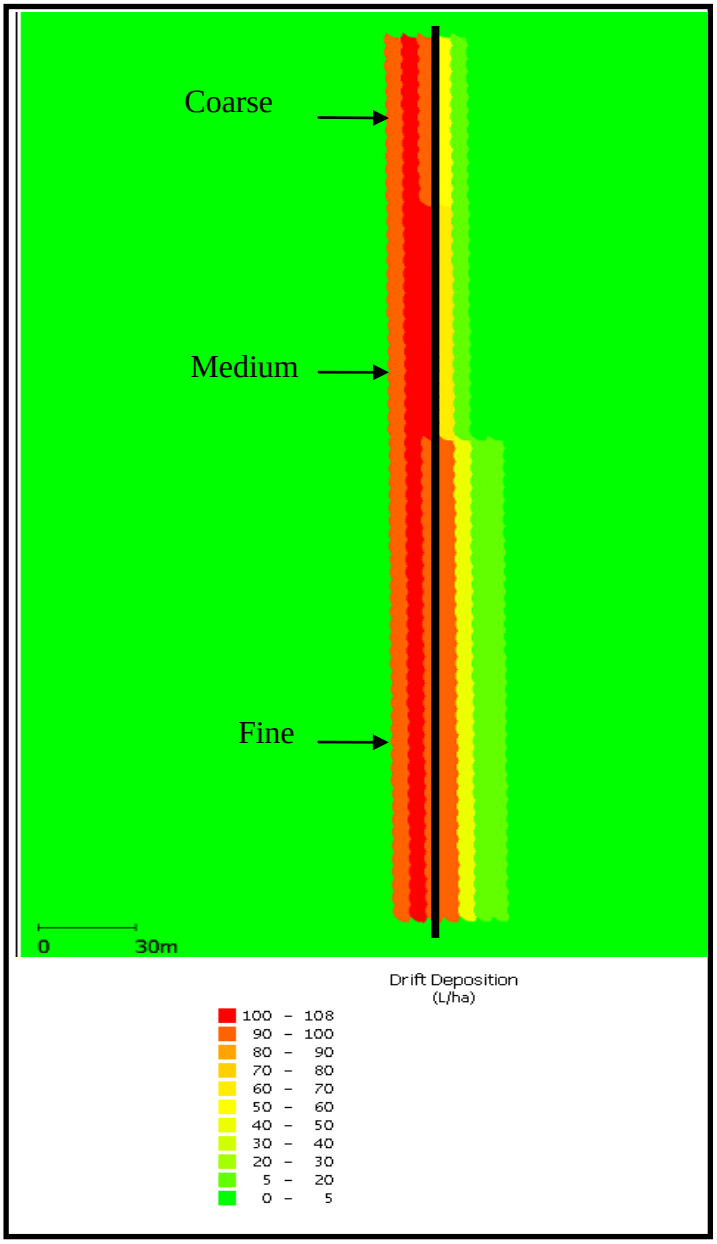

Figure 19. Predicted depositions for three different nozzle types

Depositions resulting from a wind direction of 135° relative to due east is shown in Figure 20. This figure represents spraying around a sensitive area within a field, such as a pond, and was created by changing the sprayer path within the GPS simulator. The sprayer approaches the pond from the lower edge of Figure 20 and drives counter-clockwise around the pond. The pond has an area of 0.73 ha, however spraying with the boom next to the edge of the pond reduces the unsprayed area to only 0.6 ha due to drift. The bottom left turn around the pond results in 96 L/ha being applied within the pond. Such practice could cause considerable harm to the sensitive area. Also noticeable from Figure 20 are several very high application rates that result from turning within the field as well as the wind direction. The application rate is doubled in some areas due to compiling drift.

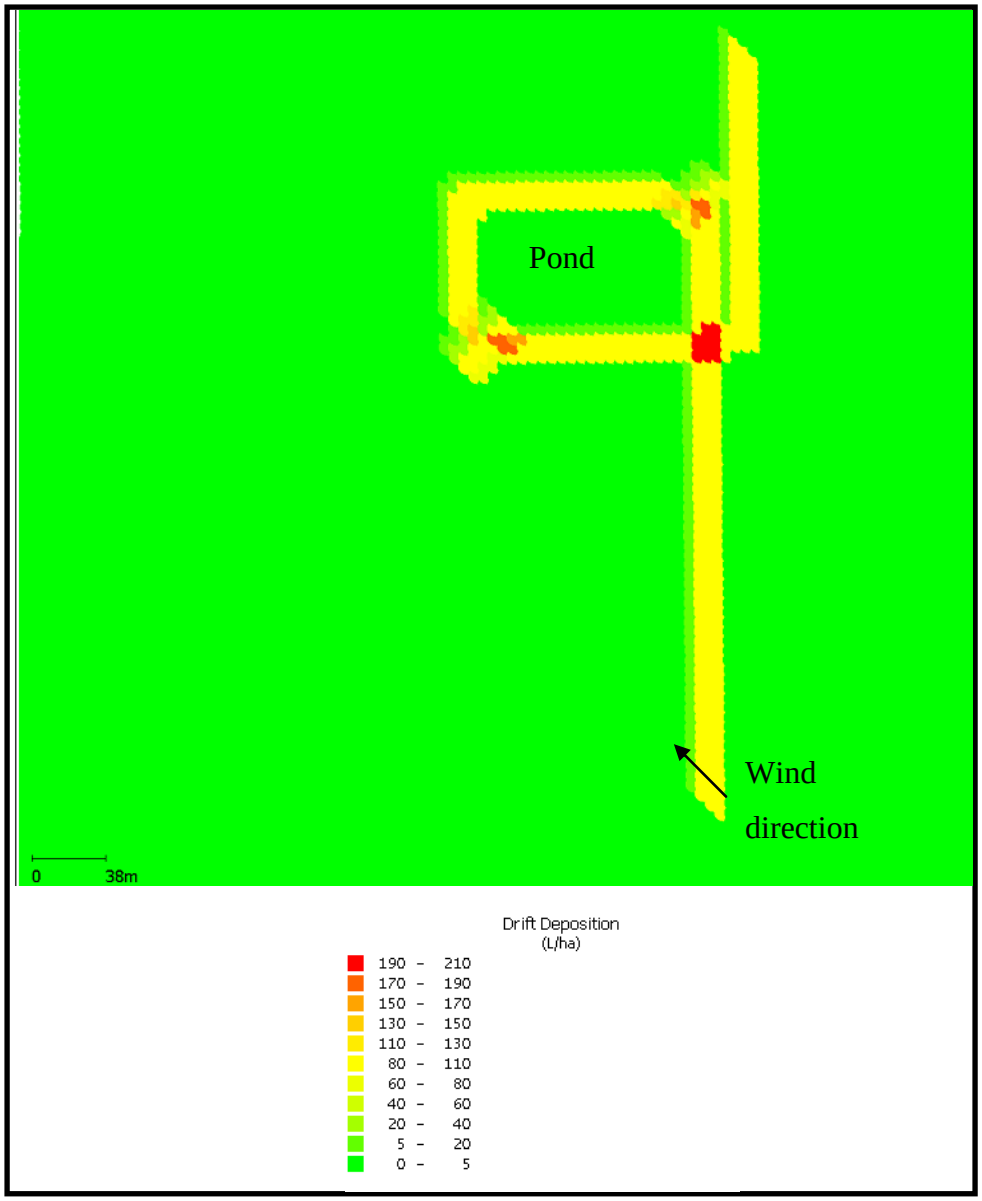

Figure 20. Depositions for simulated spraying around a sensitive area

3.4. Conclusions

The following conclusions were drawn from the review, development, and testing of a drift prediction and mapping algorithm:

- Current drift prediction models were primarily developed for academic uses. In such a form, these models do not possess the timing or spatial capabilities required for real time nozzle control.

- DRIFTSIM, selected as the base drift prediction model for the nozzle controller, is a recognized predictive model with readily available data tables for reference. In addition to the development of a regression equation from the DRIFTSIM data tables, accompanying algorithms to transform prediction of drift distances to depositions and to map drift on a gridded field were required for future nozzle control capabilities.
- Development of discrete field areas and partitioning the nozzle spectrum are inherent processes required in the evaluation approach of drift representation. Each of these processes influences overall drift resolution and predictive accuracy.
- The developed prediction and mapping program displayed successful in-lab performance, evaluated qualitatively through the ability to capture the impacts of highly influential variables on drift deposition.

Chapter 4. Acceptable Drift to Sensitive Areas

Spray drift can never be completely eliminated, however through the implementation of best application principles and the use of drift reduction technologies, applicators can reduce it to acceptable levels. The decision making process of when to change application techniques or even whether to spray or not is rooted in the fundamental question, "Is the potential for drift greater than the acceptable level of drift?". While predicting drift is highly complex, it is only half of the information required to answer this question. Determining levels of acceptable drift are equally complex and important. With the overall goal of developing a basis for acceptable levels of drift for use within a nozzle selection controller, specific objectives are as follows:

- Review current U.S. and foreign methods for protecting sensitive areas from drift.
- Formulate a methodology for handling sensitive area information in the context of the nozzle selection controller.
- Determine levels of acceptable drift based on this methodology.
- Incorporate acceptable levels of drift into the drift prediction and mapping algorithm.

4.1. Current Practices Literature Review

The EPA governs and regulates pesticide drift in the United States. The goal of the EPA is to manage pesticides so that they can provide benefits to agriculture while not producing "unreasonable adverse effects" on the environment (EPA, 2009b). Restrictions and labeling requirements for a certain pesticide are determined though an ecological risk assessment, which involves combining the pesticides exposure risk and toxicity to gauge the pesticides potential negative impact on the environment (Anon, 1983). Information concerning the toxicity level of the pesticide is required by the EPA from the manufacturer for registration. Testing is typically performed by commercial laboratories and involves determining the impact of various levels of the pesticide on non-target organisms. A list of standard use non-target organisms is shown below (Office of Pesticide Programs, 2004):

- Fish
- Birds (e.g. ducks and quail)
- Mammals (e.g. rats)

- Terrestrial plants (e.g. oats, soybeans, and corn)
- Aquatic plants (e.g. algae)
- Freshwater invertebrates

This list of target species can be expanded based on the specific intended use of a pesticide.

For these organisms, endpoint measurements such as the dose at which the active ingredient causes death in 25% of a species of organisms (LD25) value or the maximum dose of the active ingredient which produces no significant negative effects on the sensitive organism (No observable effects limit, NOEL) serve as toxicity endpoints. Endpoints are defined as "explicit expressions of the actual environmental value or its attribute that is to be protected" (Risk Assessment Forum, 1998). Typically either the organism's survival characteristics or reproductive impairment are the functional targets of the endpoints. Within the toxicity study, the most sensitive species for which data can be obtained is considered the critical toxicity level. The EPA maintains a running database, termed ECOTOX, of toxicity levels for reference and use in future registration or re-registration (Office of Pesticide Programs, 2004).

The exposure risk of the pesticide is evaluated based on anticipated frequency of use of the pesticide, potential for transport (both through drift and runoff), and locations of use relative to sensitive areas. In determining potential drift, both field collected data and drift modeling are consulted. The modeling procedure is often simplified by assuming 1% drift for ground applications and 5% for aerial application. From this information estimated environmental concentrations (EEC'S) are calculated.

The risk quotient (RQ) is defined as "the likelihood of adverse ecological effects on non-target species" (Office of Pesticide Programs, 2004) and expressed as

Equation 12. Risk quotient

$$RQ = \frac{EEC}{Toxicity}$$

where

EEC = estimated environmental concentration

Toxicity = the most critical endpoint of non-target organisms

Risk quotients are compared to EPA predefined levels of concern to determine what regulatory actions are required to reduce the risk quotient. Currently, very general labeling language is instituted to reduce drift based on these risk quotients; however with the implementation of the more scientifically based labeling revisions, buffer zones, droplet size restrictions, and wind speed restrictions would all be specified on the label to reduce drift and protect sensitive areas.

The Pest Management and Regulatory Agency (PMRA) is the governing body of spray drift in Canada. Similar to the EPA approach, PMRA tackles the protection of sensitive areas through a risk assessment. Buffer zones are the primary regulatory measure instigated to protect these areas of drift with the size of the buffer zone based on the toxicity of the pesticide and the determined level of exposure (Kuchnicki et al., 2004). PMRA uses both no-observable-effects-concentrations (NOEC) for aquatic organisms and 25% effective concentration levels (EC25, level where a 25 % reduction is seen in properties such as plant weight or emergence) in terrestrial plants to quantify the toxicity of a pesticide through testing similar that that performed for the EPA studies. Buffer zones are only required by PMRA when the sensitive areas are downwind from the point of spraying. Labels of each pesticide contain the buffer zone requirements. A recent buffer zone revision proposal has suggested including a table of factors on the label by which the linear distance of the buffer zone can be reduced if drift reduction practices, such as spraying with larger droplet sizes or using specialty equipment, are incorporated into the spraying process (shown in Figure 21) (Kuchnicki et al., 2004).

Low Boom (<60 cm)				
Wind Speed (km/h)	Spray Quality			
	Fine	Medium	Coarse	V. Coarse
1 to 8	0.8	0.2	0.1	0
9 to 16	1.2	0.6	0.3	0.1
17 to 25	1.6	1	0.6	0.2
High Boom (60-120 cm)				
Wind Speed (km/h)	Spray Quality			
	Fine	Medium	Coarse	V. Coarse
1 to 8	1.6	0.3	0.2	0.1
9 to 16	2.3	1.1	0.6	0.2
17 to 25	3.1	1.9	1.1	0.4
Low Boom, drift-reducing cones				
Wind Speed (km/h)	Spray Quality			
	Fine	Medium	Coarse	V. Coarse
1 to 8	0.6	0.1	0.1	0
9 to 16	0.8	0.4	0.2	0.1
17 to 25	1.1	0.7	0.4	0.2
Low Boom, drift reducing shrouds				
Wind Speed (km/h)	Spray Quality			
	Fine	Medium	Coarse	V. Coarse
1 to 8	0.2	0.1	0	0
9 to 16	0.4	0.2	0.1	0
17 to 25	0.5	0.3	0.2	0.1

Figure 21. Example buffer zone distance multipliers for the implementation of drift reduction methods (Kuchnicki, 2004)

In the United Kingdom, the local environmental risk assessment for pesticides (LERAP) procedure is used for protecting sensitive areas, specifically aquatic areas, from drift. A standard buffer zone width of 5 m is required for all product applications. LERAP allows for a reduction in the zone based on the pesticide application rate, the size of the waterway, and the drift reduction potential of the sprayer (which is rated as 1, 2, or 3 stars) (DEFRA, 2001). Any instance which requires a buffer zone, i.e., whenever spraying in close proximity to an aquatic area, must be documented along with any reductions made in the

buffer zone width. This document is subject to inspection by local authorities and must be maintained by the applicator.

Of all current sensitive area protection methods, Germany's is the most extensive. The German Regulatory Authority sets buffer zone widths based on toxicity information for each pesticide. A points system is then calculated by the applicator to determine reductions to this width. The points system takes into account if a waterway is flowing, the size of the waterway, drift reduction properties of the sprayer, and the presence of riparian vegetation between the sprayer and the waterway (Rautmann, 2003).

4.2. Summary of Current Methods to Define Sensitive Areas

Regulatory agencies in the US, Canada, and Europe rely on risk assessments to determine required measures to protect sensitive areas. Risk assessments consider both the toxicity of the pesticide and its potential to cause harm in assessing its overall impact on the environment. Toxicity data typically pertains to the endpoints of concentration in the environment which cause very little noticeable damage, such as the NOEL or EC25 levels. Buffer zones are the consensus first approach to reducing the impact of the pesticide on the environment. Most countries offer buffer zone reduction if drift reduction technologies are implemented.

4.3. Acceptable Drift to Sensitive Areas within the Nozzle Controller

A real-time nozzle selection controller functions as a regulatory instrument. In this role, the decision making processes should have the same scientific basis as a risk assessment. The first component of that assessment, the potential to cause damage, is handled by the drift prediction and mapping algorithm previously described. The second component, the pesticide toxicity information, is a more static variable yet is just as crucial to the controller decision making processes.

The toxicity endpoints used within EPA's risk assessment analysis represent levels of deposition in sensitive areas which the EPA deems "acceptable" in a regulatory sense, as they do not cause significant observable effects in the environment. To maintain regulatory stability as well as to instill authority in acceptable levels of drift, these levels were selected to serve as the basis for levels of acceptable drift within the drift controller. While these

levels are publically available, they do not exist in a format which can be readily used by the nozzle selection controller. EPA's risk assessments are on a pesticide by pesticide basis, as pesticides vary in toxicity. In the United States alone there are over 1,055 registered pesticide active ingredients, and more than 16,000 different pesticide products (Center for Disease Control, 2010). Additionally the toxicity studies for each pesticide exist for many different "sensitive areas". The size of the dataset required to house this information as well as the accompanying "lookup" algorithms would detract from the overall goal of the nozzle selection controller. It is anticipated that in future development of a nozzle selection controller, a more inclusive, in-depth approach to acceptable levels of drift would be explored. The following approach to levels of acceptable drift is thus a first approach, proof-of-concept method.

With the limited ability of the nozzle selection controller to account for all possible pesticides, the scope of toxicity analysis, as it pertains to the controller, was reduced to more common instances. In the Midwest United States, the most common pesticides are those applied in the production of corn and soybeans. A summary of the most commonly used herbicides, insecticides, and fungicides in corn and soybeans are shown in Table 6 (USDA, 2006).

Table 6. Most commonly used pesticides in corn and soybean production in 2005 (USDA, 2006)

	Herbicide	Acres [% of crop total]	Insecticide	Acres [% of crop total]	Fungicide	Acres [% of crop total]
Corn	Atrazine	66	Cyfluthrin	7	NA	<1%
Soybeans	Glyphosate	88	L. Cyhalothrin	6	Azoxystrobin	1%

Herbicides, specifically atrazine and glyphosate, are the predominate pesticides sprayed on both corn and soybeans. A survey by the Association of American Pesticide Control Officials (AAPCO, 1999) showed that gyphososate, atrazine, and 2, 4-D alone were responsible for over 35% of all drift complaints reported in 1998. Insecticides and fungicides have neither a pre-dominant active ingredient sprayed nor are they used as extensively as herbicides, however they are generally thought to be more toxic to aquatic species and thus cannot be entirely ignored within the scope of the nozzle controller.

In addition to the active ingredients within a pesticide, the non-target organism characteristics also have an impact on the toxicity of a pesticide and thus acceptable drift endpoints. In reality, any organism other than the targeted pest can be considered a sensitive or non-target organism. As with pesticide types, it was concluded that the scope of the controller should account for the more common, in terms of violations, sensitive area types. The AAPCO survey concerning drift complaints queried which areas were the subject of most drift complaints. Results of this study are shown in Figure 22.

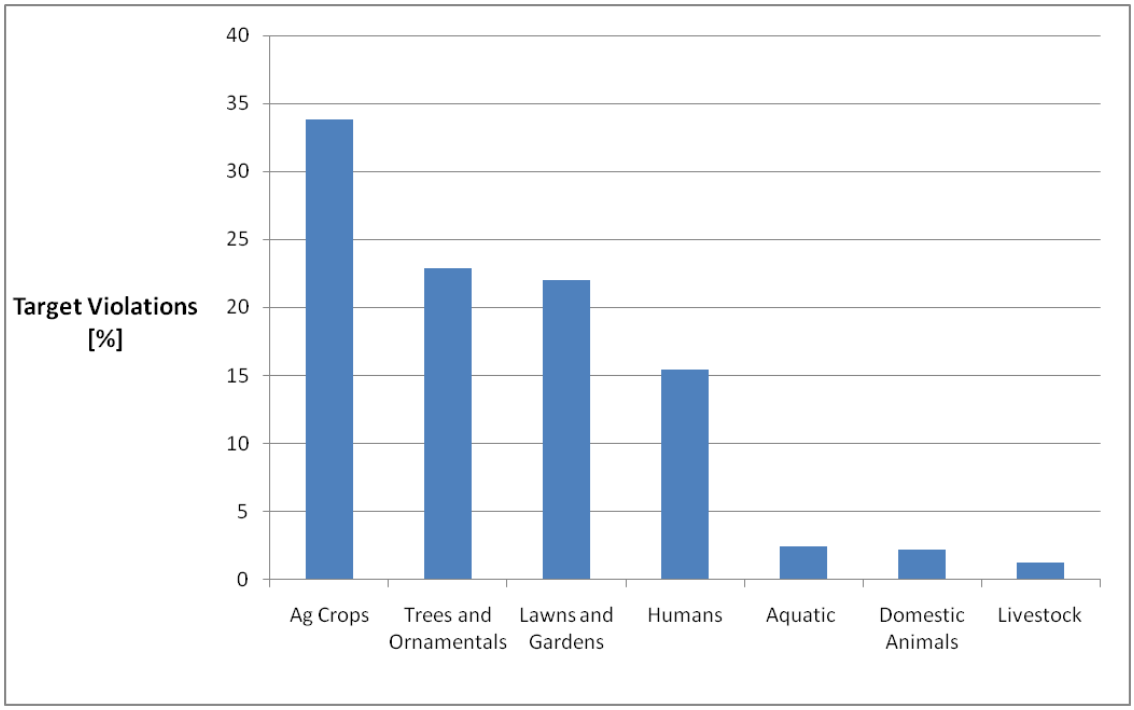

Figure 22. AAPCO reported drift complaint distribution

Agriculture crops are the target of the majority of complaints due to their typical close proximity to sprayed areas as well as increased concern of economic impacts. Surprisingly, aquatic areas have a very low percentage of complaints possibly due to difficulty in determining the source of contamination.

EPA ECOTOX database was consulted to evaluate toxicity endpoints of the common pesticide/sensitive area pairings. Both NOEL and EC25 levels were recorded when available. ECOTOX contains thousands of pesticide categories and is an excellent source for toxicity information however it is not an all inclusive database. Additional sources were also

consulted to try to obtain a more complete database of toxicity endpoints of pesticide/sensitive area pairings.

Parallel to its use within risk assessments, toxicity endpoints provide levels of drift deposition which are acceptable in sensitive areas. The nozzle decision making process is then a comparison of the predicted drift to the acceptable drift and a modification of the nozzle selection to maintain an acceptable amount of drift. This method of operation requires the acceptable level of deposition to either be a constant, hard-coded value or for the applicator to enter acceptable levels of deposition in some form. In the development of the drift controller, it was determined the most flexible, user-friendly method of handling sensitive area information is an operator entered, sensitivity category approach. High, medium, and low sensitivity levels were derived from the dataset and pertain to the action of the pesticide within a sensitive area, combining the characteristics of both the pesticide active ingredients and sensitive area. Pesticide-sensitive area combinations were separated into high, medium, and low sensitivity groups based on their similar toxicity endpoints as follows:

High Sensitivity	**Medium Sensitivity**	**Low Sensitivity**
Herbicide/ Human	Herbicide/Livestock	Insecticide /Adjacent crops
Herbicide/Aquatic	Insecticide /Livestock	Insecticide /Pasture and hay grasses
Herbicide/Adjacent crops	Herbicide/Pasture and hay grasses	Insecticide /Conservation areas
Insecticide/Aquatic	Herbicide/Conservation areas	Fungicide /Pasture and hay grasses
Insecticide / Human	Fungicide /Livestock	Fungicide /Conservation areas
Fungicide/Aquatic		Fungicide /Adjacent crops
Herbicide/Organic crops		
Herbicide/Bees		
Insecticide/Organic crops		
Insecticide/Bees		
Fungicide / Human		
Fungicide /Organic crops		
Fungicide /Bees		

For nozzle selection, the controller requires definitive levels of acceptable deposition corresponding to the high, medium, and low sensitivity categories. Levels for these respective categories were derived generally from the most sensitive or lowest deposition levels within each group and were 0.29 $\frac{mg}{m^2}$, 29 $\frac{mg}{m^2}$ and 72.5 $\frac{mg}{m^2}$ of active ingredient for the high, medium, and low categories respectively. In terms of concentration levels, which are a more conventional representation of toxicity endpoints, a conversion factor assuming a 0.3 m deep water body can be multiplied through resulting in mass concentrations of 1 ppb, 100 ppb, and 250 ppb respectively. A third form of acceptable deposition specifically applicable to the pesticide regulatory sector is representation of concentration derived from swabbing a small area (10 cm^2) and diluting the resulting mass within 100 ml of water. Corresponding thresholds to the high, medium, and low sensitivity categories in this form are 2.9 ppb, 290 ppb, and 725 ppb respectively.

The location and sensitivity category are required by the nozzle controller for decision making and ultimately protection of a sensitive area. Pesticide concentration is

needed to determine the actual volumetric deposition ($\frac{L}{ha}$) which corresponds to an acceptable level of deposition of the active ingredient ($\frac{mg}{m^2}$). A user interface was developed to run in conjunction with the drift prediction and mapping algorithm, allowing for inputs of the sensitivity classification (through three "radio" buttons) and four corners of a quadrilateral enclosing the sensitive area. Corners are defined in terms of latitude and longitudes as shown in Figure 23.

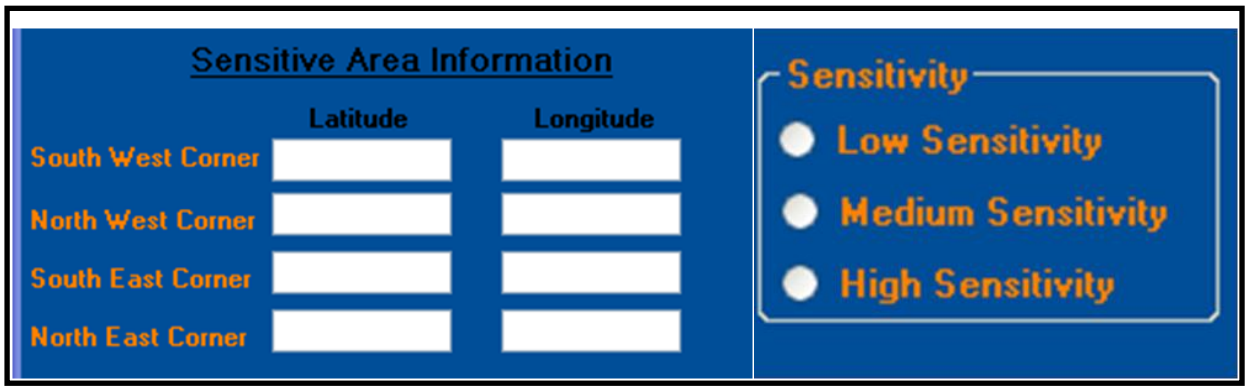

Figure 23. Definition of sensitive areas (location and sensitivity) through user interface

A second mapping algorithm, in addition to the predicted deposition mapping scheme, generates an acceptable deposition grid. Grid cells within the acceptable deposition grid are assigned identical spatial coordinates to corresponding grid cells within the predicted deposition grid, producing two grids representing the same field. Acceptable deposition levels are written to all grid cells recognized as being contained within a respective sensitive area. Multiple sensitive areas can be entered through the user interface. With the mapped acceptable deposition levels, the controller contains a magnitude and position of areas to protect from excessive amounts of drift.

Chapter 5. Nozzle Selection Basis

Droplet size is the most influential variable effecting drift; therefore it is the subject of action in reducing drift within the context of the nozzle selection controller. Implementing larger droplet sizes however, has consequences. It often believed that increasing droplet size reduces efficacy, thus the motivation to spray a smaller droplet size.

The overall goal of the nozzle selection controller is to protect sensitive area from drift. When drift is of a concern, based on weather conditions and the location of the sprayer in the field, the controller selects the nozzle which reduces predicted levels of drift to less than the acceptable levels of deposition in sensitive areas. In instances where potential for drift damage is reduced, spraying large droplets could needlessly reduce efficacy. In order to incorporate efficacy conservation into the drift controller the following objectives were pursued:

- Determine the impact of droplet size on efficacy, summarized by a droplet size range for maximum efficacy, through a literature review
- Generate a control algorithm within the nozzle controller to optimize efficacy while maintaining acceptable levels of drift.

5.1. Literature Review

Increasing use of drift reduction nozzles has led to increased research concerning the impacts of droplet size on efficacy. It is generally believed that the influence of droplet size is specific to pesticide type and mode of action (contact or systemic). Contact pesticides destroy pests based on modes of action occurring, as the names suggest, at the contact point. Systemic pesticides translocate from the point of contact to other parts of the pest, or host organism, where they cause inhibitory effects. Pesticide classes were divided into contact herbicides, systemic herbicides, insecticides, and fungicides to determine the relationship between droplet size and efficacy within each class.

McKinlay et al. (1974) studied the impact of droplet size on the toxicity of a contact herbicide, paraquat, within sunflowers. Droplet sizes were varied from 100μm to 350μm and the effects observed on individual sunflower plants. Toxicity, as measured by the amount of visible leaf damage, decreased as the droplet size increased. Contrary to these findings,

Douglas (1968) found that both paraquat and diquat had increased activity as the droplet size was increased from 250 μm to 450 μm however further increasing the droplet size to 1000μm decreased activity. Douglas defined activity as the area of necrosis per gram of active ingredient applied. Prokop and Veverka (2003) and Shaw et al. (2000) did not find droplet size to have a significant impact on efficacy for bentazon and acifluorfen respectively. In both cases droplet size ranges subjected to testing were from about 200 μm to 450 μm.

McKinlay et al. (1972) determined that a common systemic herbicide, 2, 4-D, was much more efficacious in the form of small droplets (100 μm) when compared to large droplets (400 μm) as evidenced by the seedling quantity and stem curvature of sunflowers. Medium size droplets (200 μm) required three times the pesticide concentration while large droplets (400 μm) took six times the concentration of small droplets to produce the same negative effects on the sunflower. Wolf et al. (1992) specifically analyzed the impacts of droplet size on adsorption and translocation of 2, 4-D in oriental mustard. Increasing the droplet size from 198 μm to 2760 μm did not impact adsorption however translocation decreased as the droplet size increased. Overall effects on the plant itself were not recorded. Feng et al. (2003) also found retention of glyphosate to decrease with increasing droplet size; however, adsorption increased leading to an overall greater translocation of the active ingredient to the roots of corn. Prasad and Beresford (1992) observed the same efficacy for glyphosate, hexazinone, and triclopyl as droplets sizes were increased from 155 μm to 435 μm; however, further increasing droplet size significantly reduced efficacy as measured by the change in weight of plants after spraying. Jones et al. (2002) performed in-field spaying with three droplet spectrums during glyphosate application ranging from 99 μm to 582 μm and saw no significant change in efficacy. Wolf (2000) tested the impact of drift reduction nozzles on efficacy and found that only 16% of the 19 herbicides applied to 27 different weeds (513 total cases) displayed significant relationship between droplet size (nozzle selection) and efficacy. The significant cases were all for herbicides within the same subclass, which is seldom used in the Midwest.

Very little research has been done on the relationship between droplet size and the efficacy of insecticides. Sumner et al. (2007) found through in-field testing that the control of stinkbugs in cotton is significantly better for drift reduction nozzles when compared to hollow cone nozzles due to their larger produced droplet sizes. Sumner suggest that the smaller droplets, while having better coverage ability (Smith et al., 2000), do not possess enough energy to sufficiently penetrate the dense canopy of the cotton to provide efficacy to the lower leaves of the plants.

Sumner's claims are further supported by testing aimed at determining the impacts of droplet sizes on fungicide efficacy. Ozkan et al. (2006) found medium droplet sizes resulted in greater coverage in the lower and middle portions of dense canopies of soybeans when compared to fine and coarse droplets. Bretthauer et al. (2008) similarly observed greater control of soybean rust with very course droplet sizes. Hanna et al. (2006), Prokop and Veverka (2006), and Derksen et al. (2001) did not find droplet size to be a significant factor influencing efficacy of fungicides.

5.2. Conclusions

The optimum droplet size for contact herbicide efficacy balances the need for droplets small enough to provide coverage of the target yet large enough to prevent complete evaporation prior to adsorption of the active ingredient into the plant. Review of literature suggests a range of droplet sizes from 150-350 μm where efficacy is maintained however there are certainly exceptions to this range (specifically for paraquat and diquat).

While several cases exist where small smaller droplets (down to 100 μm) produce greater efficacy (McKinlay et al., 1972) and greater translocation (Wolf et al., 1992), the majority of researchers agree that systemic herbicide efficacy is independent of droplet size until a threshold level is reached. This threshold level is determined by the plant-chemical combination. Systemic herbicides rely on the retention, adsorption, and translocation processes to function. Adsorption increases as the droplet size increases due to an increased amount of active ingredient per unit area of the leaf (thus a greater transfer gradient). Translocation decreases when cell lysis occurs at a threshold value of pesticide concentration, and thus a threshold droplet size. This lysis causes the active ingredient to be barred from other cells. The minimum droplet size producing lysis for common application

conditions (glyphosate to weeds), is around 400 μm, as determined by Prasad and Beresford (1992) and Feng et al. (2003). Numerous other studies have found that the adsorption increase and translocation decrease balance each other out in terms of efficacy impact, resulting in no significant effect on efficacy for a wide range of droplet sizes (Wolf, 2000; Jones et al., 2002; Wolf et al., 1992). A suggested droplet size from these findings for acceptable efficacy is 100 μm-400μm.

Limited insecticide relation to efficacy studies agree that a medium size droplet (200 μm-350 μm) maintains acceptable efficacy for contact applications where deposition into the lower canopy is important (as for fungicides). Insecticide function relies on coverage of the plant for protection against pests. While coverage is higher in the upper canopy for smaller droplet sizes, penetration into the lower portions of the canopy is minimal (Bretthauer et al., 2008; Ozkan et al., 2006). A balance between small droplets for increased coverage and large droplets for increased penetration is achieved at the medium droplet size.

Research concludes that contact fungicide efficacy, similar to insecticide efficacy, is optimized when medium droplets (200 μm-350 μm) are applied (Bretthauer et al., 2008; Ozkan et al., 2006). These droplets have the ideal size to produce coverage in all sections of the canopy.

Figure 24 summarizes the resulting ranges of droplets sizes derived from the literature review where maximum efficacy is achieved and maintained for systemic herbicides, contact herbicides, insecticides, and fungicides.

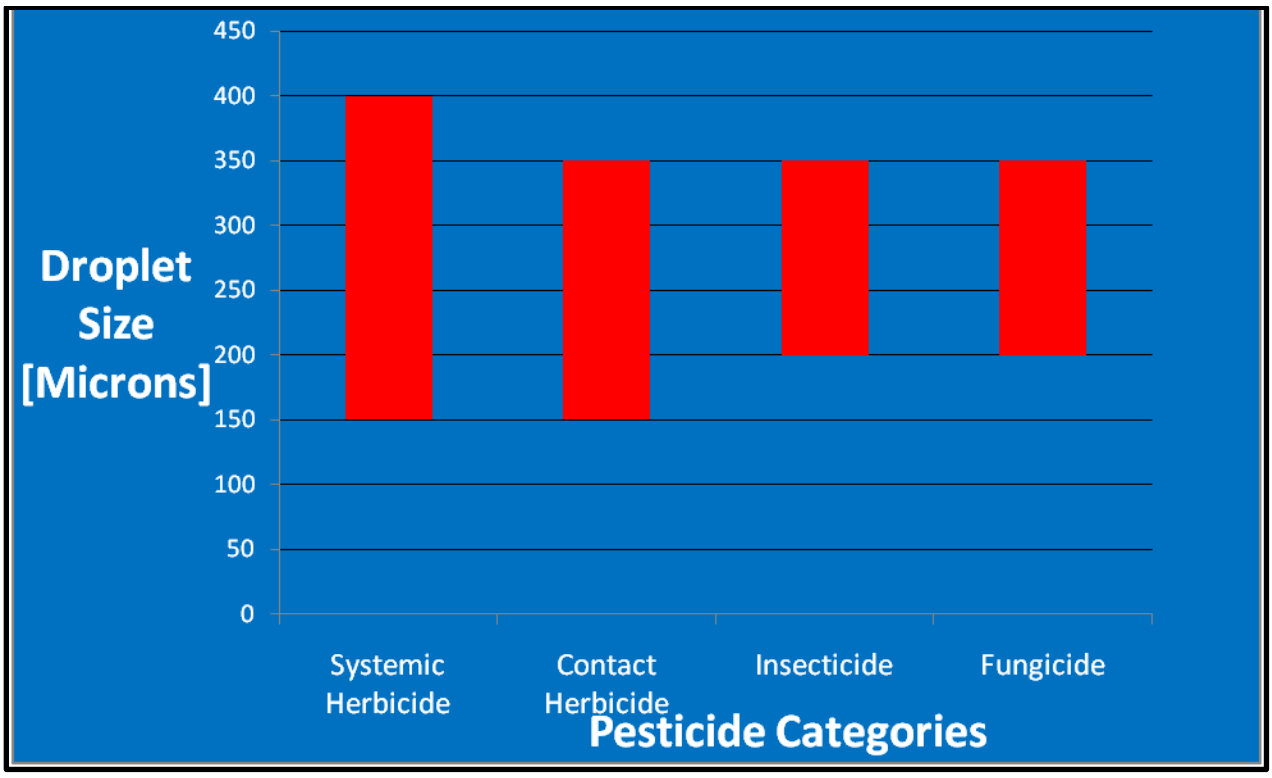

Figure 24. Ranges in droplet sizes where efficacy is maintained for four pesticide classes derived through a literature review

5.3. Incorporation of Efficacy Information into Controller

Protecting sensitive areas from drift is the primary objective of the nozzle controller. Maximizing efficacy is a secondary motivation in nozzle selection. The preceding literature review revealed that optimizing efficacy is at a minimum pesticide class specific (herbicide, insecticide, fungicide),; however true optimization is dependent on the specific active ingredient being applied. As is the case with acceptable drift to sensitive areas, it is outside the scope of a prototype controller to include optimal nozzles for the over 16,000 US registered pesticides. To provide maximum flexibility and reduce the overall complexity of the controller, a series of radio buttons was added to the user interface to allow applicator input of a default nozzle which is assumed by the controller to produce maximum efficacy. A flowchart of the nozzle selection process based on predicted deposition, acceptable deposition, and optimal efficacy nozzle (default nozzle) is shown in Figure 25, highlighting the primary importance of protecting sensitive areas.

Four states of the nozzles are shown in Figure 25: fine, medium, coarse, or all nozzles off. As is indicated by the “looping” structure of the decision making process, nozzles are updated after each drift prediction. The approach assumes a linear decreasing efficacy with increasing droplet size.

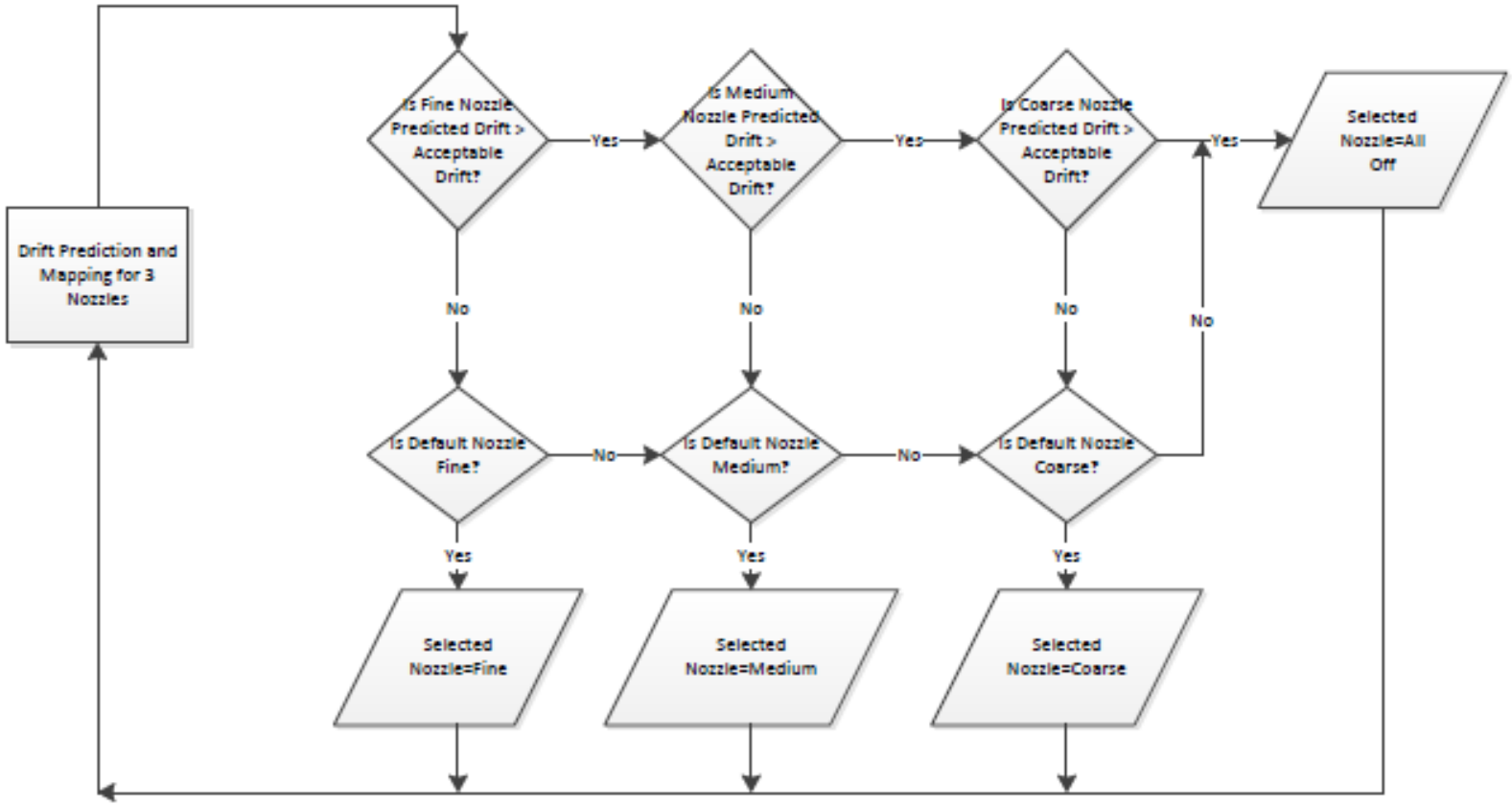

Figure 25. Flowchart of nozzle selection process based on maximizing efficacy while maintaining acceptable drift deposition

Chapter 6. Drift Controller Implementation

In-field nozzle selection control revolves around the central question, “Is the predicted drift greater than the acceptable level of deposition in an identified sensitive area?”. The drift model and mapping algorithm is the foundation for drift prediction, while the categorized toxicity endpoints derived from EPA and independent studies comprise the levels of acceptable deposition. With a scientific basis for these two components in place and a tier 1 simulator program established, the stage is set for the development of a real-time nozzle selection controller. Specific tasks in the controller development are as follows:

- Establish controller input/output requirements
- Integrate sensitive area protection into prediction and mapping algorithm
- Generate an interface for user inputs and displaying of outputs
- Select and implement required sensors

6.1. Input/Output Requirements

Inputs to the nozzle selection controller are composed of all pieces of information necessary for the nozzle selection process. Nozzle selection is made up of four functions: drift prediction, drift mapping, toxicity evaluation, and efficacy optimization. Drift prediction inputs are composed of all variables within the prediction equation: temperature, humidity, wind speed, boom height, initial droplet velocity, and droplet size. Deriving deposition levels from the drift distances relies on the flow rate, boom width, nozzle spacing, vehicle speed, grid width, and grid length. Mapping of the drift is dependent on wind direction, and sprayer position in the field. Toxicity evaluation requires acceptable deposition levels and a location of the sensitive area. The simplified approach of efficacy optimization described in the nozzle selection process is reliant on only a single additional input, the default or highest efficacy nozzle.

The output from the controller is a physical changing of nozzles on the sprayer. The target vehicle for implementation (SpraCoupe® model 7650, AGCO, Duluth, GA) was pre-outfitted with three nozzle types, fine, coarse, and very coarse nozzles (Figure 26). While a fine, medium, coarse configuration would have provided a more linear drift reduction scheme

with changing nozzles, the expense necessary to refit the 42 nozzle groups on the boom made this option unviable. The prior method of nozzle selection on the targeted vehicle was through a three-way switch in the cab which actuated individual electrical solenoid valves via a relay corresponding to each nozzle type. For compatibility with the existing system, electric solenoids were maintained as the method for nozzle selection. Mirroring the manual nozzle selection process, the required controller output is an electronic actuation signal to the appropriate nozzle selection relay. Two secondary outputs, based on the project objectives, are the test files of both the predicted deposition levels and the conditions (weather and sprayer application) measured during application.

Figure 26. Very coarse, coarse, and fine nozzle bodies with activating solenoids on test machine

6.2. Controller Components

6.2.1. Program

The drift prediction and mapping portion of the nozzle selection controller is the heart of the control process. As previously described, nozzle selection is based on the fundamental question, "Is the predicted drift deposition greater than the acceptable levels of deposition to a sensitive area?". The predicted deposition grid and the acceptable deposition grid provide a definitive, scientific basis by which to answer this question.

Tier 1 program prediction and mapping is performed on a continuous basis. Each prediction iteration represents a unique calculation of nozzle/boom deposition at a discrete point in space and time and thus a unique nozzle control sequence. The area-of-interest in the control sequence includes all grid cells for which predicted deposition levels are updated. Sprayer position, wind direction, and drift distances predicted by the program dictate the grid cells which are updated and thus the area-of-interest within the control iteration. In addition to grid cells updated based on the sprayers look-ahead distance, the "fill-in" region is also a subset of the area-of-interest (as shown in Figure 27). A sequence was added to the tier 1 program to evaluate "Is the predicted drift deposition greater than the acceptable deposition?",,for each grid cell within the iteration's area-of-interest.

Drift is predicted for all nozzles on-board the sprayer. Based on the target test vehicle, fine, coarse, and very coarse predictions are made and compared to acceptable depositions for each iteration. If the predicted deposition within any the grid cells in the area-of-interest is greater than the acceptable deposition in the corresponding sensitive area grid cell, a nozzle specific flag is raised signaling that if the corresponding nozzle is selected for application, in theory the sensitive area will be contaminated.

The logic shown in Figure 25 was added to the program to perform nozzle selection. Flag values are the basis for answering each of the questions within the flowchart and ultimately nozzle selection. Upon determining the correct nozzle for application, the program relays a nozzle selection message to a controller board (described in section 6.2.5). Through the implementation of the look-ahead distance, the control board is able to make changes to nozzle selection prior to application within the area of interest.

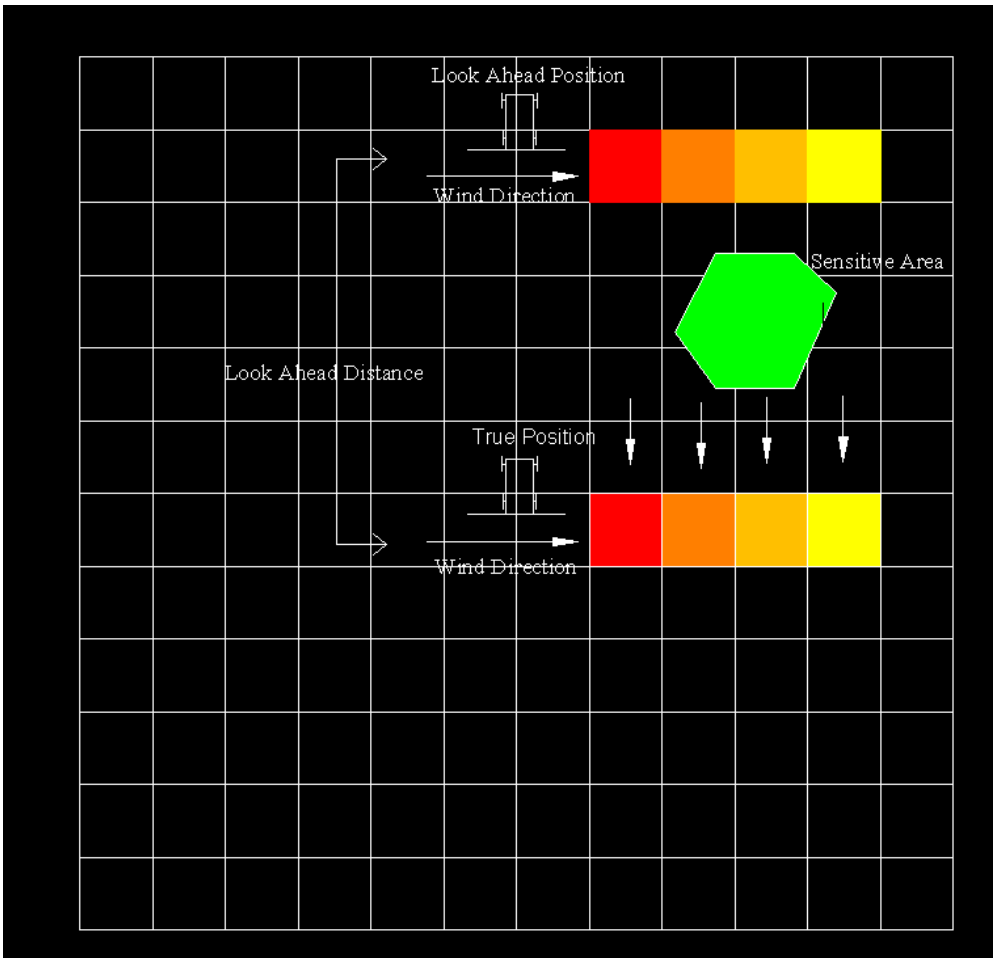

Figure 27. Area-of-interest between true sprayer position and look-ahead position with an encountered sensitive area

The nozzle selection controller was programmed in C++. To optimize computing time a total of three threads were implemented. The first thread handles the drift prediction and mapping algorithm. Thread number two maintains a user interface described in Section 6.2.4. The third thread maintains an updated text file with as-applied operating conditions. The program was installed on a 1.69 GHz computer for implementation. On this operating platform, the update rate was slightly faster than 0.5 Hz, falling short of the desired 2 Hz goal. Simulation in the lab on a higher performance computer (2.83 GHz) resulted in an update rate of 1.8 Hz. With the high dependency of update rate on operating systems and the rapid development of field computers, this shortcoming was seen as temporary. The program itself was formatted as a header file, with the anticipation of its incorporation into additional

programs, and is 414 Kb in size. Predicted deposition text files maintained by the program are 31 Mb in size and are stored within the electronic folder housing the programs executable file.

6.2.2. Sensors

To reduce operator interaction, it was desirable to automate inputs to the nozzle selection controller when feasible. Specific targets of automated or system inputs are all variables which rapidly change in the field during spraying. Weather and application variables are the two general classes of variables which are both rapidly changing and are also highly influential to the nozzle selection process. As with most processor based control systems, the most direct approach to automating inputs is through the use of electronic sensors.

Weather variables include the temperature, humidity, wind speed, and wind direction. The first three of these variables are independent variables in the drift prediction equation, while the wind direction is applied in the mapping algorithm to place deposition within the field. Multiple sensors are readily available to measure weather conditions, including integrated systems which act as complete weather stations. A Maretron® (Phoenix, AZ) WSO100 weather station (Figure 28) was selected to sense weather conditions and interface with the nozzle selection controller.

Figure 28. Maretron weather station (Maretron Inc.) providing measure of temperature, humidity, wind speed, and wind direction

The WSO100 is specifically intended for use in marine environments such as on ships or sail boats, however as it is designed to be mounted on a moving vehicles, its uses are

readily extended to agricultural purposes. The weather station contains sensors to measure wind speed, wind direction, relative humidity, temperature, and barometric pressure within a waterproof enclosure. Wind speed and direction are measured through the use of ultrasonic sensors, providing accurate wind parameters at fast update rates when compared to the more traditional anemometer weather stations. Table 7 displays the resolutions and ranges of measure for each of the weather station sensors.

Table 7. Weather station sensor accuracies, ranges, and resolutions

	Accuracy	Range	Output Resolution
Wind Speed	± 2%	0-51 m/sec	0.01 m/sec
Wind Direction	± 3°	0-360°	0.0001 rad
Temperature	± 1°C	–25 - 50°C	0.01°C
Humidity	± 5%	0-100%	0.004%

An internal processor on the WSO100 performs the measurement and communication of sensor readings. The measurement rate of each sensor is programmable. Default update rates of the temperature and humidity sensors are 2 Hz while the update rate of the more variable wind speed and wind direction measurements is 10 Hz. Due to the variable nature of the wind measurements, the WSO100 internally dampens the changes in speed and direction using a programmable dampening period.

The WSO100 is set up for Controller Area Network (CAN) bus interfacing. As its intended use is in the marine sector, the NMEA 2000 standard protocol is the basis of operation. The NMEA 2000 protocol is build on top of the J1939 automotive industry standard with slight modifications to message identifiers and cabling requirements. Two different messages are sent from the WSO100 containing the wind data and the atmosphere data at each respective update rate. A definition and layout of the two messages are shown in Table 8.

Table 8. Weather station CAN message definition and layout

PGN	Description	Data Bytes							
		0	**1**	**2**	**3**	**4**	**5**	**6**	**7**
130306	Wind Data	Field Id.	Wind speed low	Wind speed high	Wind direction low	Wind direction high	Wind ref.	Not used	Not used
130311	Environment Data	Field id.	Temp. ref.	Temp low	Temp high	Humidity low	Humidity high	Pressure	Pressure

Wind speed and wind direction measurements were taken over a 2 minute time interval in the field when wind was “light and variable” to determine if the default dampening of the wind measurements required adjustment. A Vector (Stuttgart, Germany) CANcaseXL data logger was used to collect both wind speed and wind direction data and write the collected data to a text file. The position of the weather station was held stationary through the duration as to not induce artificial directions and velocity. Plots of wind speed and wind direction are shown in Figure 29 and Figure 30, respectively.

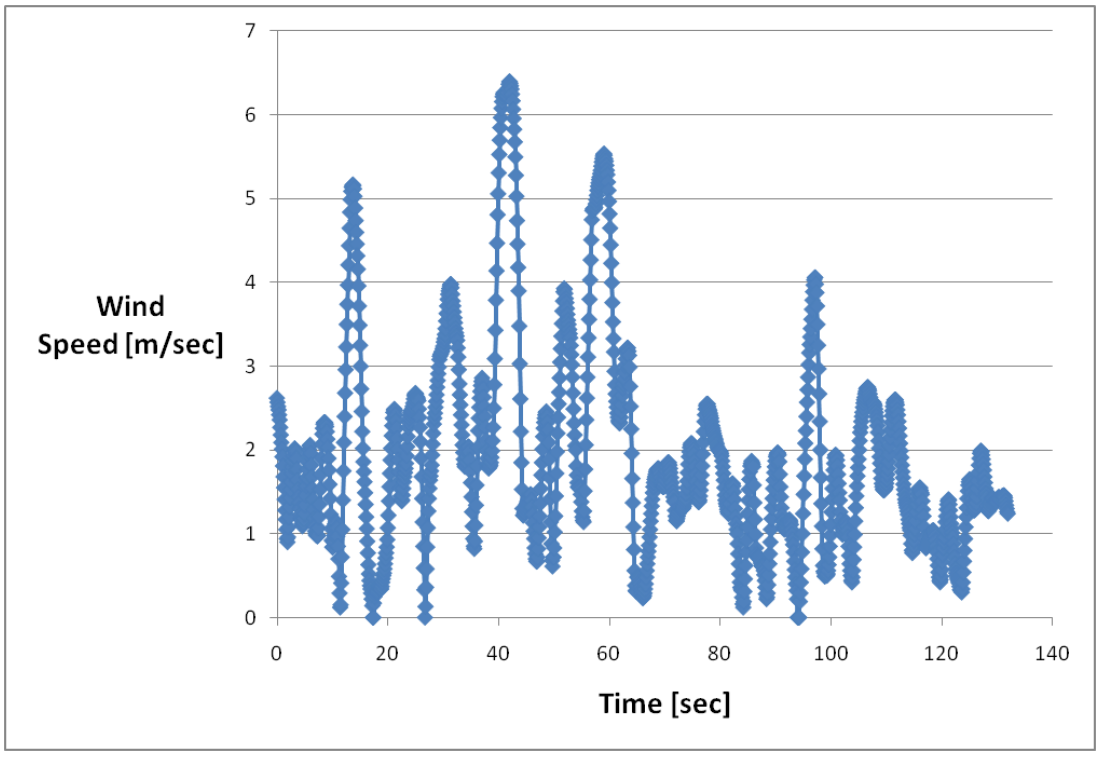

Figure 29. Wind speeds (measured from a stationary position) over two minute duration

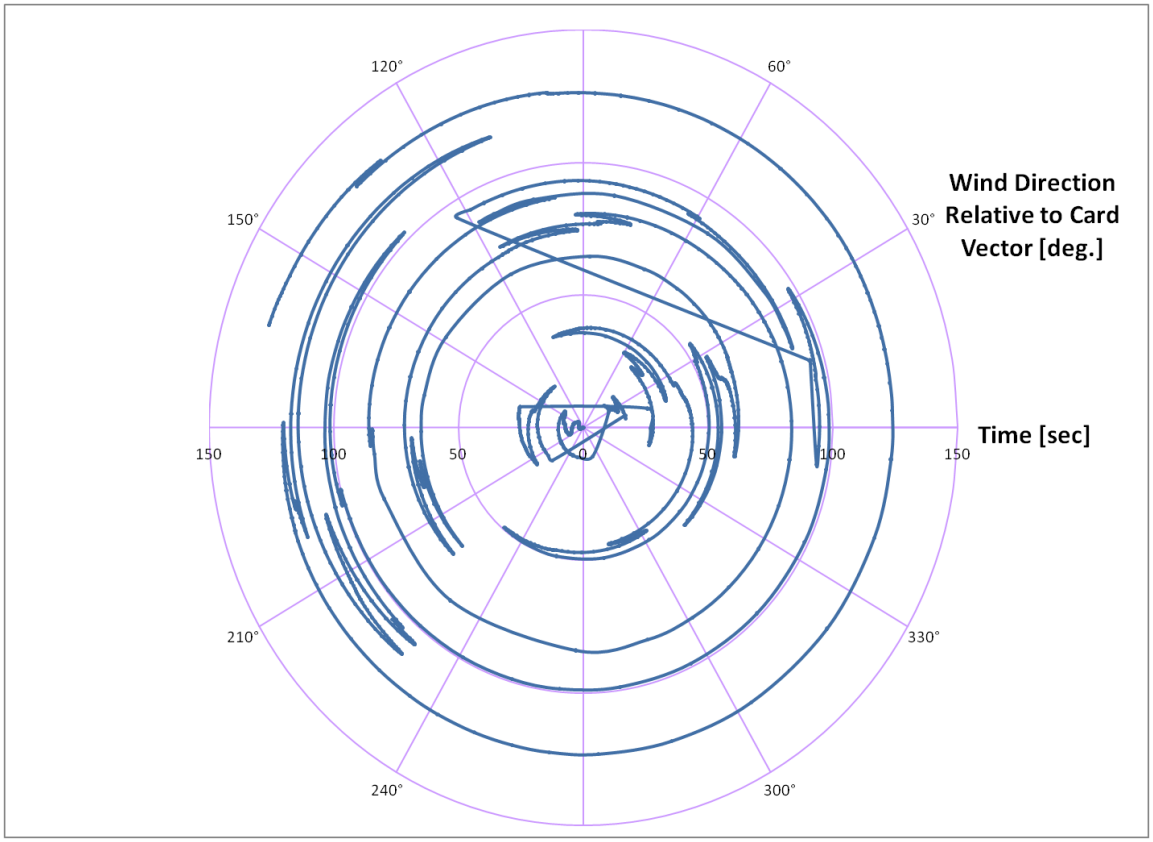

Figure 30. Wind direction (measured from a stationary position) over two minute duration

Wind speed fluctuations throughout the time duration of measurement are gradual and supported by several data points of measurements. This behavior suggests that the dampening of the wind speeds sufficiently reduces both noise and un-sustained wind gusts. The wind direction plot displays wind position in cylindrical coordinates with the time duration as the radial magnitude. The constant increase in radial magnitude represents the passing of time. Points are connected in measurement sequence therefore perceived breaking of the circular patter represents large wind direction fluctuations. Overall, as with wind speeds, the wind direction maintains continuous increases and decreases therefore it was concluded that the default dampening resulted in a sufficient representation of wind speed and wind direction for use within the nozzle selection controller.

Mounting the weather station onboard a vehicle results in wind measurements which are relative to the vehicle. Wind speed in the context of the drift prediction equation derived from DRIFTSIM, is absolute (or relative to a stationary point within the field), as DRIFTSIM

assumes droplets are released from stationary nozzles. While the vehicle speed will induce an additional initial droplet speed vector, the droplet's trajectory is dominated by terminal velocities which in the horizontal plane are equal to the absolute wind speed with a heading equal to the absolute wind direction. An algorithm was added to the controller to return absolute wind speed and direction from relative wind speed, direction, vehicle speed, and vehicle travel direction (derived from successive GPS coordinates).

Like the weather variables, boom height is an application variable which is used in the drift prediction equation. Recently developed boom self-leveling systems, such as the Norac® (Fridley, MN) AutoBoom system, use ultrasonic sensors to determine boom height above either the crop or the ground based on desired performance. With the perceived eventual incorporation of a self-leveling system into the nozzle selection controller, a stand-alone ultrasonic sensor (model PING))), Parallax, Rocklin, CA) was selected to measure boom height. The sensor package includes both an ultrasonic transmitter and receiver in a single package. A 40 KHz sonar pulse is emitted by the ultrasonic transmitter, travels until it reaches an obstruction, reflects off the obstruction, and is ultimately received back by the ultrasonic receiver. The PING))) sensor is designed to easily interface with microcontrollers, and accurately measures proximities up to 3 m. A single input/output pin receives a 5 volt input pulse from the microcontroller, emits a sonar pulse when the pin goes from high to low, then holds the pin high until the emitted pulse is received back by the senor. The travel distance of the pulse can be calculated based on the speed of sound and the time duration for which the pin is held high.

Figure 31. Ping))) ultrasonic sensor (Parallax Inc.) instrumented to measure boom height

The accuracy of the ultrasonic sensor is predominately attributed to the reflective ability of the target-distance measurement objective, and the speed of sound assumption. In

the context of drift prediction, the target measurement is the distance between the nozzle and the plane on which the droplet ultimately deposits. When spraying in a vegetated area, the deposition plane is highly variable as droplets can deposit within the vegetation or on the ground. When considering the ground as the plane of deposition, additional complexities of consideration are variable wind speeds and directions generated by the canopy near the ground. Due to the uncertain nature of accounting for these complexities, the raw ultrasonic distance measurement of the irregular vegetated surface was assumed true "boom height" within the context of drift prediction.

The speed of sound is a function of the air stiffness (the air bulk modulus) and the air density. Bohn (1988) expressed the speed of sound as a function of the air temperate and molecular mass as

Equation 13. Speed of sound as a function of air temperature

$$speed\ of\ sound = \sqrt{\frac{\gamma * R * T}{M}}$$

where

γ=heat capacity ratio

R=universal gas constant

T=temperature

M=molecular mass of air

Varying temperature from 10 °C to 30 °C corresponds to a change in speed of sound of 12.77 m/sec. A maximum speed-of-sound estimate error over this temperature range results in less than a 5% error in boom height measurement. Within the context of the nozzle selection controller, a boom height error of 5% is negligible relative to the highly variable ground surface and canopy over the area for which each drift prediction is applied and the 0.65 coefficient of determination of the prediction equation. A constant speed-of-sound at 20 °C (332 m/sec) is applied within the nozzle controller for calculating boom height.

Existing sprayer sensors were utilized to obtain the droplet initial velocity, the flow rate, and the vehicle speed. Most late model self-propelled sprayers are equipped with rate controllers which require sensors for measuring each of these variables. The nozzle selection

controller was implemented on a SpraCoupe 7650 sprayer which uses radar for speed sensing, and electronic pressure and flow sensors for measuring fluid dynamic variables. Interfacing with the rate controller on this machine is done via the sprayer CAN bus. In all, the sprayer contains three busses: the engine bus, the proprietary bus, and the virtual terminal bus. The virtual terminal bus contains all information displayed to the operator and the variables required for the rate controller therefore tapping into this bus was used to access the outputs from these sensors. Reverse engineering techniques were implemented to identify which messages on the bus contained data corresponding to each of the three sensors, as well as correlating the data within each message to sensor outputs.

The CANcaseXL data logger was the primary tool used to analyze and record CAN messages within the reverse engineering procedures. For each sensor of interest, operating conditions were varied over a typical operating range. The virtual terminal displayed each of the variables of interest and was used as the true value for each variable. CAN outputs were stored in a text file via the CANcaseXL. The data cells within the CAN messages were observed during testing to identify which message corresponded to each variable. After testing, the text file was uploaded into Microsoft® (Redmond, WA) Excel to determine the resolution and offset of the appropriate message bytes. A summary of all CAN messages used within the nozzle controller are shown in Table 9.

Table 9. Definition of CAN messages incorporated within the nozzle selection controller

Variable	PGN	Resolution	Offset
Pressure	59008	0.575 KPa	0
Flow rate	59008	0.0014 L/sec	0
Vehicle speed	61474	0.001 m/sec	0
Temperature	130311	0.01C	-273.15
Humidity	130311	0.004%	0
Wind speed	130306	0.01 m/sec	0
Wind direction	130306	0.0001 rad	0

For use within the drift prediction equation, the droplet initial velocity was calculated from the pressure. The pressure sensor is located on the sprayer boom, near the nozzles; therefore it is assumed that the pressure at the sensor is equal to that at the nozzles (internal).

An energy balance based on Bernoulli's equation allows the droplet velocity to be calculated as

Equation 14. Initial exit velocity of the droplet as a function of inlet pressure and flow rate

$$Exit\ velocity = \sqrt{\frac{2 * P}{\rho} + \left(\frac{4 * Q}{\pi * D^2}\right)^2}$$

where

P = pressure at the sensor

ρ = density of water

Q = volumetric flow rate of fluid to a single nozzle

D = diameter of the tube carrying volume to the nozzle

The pressure is obtained from the pressure sensor. Volumetric flow rate is determined from the flow rate sensor and knowledge of the number of nozzles on the boom, as the flow rate measured by the sensor is for the entire boom. The diameter of the tube was determined from tube specifications.

6.2.3. GPS Inputs

Mapping of the predicted drift in the field is dependent an accurate measure of the sprayer position. While this position is only critical relative to sensitive areas, the commonplace existence of GPS systems on commercial sprayers provides a reliable source of absolute sprayer position within the field and was therefore chosen as the input of sprayer position within the nozzle selection controller. Latitude and longitude positions are input serially to the controller through National Marine Electronics Association (NMEA) strings, specifically the GGA data string. Within the controller, latitude and longitude coordinates are converted over to sprayer location on the field grid as described by Equation 10 in Section 3.2.2.2. Position accuracy is dependent on both the gridding resolution and the GPS accuracy. An RTK GPS system was selected to reduce GPS pass-to-pass accuracy to less than 1 cm. GPS update rate was set to 4 Hz to provide GPS inputs to the controller at a faster rate than the controller update rate, thereby not limiting the system performance by the GPS inputs.

6.2.4. User Interface Development

In addition to the rapidly updated inputs to the drift prediction model, nozzle selection requires inputs more readily defined by the applicator. User inputs include area sensitivity classification (high, medium, or low), sensitive area location, pesticide concentration, default acceptable drift to "non-sensitive" areas, default nozzle, and grid length. A user interface was developed to handle each of these inputs through text boxes and radio buttons as shown in Figure 32. As previously mentioned, one of the three program threads monitors user inputs during operation of the nozzle selection controller; therefore changes which are made during spraying to any of the textboxes results in a real-time change within the nozzle selection controller.

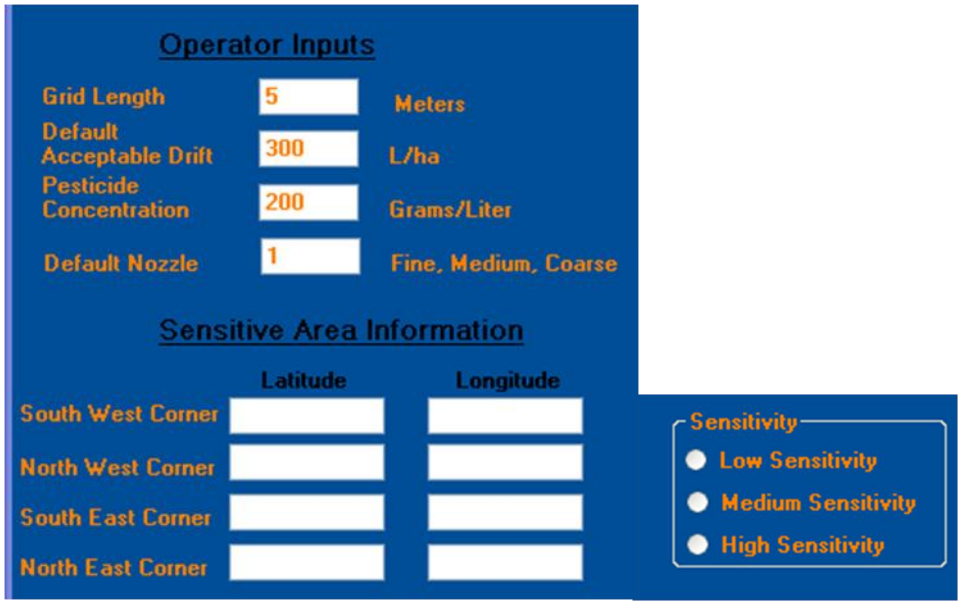

Figure 32. Developed user interface for applicator inputs

The user interface was further developed to provide informative outputs to the applicator. All sensor based inputs are displayed on the user interface as shown in Figure 34. Through the use of colored picture boxes, predicted drift is displayed to scale on a representative field layout. A legend is shown in the far right-hand side of the interface to provide reference values to the deposition colors. The user interface thread handles real-time mapping to the user interface thereby not impacting the update rate of the program. While the

goal of the nozzle selection controller is to automate sprayer operating parameters, specifically the nozzles, the purpose of the user interface display is to encourage the manual implementation of best spraying practices through a visual representation of the extent of drift. A close-up of the mapping region is shown in Figure 33, while the entire user interface is shown in Figure 34.

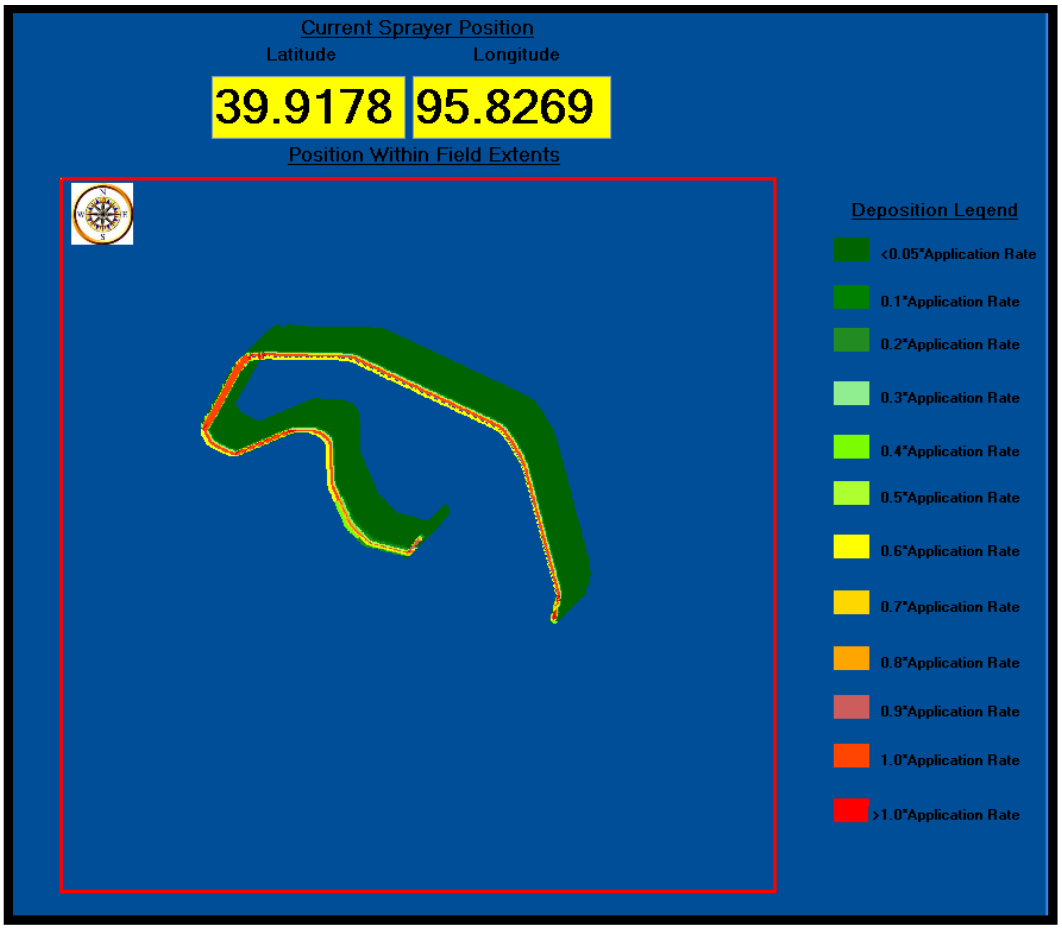

Figure 33. Real-time updated mapped deposition on user interface

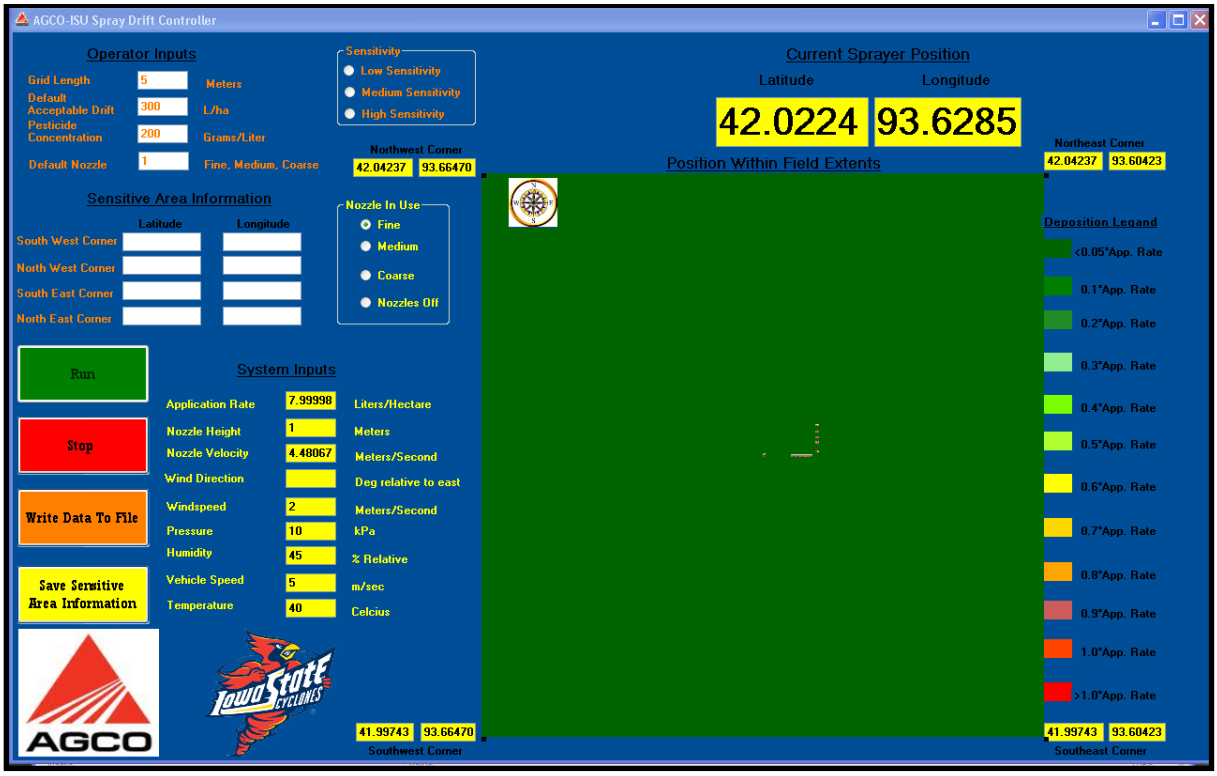

Figure 34. Full user interface for automated nozzle controller

Buttons were added in the lower left hand of the user interface for user instigated operations. The “Start” button initializes automated nozzle control to protect sensitive areas. The “Stop” button is the antithesis of the start button, whereby nozzle control reverts back to manual selection through the three way toggle switch in the cab. “Write Data to File” will write out the predicted deposition levels to a text file for recordkeeping purposes for in-depth analysis (.txt file shown in Table 4). The “Save Sensitive Area Information Button” integrates information input by the applicator into the sensitive area information text boxes and radio button into the nozzle selection process. An unlimited number of sensitive areas can be input by the applicator. Once areas are input, they are drawn within the user interface represented field for visual recall during spraying.

6.2.5. Hardware and Interfacing

With the serial input/output limitations of the nozzle selection controller program run on the laptop, a hardware bridge was required to interface with the sensor inputs and nozzle selection outputs. A control board developed at Iowa State by Dr. Matt Darr was selected to serve as this bridge. The board contains a PIC18F processor along with four MOSFETS, a serial communication chip, CAN transceiver, and four H-bridges making it a highly flexible for control uses (see Figure 35).

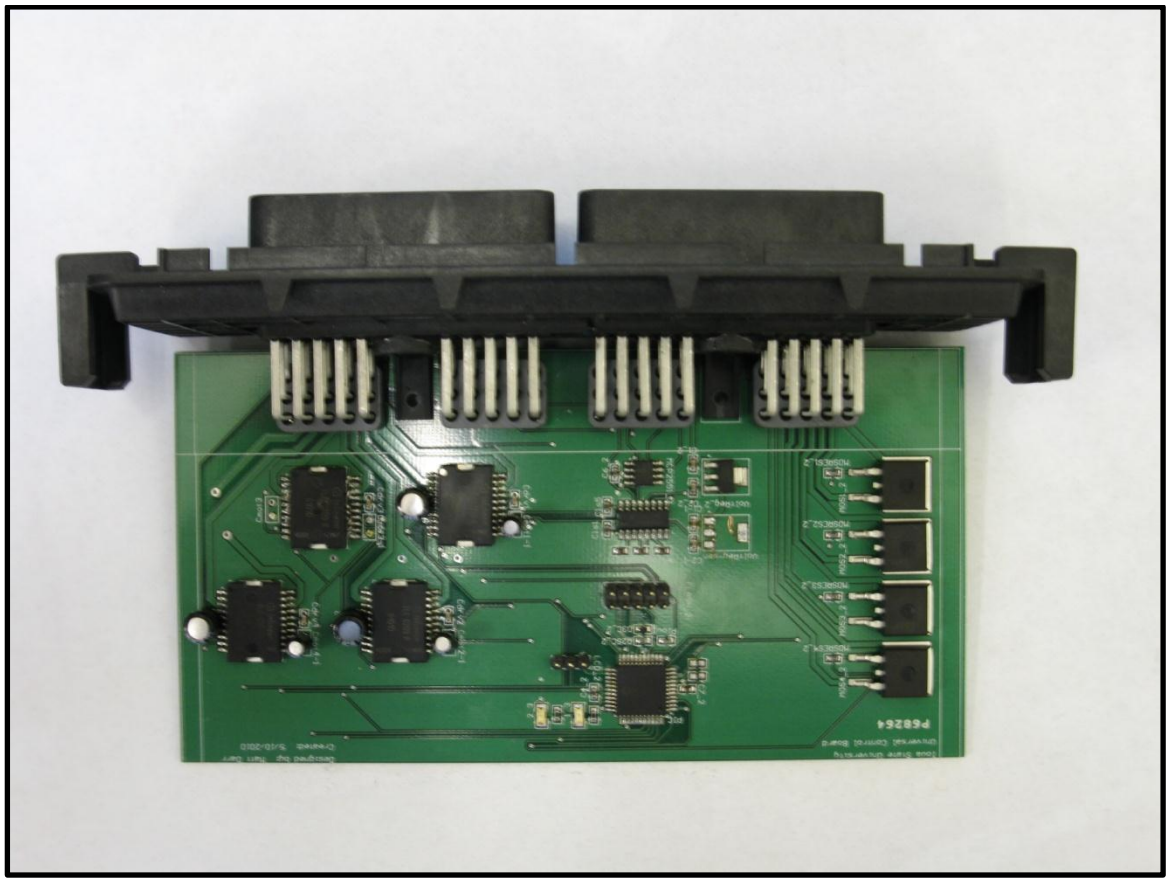

Figure 35. Controller board implemented to record CAN data, serially communicate with laptop (running prediction algorithm), and transition nozzles

The control board serves as the hub of communication for the nozzle selection system. Application variables (vehicle speed, flow rate, and pressure) are all readily available on the sprayer CAN bus along with weather variables, as the weather station was added as a

node to the existing sprayer bus. The control board was added as a second node to the sprayer bus to receive each application and weather message and relay the messages serially to the software program running on a laptop in the sprayer cab. Control of the boom height sensor is also maintained by the control board, which administers a boom height measurement after all other weather and application variables have been updated on the CAN bus. A single serial message is output at 2 Hz (based on the most limiting sensor update rate) and contains 18 bytes of data. As each of the measured variables exists as a word data type, two bytes were required for each weather or application variable, plus an additional two bytes to mark the beginning and end of the message for recognition by the nozzle selection program. Oscillator limitations of the control board limited the baud rate of the serial message to 9600 however based on the low amount of data transferred this low baud rate did not inhibit the control process. The prediction and mapping algorithm program run on the laptop receives serial data from the control board and stores all data within a buffer. As the control board update rate may be faster than the prediction algorithm update rate (based on the computer operating system), only the most recent set of weather and application conditions present within the buffer are applied to prediction.

Serial communication between the control board and nozzle selection program provides the data required for electronic nozzle selection. The nozzle selection program determines which nozzle, if any, should be used for application. After each serial message containing the new sensor variables is input to selection program, an output is sent back to the control board with a single byte corresponding to which nozzle to select. A "49"corresponds to the fine nozzle, a "50" to the coarse nozzle, and "51" to the very coarse nozzle. Any other value received by the control board results in a "no spray" condition. The control board processor deciphers the serial input message and provides a path to ground through the appropriate MOSFET corresponding to the desired nozzle selection. A wiring schematic of the nozzle solenoid valve interface with the control board is shown in Figure 36.

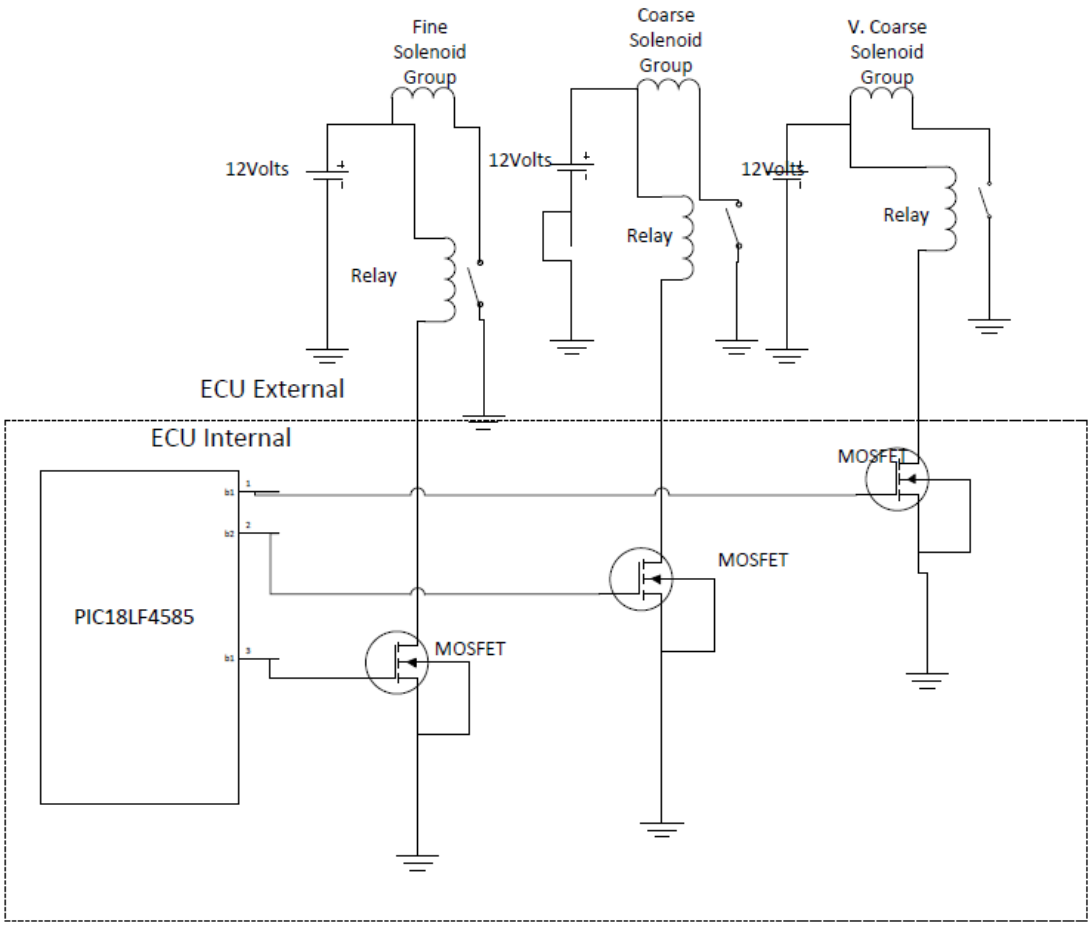

Figure 36. Circuit schematic of interfacing between nozzle solenoid valves and control board

A visual description of the interfacing of all components within the nozzle selection controller is shown in Figure 37.

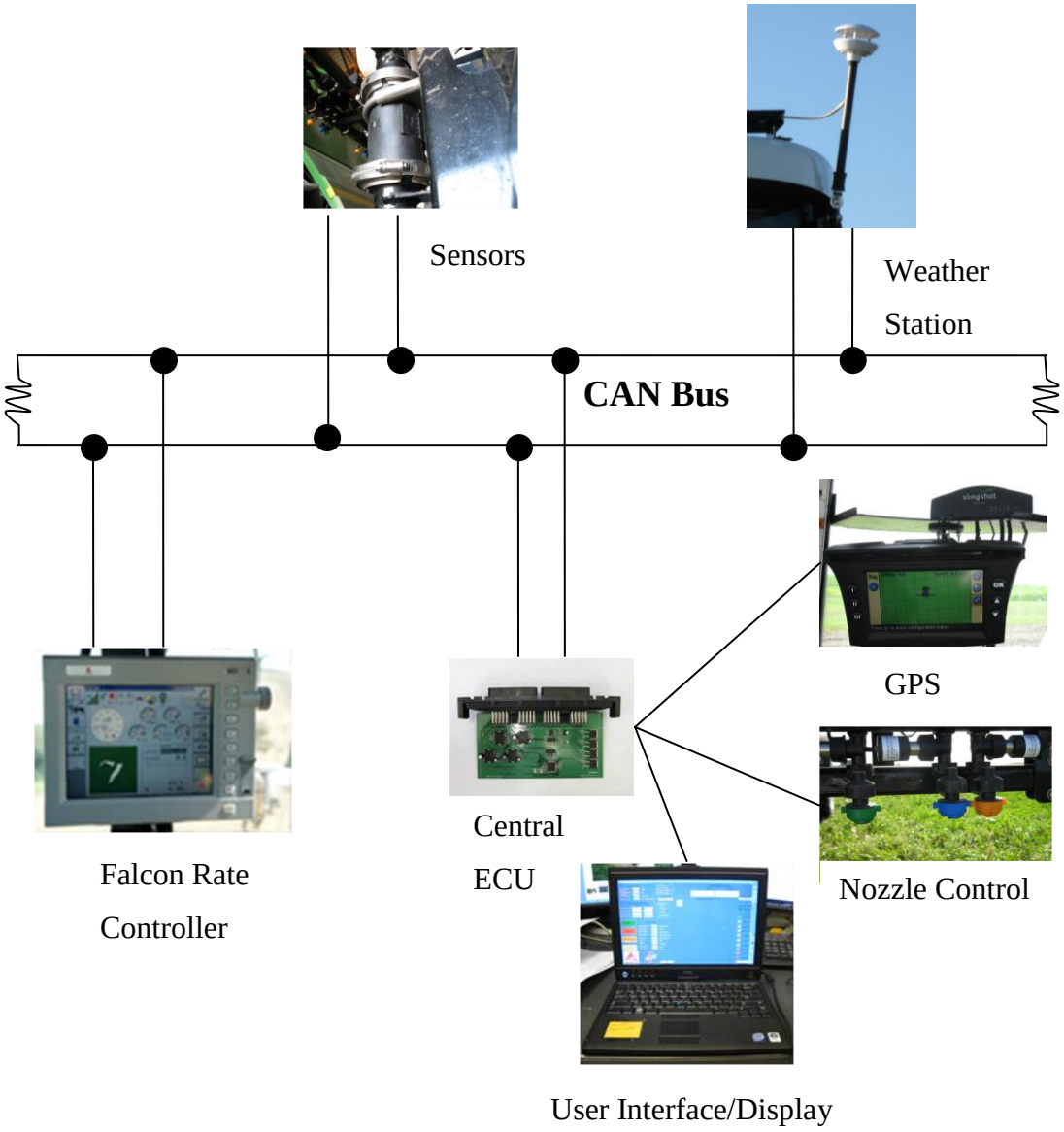

Figure 37. Interfacing of nozzle controller (run on the laptop), with sensors, control board, and nozzles

Chapter 7. Testing

In-field testing of the developed nozzle selection controller was performed to evaluate performance in a practical setting. Specific objectives of the in-field testing were as follows:

- Generate a proof-of-concept dataset, evaluating both the controller's theoretical and experimental capabilities to protect sensitive areas from drift.
- Qualitatively and statistically evaluate the predictive accuracy of the model and mapping sequence within the controller through comparison of predicted depositions to experimentally measured in-field depositions.
- Conclude sources of errors based on in-field weather measurements and experimentally measured depositions.

7.1. Test Equipment

The physical components described in the implementation section were installed on a SpraCoupe 7650 self-propelled sprayer (Figure 38) for testing. A bracket was mounted within the sprayer cab to secure a laptop running the developed nozzle selection software program. The bracket positioned the computer keyboard within arm's reach of the operator for easy interfacing (Figure 39).

Figure 38. Spra-Coupe 7650 test vehicle

Figure 39. Laptop mounted in cab under rate controller

The boom height sensor was mounted on the underside of the center boom section, adjacent to the nozzles such that boom components did not interfere with proximity readings. Figure 40 displays the mounting of the weather station such that horizontal wind speed and wind direction vectors were not induced by sprayer geometry. While more representative wind variable measurements, in terms of effect on droplet trajectories, are at the release height of the droplets (the boom height), placement at this height would have resulted in disturbances from turbulence around the vehicle.

A Trimble® (Sunnyvale, CA) EZ-Guide 500 receiver provided uncorrected GPS inputs. To further increase the GPS accuracy, a Raven® (Sioux Falls, SD) Slingshot™ RTK modem was used to provide GPS correction through the Iowa CORS network. Mounting of GPS and RTK cellular antennae' are shown in Figure 40 with the EZGuide 500 mounted display and Slingshot modem shown in Figure 41.

Figure 40. Weather station, RTK cellular and GPS antennas

Figure 41. EZGuide 500 and Slingshot modem

The control board was mounted within the sprayer cab for easy interfacing with both the virtual terminal CAN bus and the software program run on the laptop. As previously mentioned, the test sprayer was wired for manual nozzle selection through the use of a three

way toggle switch in the sprayer cab. Rewiring of the nozzle selection was performed per the wiring diagram in Figure 36, to transfer nozzle control to the control board.

The test sprayer was equipped with fine, coarse, and very coarse classified Delevan (Mendota Heights, MN) Varitarget nozzles (Figure 42), which maintain a relatively constant droplet size as the flow rate through the nozzle is varied. A variable area pre-orifice plunger (component 1 in Figure 43) and variable area nozzle orifice cap (component 2) adjust based on the flow rate and developed pressure. The plunger position establishes both the orifice area and the pre-orifice area. Pressure applied by the plunger to the diaphragm-like nozzle cap creates the orifice opening, while the varying diameter of the plunger generates control over the pre-orifice area. At low flow rates and thus low operating pressures, a compressed spring (component 3) within the nozzle body applies a large force to the plunger which in turn presses against the nozzle cap creating a very small opening. Greater pressures are generated in the nozzle from increased flow through the nozzle. As pressure increases, forces exerted on the plunger compress the spring within the nozzle body. Compression of the spring causes the plunger to travel away from the nozzle cap, increasing the orifice size, while at the same time increasing the pre-office area. The combination of varying pre-orifice and orifice maintains a constant droplet size as well as spray angle (Bui, 2005). Duggupati (2007) evaluated the nozzle spectrum characteristics of the Varitarget nozzle and found constant nozzle classification for droplet size as indicated by spray quality based on ASABE 572.1 over nozzle pressures from 10-50 psi. Varitarget nozzles have become increasingly popular in the variable rate agriculture sector due to these capabilities. Nozzle spectrums of each of the three nozzles on the test vehicle were determined from lab testing and hard-coded within the nozzle selection controller (in place of those used for the fine, medium, and coarse nozzles in the simulator testing, Section 3). Spectrums were defined in terms of 10 droplet sizes, consistent with the tier 1 controller approach.

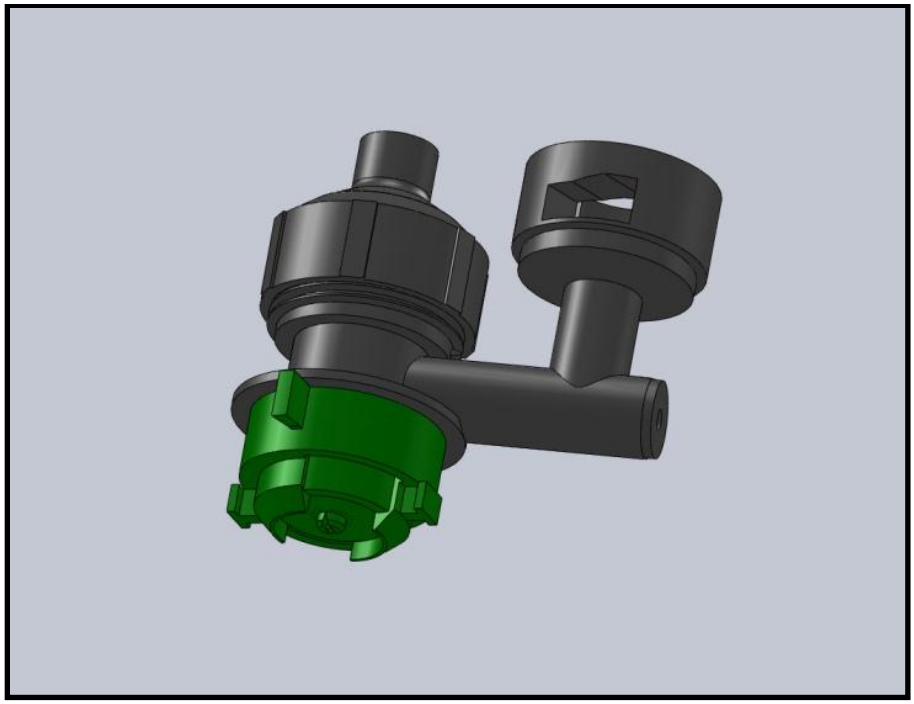

Figure 42. Delevan Varitarget nozzle

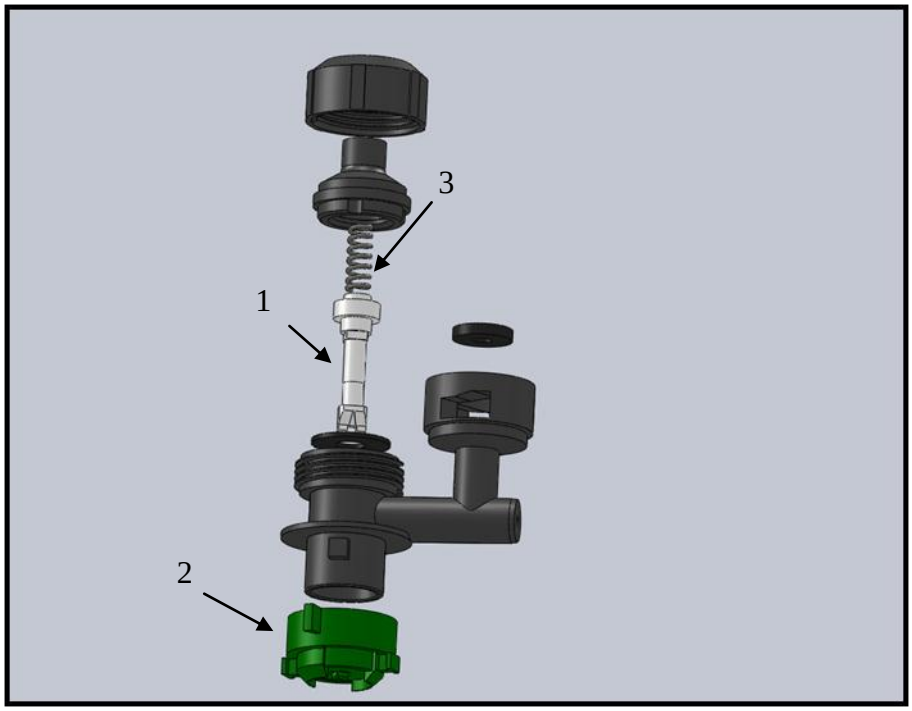

Figure 43. Components of the Varitarget Nozzle

7.2. Proof-of-Concept Testing Procedures

Motivation for proof-of-concept testing was to evaluate the nozzle controller's ability to protect sensitive areas through the transitioning of nozzles when sensitive areas are encountered during spraying. On a theoretical protection and performance basis, the key measurements for proof-of-concept testing are mapped predicted drift and mapped acceptable levels of drift. Proof-of-performance is then a comparison of the "as-applied" predicted drift to the acceptable levels of drift for a true in-field spraying event. On a practical performance evaluation basis, experimentally determined depositions in sensitive areas resulting from spraying with an activated nozzle selection controller are compared to acceptable depositions.

Proof-of-concept testing was conducted in a tilled 2.8 hectare field located on the Iowa State University Agricultural Engineering and Agronomy farm. A single sprayed swath along the "AB'" line shown in Figure 44 constituted a "spraying event" used to evaluate the performance of the automated nozzle selection system.

Figure 44. Test field layout and "AB" line

Throughout spraying, the nozzle selection program was relied upon to record both the mapped predicted depositions, mapped acceptable levels of deposition, and the operating

conditions including the nozzle in use at each point within the field. Measurement of experimental deposition levels was performed according to the ASABE standard for measuring drift deposits from ground sprayers, ASBAE S561.1 (2009). White Kromekote paper cut into 2 cm by 3 cm sections served as experimental drift collectors within the testing. The sprayed volume was water with a 0.275% concentration of Tracer Hot pink Dye (Precision Laboratories, Waukegan, IL.), as was used by Hanna et al. (2006). The dye-Kromekote paper (Figure 45) method produces a droplet stain with a sharp, distinct edge, and is a popular approach to high volume in-field drift measurements (Barry et al., 1978, Maksymiuk and Moore, 1962).

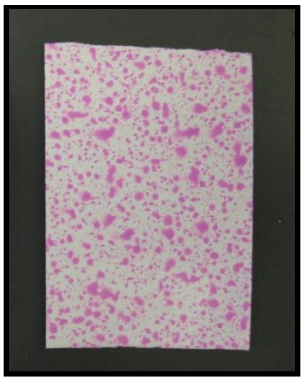

Figure 45. Dyed Kromekote card

Two simulated sensitive areas were flagged-out within the test field at distances from the boom edge which were pre-determined to require nozzle transitioning based on typical operating conditions. Cards were placed along the border of, and within the sensitive area, for each of the two sensitive areas, as shown in Figure 46. The defined card placement provides analysis of depositions within and around the close proximity of sensitive area. Each card was labeled based on its row (defined parallel to the sprayer path) and column (perpendicular to the sprayer path) position relative to the sensitive area for later correlation of depositions to positions within the field. Modified paperclips were attached to the cards and pushed into the ground as shown in Figure 47 to prevent displacement of the cards by the wind.

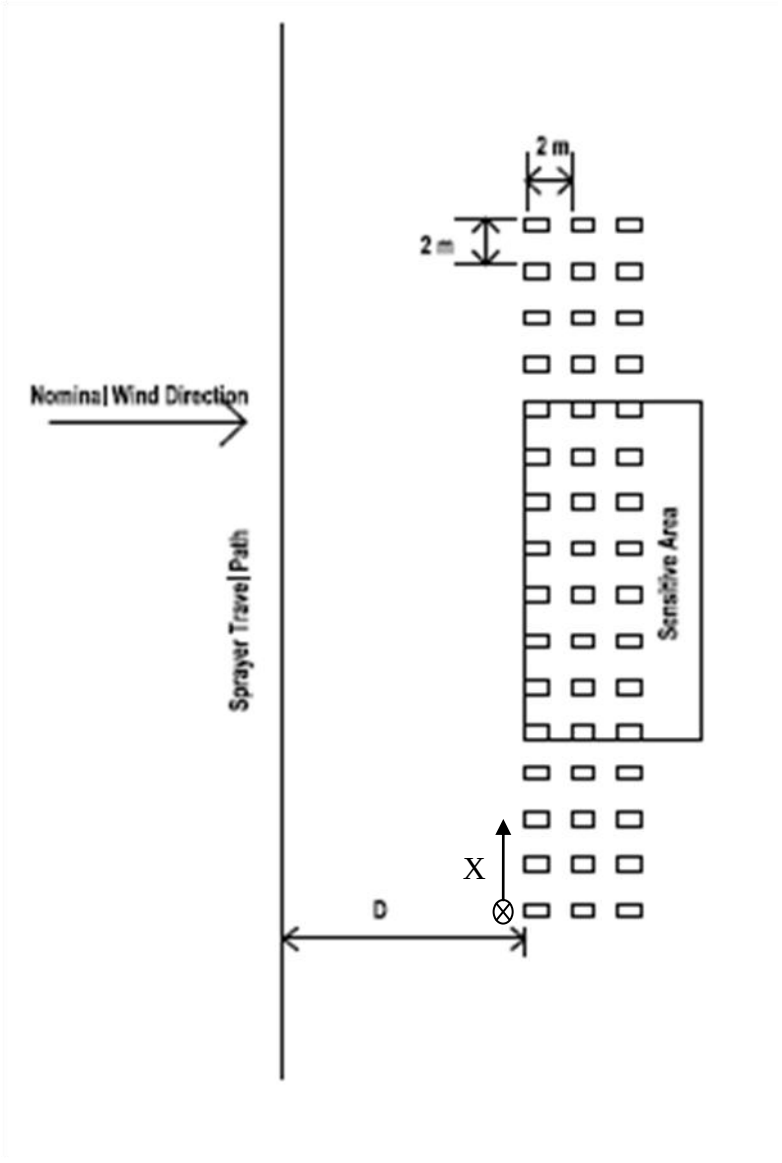

Figure 46. Measurement card placement for proof-of-concept testing showing origin for x-axis as referenced in Figure 56-Figure 59

Figure 47. Kromekote collection card with paperclip fixture

The first sprayer-encountered sensitive area, “A”, was located at a distance 78 m from the boom edge while the succeeding encountered area , “B”, was 9 m from the boom edge (see Figure 48 for sensitive area locations within field). Under anticipated operating conditions during the tests, highly sensitive areas at both “A” and “B” would result in coarse nozzle selection and “no-spray” nozzle states respectively. Similarities between the coarse and very coarse nozzle spectrums did not present a predictable situation where a very coarse nozzle would be selected rather than the coarse nozzle therefore only two sensitive areas were used to generate a total of three nozzle conditions, as fine nozzles were set as the default nozzle.

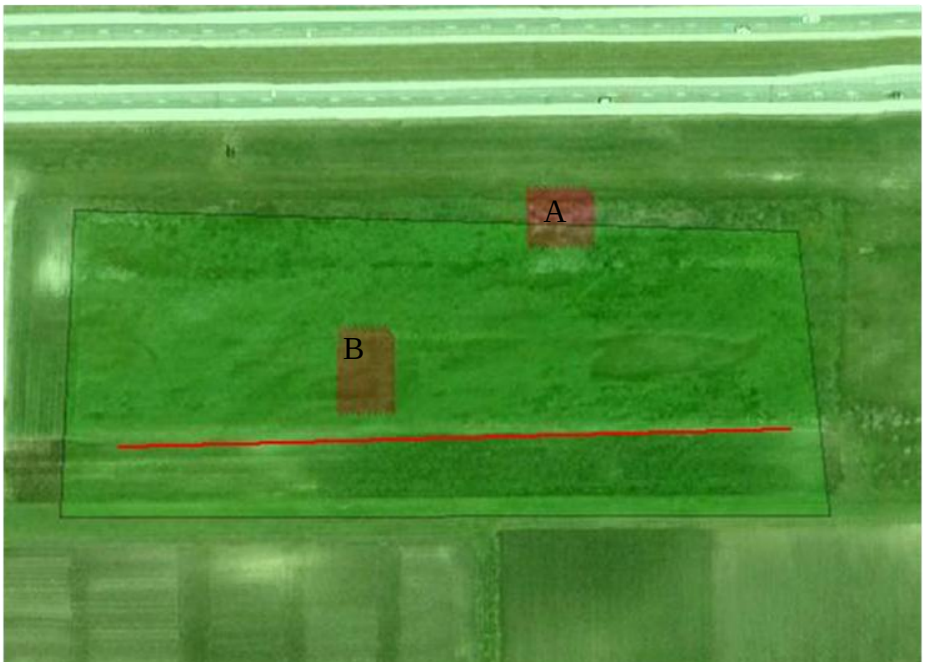

Figure 48. Sensitive areas relative to centerline of travel within proof-of-concept test field

Proof-of-concept testing was conducted on October 8, 2010 at 3:30 pm central time. Due to difficulties in maintaining ambient weather conditions, only a single repetition was performed. The sprayer was positioned at the east most point of the "AB" line of travel. Wind conditions were monitored until the wind speed was comparable to that used in sensitive area selection and placement and the wind direction stabilized to relatively due North heading. With the desired conditions reached, the sensitive area sensitivity levels (both High) and locations were input to the nozzle selection controller via the developed interface. Additional user inputs were as follows:

Grid length: 2m
Default Acceptable Drift: 1000 L/ha
Pesticide Concentration: 100 g/L
Default Nozzle: Fine

When the desired conditions were obtained, the nozzle selection controller was engaged and spraying commenced along the "AB" line which was marked with high-

visibility flags. An application rate of 100 L/ha was maintained throughout the duration of the swath through the use of the sprayer's rate controller. Upon completion of the test, both the acceptable levels of drift and predicted drift deposition levels were written to test files for later analysis though the user interface. Kromekote cards were allowed to dry within the field prior to collection. Cards were stored within sealed bags to prevent the future effects of moisture on the droplet stains.

Depositions on the field collected cards were measured through the use of WRK DropletScan™ (Lonoke, AR). Effectiveness of this system in measuring droplet sizes for downwind drift collections was confirmed by Wolf (2003) and Hoffman and Hewitt (2004). DropletScan™ measures the deposition on card surfaces through the application of imaging algorithms to scanned images. The algorithms use spread factors (the ratio of droplet diameter on the card to pre-deposition diameter) to relate color contrasts on the card surface to a total volume deposited on the card. Known scanned areas are applied to derive volume per unit area measures.

The accuracy of DropletScan™ is highly dependent on the use of spread factor representative of the liquid-paper interface. Barry et al. (1978) developed relationships between spot diameters, as measured under the microscope, and pre-deposition droplet diameters controlled through the use of a vibrating reed apparatus. Relationships were determined for a wide variety of pesticides as well as dyes on Kromekote paper. Amongst dyes, relationships were similar, however between dyes and pesticides relationships were highly different. Rhodamine dye produced a relationship of

Equation 15. Rhodamine dye spread on Kromekote paper

$$Spot\ diameter = \frac{predeposit\ diameter + 19.32}{1.81}$$

With the low variability in dye relationships and similar properties between Rhodamine and Tracer dye, the Rhodamine spread factor was used within deposition analysis.

Predicted drift and acceptable deposition levels were determined from the nozzle controller's output text file. Depositions were determined both numerically, directly from the text files, and visually using SMS. The controller's theoretical and experimental ability to protect sensitive areas was determined from comparisons between drift predicted by the

controller, measured deposition on the Kromekote cards, and acceptable deposition for the sensitive areas.

7.3. Predictive Accuracy Testing

7.3.1. Background

The controller's ability to protect sensitive areas within the field hinges upon its predictive accuracy. An overpredicting controller will prematurely select larger droplets for application resulting in unnecessarily reduced pesticide efficacy. Underprediction can have even more detrimental impacts, as excessive drift will be allowed to deposit in sensitive areas resulting in environmental damage. Accuracy, in the context of the drift controller, is a measure of how well predicted drift compares to true in-field drift. Testing was conducted to quantify the automated nozzle selection controller's predictive accuracy.

Wind tunnel testing is often chosen to replace in-field testing in evaluating the accuracy of a drift prediction model. The controlled environment of the tunnel allows single variables to be changed in a step wise fashion to generate a wide dataset for model evaluation. While convenient, wind tunnel testing does not truly represent the drift phenomenon which occurs in the field. The spatial aspects of drift due to sprayer position and wind direction require in-field testing to fully evaluate predictive ability. Methods of predictive model evaluation through in-field testing were reviewed prior to formulating a test plan for evaluating the nozzle selection controller's predictive accuracy.

Prior researcher's methods to evaluate predictive accuracy in the realm of spray drift tend to be more qualitative in approach as opposed to quantitative. Ellis and Miller (2010) compared predicted and experimental depositions at various distances from the boom edge for 13 different sets of operating conditions. Conclusions were drawn concerning predictive ability through the visual analysis of predicted and experimental depositions plotted on the same *y* axis versus distance from the boom edge on the *x*-axis. A cumulative plot of all predicted deposits versus measured deposits (as a percent of the application rate) was used to visually determine overall predictive ability as the ideal relationship between these two variables would be linear with a *y* intercept of zero (see Figure 49). This is a common method of model evaluation, also used as the primary method of accuracy analysis in works by Teske

et al. (2001, 2004) for the AGDISP model and Holtermann et al. (1997) for the IDEFICS model.

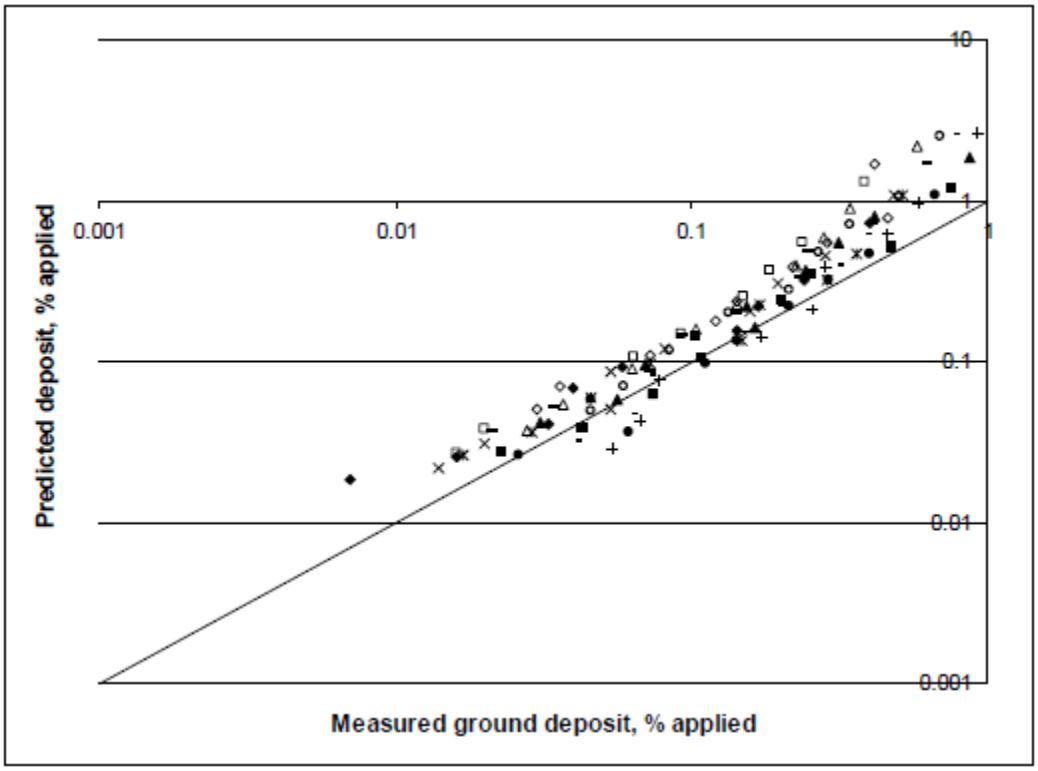

Figure 49. Collective plot of predicted deposition versus experimental deposition commonly used to evaluate predictive accuracy (Ellis and Miller, 2010)

Lebeau et al. (2009) determined the predictive ability of his plume model used for real-time prediction using data from five trials conducted with varying wind speeds and plant heights (effective boom height). Accuracy was evaluated by qualitatively comparing tabled percent deposition values of the predicted and in-field measured depositions. Nuyttens et al. (2007) expanded upon the graphical approaches of Ellis and Miller, Teske et al., and Holterman et al. by calculating the significance of the correlation coefficient for his dataset for a regression line similar to that seen in Figure 49.

7.3.2. Procedures

With the ability to predict drift based on real-time operating conditions comes an opportunity to perform more in-depth statistical analysis on predictive accuracy of a drift.

Prior methods of drift model evaluation have measured weather conditions but used "average" or mean weather during the test rather than adjusting for drift in much smaller "real time" steps. A test plan was developed with the anticipation of generating data through testing which would provide a basis for an innovative statistical evaluation of the drift prediction model using real-time weather to affect predicted drift.

A significant limitation in in-field testing is the inability to vary and select weather conditions at will. In evaluating predictive accuracy of a model, conclusions can only be drawn for predictive accuracy at the set of conditions encountered during testing. It was determined that the scope of the nozzle-controller predictive accuracy testing would be limited to typical operating conditions. To provide variability and increased understanding of the predictive ability, five general sets of operating conditions were selected to serve as treatments, with wind speed and boom height as the two principle subjects of variability. The fine nozzle type was selected as the primary target of analysis as it produces high drift potential cases, however test 5 was conducted with a coarse nozzle to generate a single low drift potential condition. The five test cases were as follows:

Test 1	Test 4
Low wind	High wind
High boom	High boom
Fine nozzle	Fine nozzle
Test 2	Test 5
Low wind	Low wind
Low boom	Low boom
Fine nozzle	Coarse nozzle
Test 3	
High wind	
High boom	
Fine nozzle	

Low wind speed is defined as encountered winds ranging from 1-5 m/sec, while high wind speeds range from 5-8 m/sec. Low boom heights are approximately 1 m while high boom heights are 1.2 m. It was initially determined that a greater range in boom heights should be implemented within the treatments, however this detail was overlooked during the testing resulting in less distinguished low and high boom heights. This development led to reduced scope of model accuracy validation, however the overall subject of the testing was not compromised.

The automated nozzle selection controller was implemented as described within the proof-of-concept testing. With the goal of comparing predicted and experimental depositions, measurements collected for accuracy testing include the in-field depositions collected on Kromekote paper, depositions at positions as predicted by the controller, and real-time updated operating conditions during testing. As in the proof-of-concept testing, the controller's logging abilities were used to record predicted depositions as well as operating conditions. Depositions were collected on Kromekote cards.

The proof-of-concept test field on the Iowa State University Agricultural Engineering and Agronomy farm served as the test site for the predictive accuracy testing. The field layout for predictive accuracy testing is shown in Figure 50. Cards were placed from 0-50 m from the edge of the boom in 2 m increments, thus constituting a "card vector". Ten card vectors were placed in the field for each set of test conditions with 50 m between each card vector. Fifty meter spacing allows for wind direction variability up to 45° without deposition from a single card vector overlapping an adjacent card vector per ASBAE S572.1. Test days were selected based on wind direction, wind direction stability, and wind speed to satisfy the test design criteria. In order to maintain the desired card vector spacing to prevent overlap, field dimensions required either due north or due south wind directions. Wind direction variations from due north or south of less than 20° were desirable to reduce the potential for overlap on adjacent card vectors.

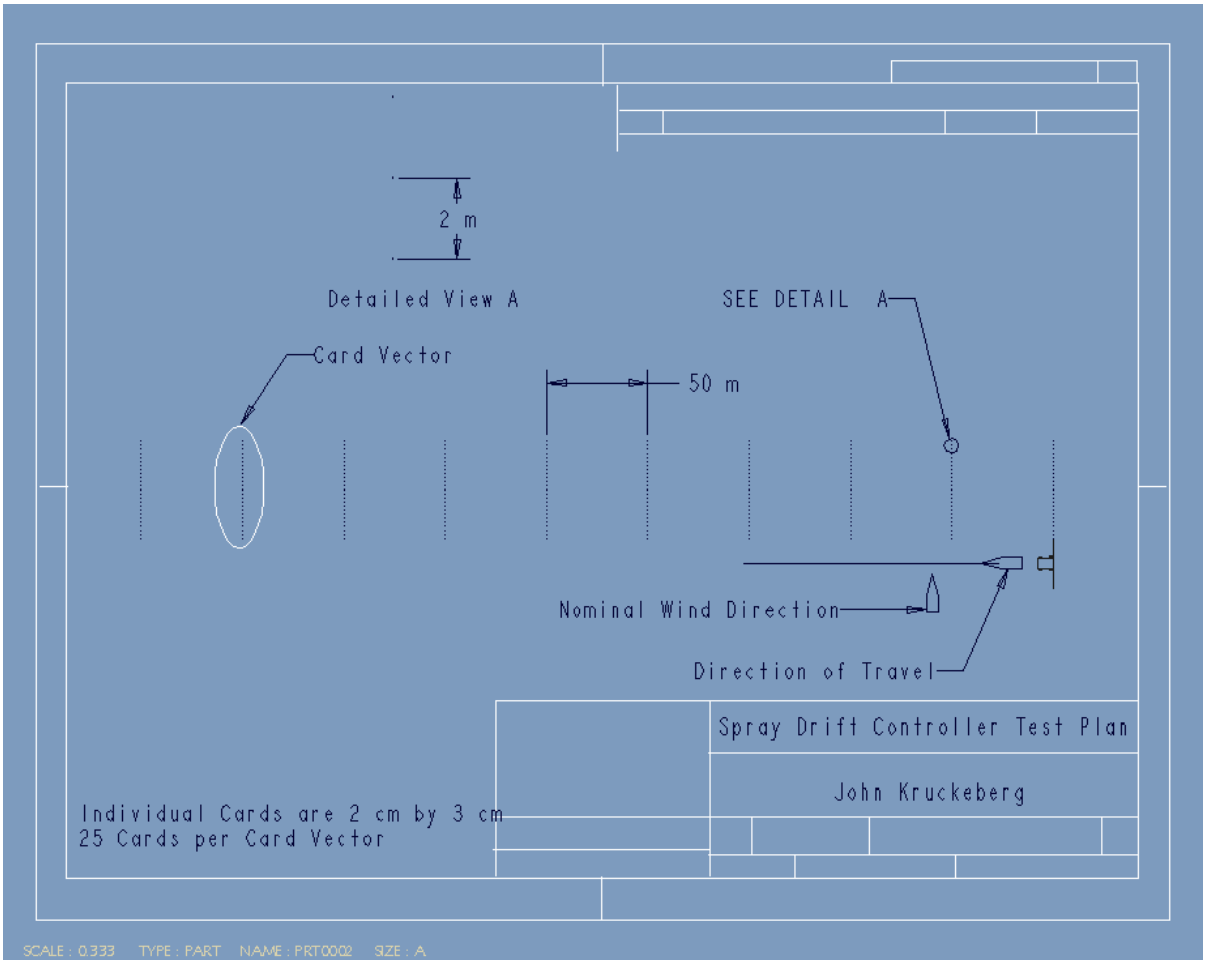

Figure 50. Field layout and card placement in model accuracy testing

Kromekote cards were labeled on the same row column basis as in the proof-of-concept testing, with columns consisting of the 10 card vectors and rows of the 26 (0-50 m at 2 m intervals) positions within the vectors. Latitude and longitude coordinates were recorded for the location of card 0 within each column for later linking of card vectors with predicted depositions.

Testing was conducted on three different days to acquire the appropriate wind conditions. Tests 1 and 2 were performed on September 28, 2010 when low wind speeds were observed, tests 3 and 4 on October 2, 2010 as high wind speeds were present, and test 5 on October 5, 2010 when low wind speeds were observed. Prior to each test, in-field conditions were monitored through the interface of the nozzle selection controller. When

conditions, most notably wind speed and direction, stabilized and were in the desired ranges, user inputs were established in the nozzle selection controller as follows:

Grid length: 2 m

Default Acceptable Drift: 1000 L/ha

Pesticide Concentration: 100 g/L

Default Nozzle: Fine (Tests 1, 2, 3, 4)/Coarse (Test 5)

Sensitive areas were excluded from the inputs to prevent varying nozzle selection. The high default acceptable drift level assured that the fine nozzle would be selected for tests 1-4, while on test 5 the coarse nozzle was input as the default nozzle for complete application with the coarse nozzle.

Each test consisted of a single swath along the "AB" line (Figure 51 and Figure 52). Predicted depositions and operating conditions were monitored and recorded by the drift controller at an update rate of 0.5 Hz. The "AB" line was extended 50 m beyond the last card vector to allow potential wind direction impacts to be consistent for all card vectors. Predicted deposition and operating condition text files were saved after the completion of each test for later analysis. Table 10 displays the average conditions for each of the five tests. Wind directions specifies the direction relative to parallel to the card vectors, with positive directions indicating westward tending (out of the east blowing to the west) winds and negative directions indicating eastward winds. Varying pressures were derived from slightly varying vehicle speeds, as flow rate was adjusted to maintain a consistent application rate (~70 L/ha).

Table 10. Average operating conditions recorded during each of the 5 tests (standard deviations shown for wind measurements)

	Temp [C]	Hum [%]	Wind Speed (std.) [m/sec]	Wind Dir. (std.) [deg.]	Boom Height [m]	Pressure [kPa]	Nozzle Type
Test 1	22.5	52.7	3.9 (1.1)	4.0 (13.5)	1.2	162.1	Fine
Test 2	22.5	52.6	1.2 (0.4)	4.0 (14.8)	1.0	236.5	Fine
Test 3	11.2	67.2	5.4 (1.17)	-7.0 (16.0)	1.2	216.0	Fine
Test 4	12.2	61.3	6.4 (1.87)	-15.0 (19.3)	1.2	160.7	Fine
Test 5	19.5	44.4	3.4 (1.1)	22.0 (50.3)	1.0	279.1	Coarse

Kromekote cards were analyzed as in the proof-of-concept testing with depositions being measured for each card. Predicted depositions at the position of each card were determined from the compiled text files. Both predicted and experimental depositions were input to Microsoft Excel for analysis.

Figure 51. In-field drift from accuracy testing

Figure 52. In-field drift resulting from accuracy testing

Chapter 8. Results

The automated nozzle selection controller's functionality was evaluated using both qualitative and quantitative techniques. Qualitative techniques mirrored those commonly used by other researchers in evaluating predictive ability of drift models. A method for quantitative analysis was developed to statistically determine the model's predictive ability and allow for objective comparison to other prediction models.

8.1. Proof-of-Concept Results

The goal of proof-of-concept testing was to evaluate the ability of the nozzle selection controller to both theoretically and experimentally protect sensitive areas from excessive amount of drift (greater than acceptable levels). Qualitative methods were relied upon to evaluate each of these capabilities.

Predicted drift depositions for the proof-of-concept testing were uploaded into SMS to evaluate theoretical sensitive area protection. Predicted and acceptable deposition levels as represented in SMS are shown in Figure 53.

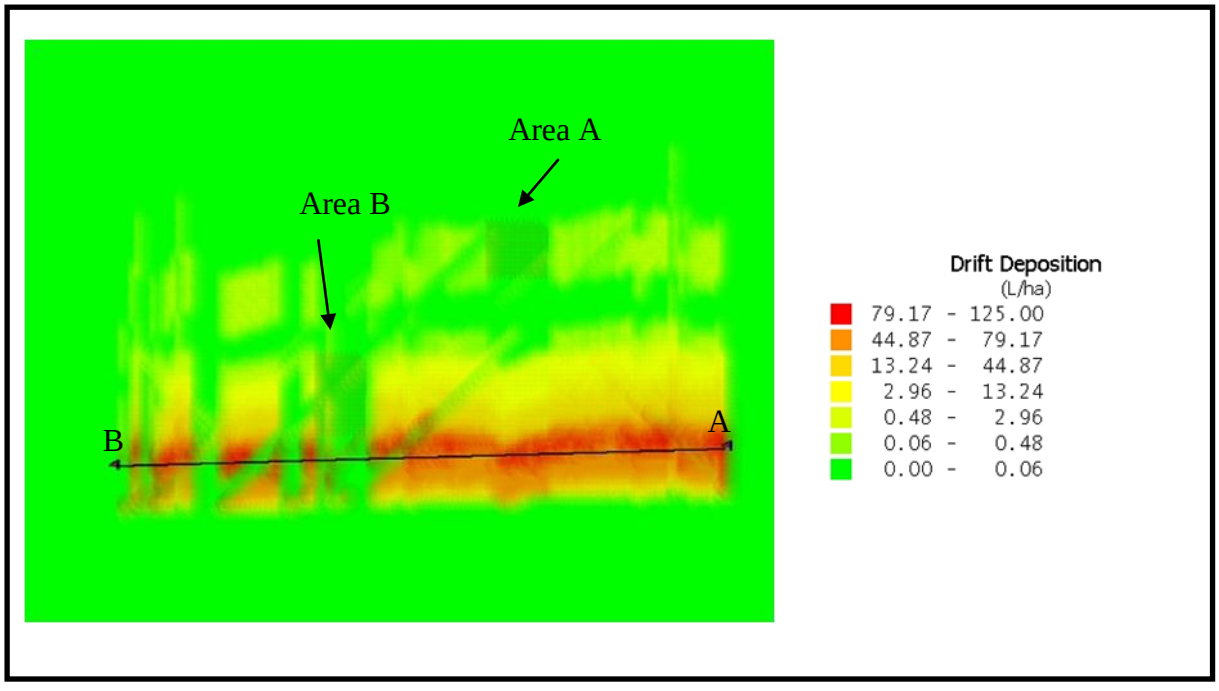

Figure 53. Predicted deposition and sensitive areas within proof-of-concept testing

Each of the sensitive areas in Figure 53 has an acceptable deposition level of 0.029 L/ha which corresponds to a highly sensitive area. Transitioning of the nozzles by the activated selection controller is clearly evidenced by the predicted drift profile. Beginning at point “A”, the sprayer applied with a fine nozzle. While large amounts of drift occur when spraying with the small droplet sizes of the fine nozzle, the absence of a sensitive area in close proximity to the sprayer causes the controller to focus on maximizing efficacy rather than the reduction of drift. As the sprayer continues down the “AB” line toward sensitive area “A”, the controller recognizes that the fine nozzle theoretically produces drift levels exceeding those established as acceptable for area “A”. The controller determines that the coarse nozzle is the highest efficacy producing nozzle which does not result in excessive drift to area “A” therefore the application nozzle is transitioned from fine to coarse. When the controller recognizes that the fine nozzle no longer violates the acceptable drift levels of sensitive area “A”, it is re-selected for application. Continuing along the “AB” line, area “B” which is near the boom edge, is encountered. For this area, the controller predicts each of the three on-board nozzles, if implemented, would produce excessive drift within area “B”, therefore a “no-spray” condition is selected. Continuation past area “B” re-instates the fine nozzle.

An interesting control sequence occurs when the wind direction suddenly shifts after the sprayer has passed sensitive area “B”. A -45° wind direction causes spray to drift “back” onto the sensitive area, therefore an additional “no spray” condition is required to protect area “B”. Once wind direction returns to due north, the fine nozzle is re-selected for application to maximize efficacy. A higher resolution representation of the predicted depositions with the selected nozzles is shown in Figure 54 with a detailed nozzle selection profile, as recorded by the controller, relative to position on the “AB” line is shown in Figure 55.

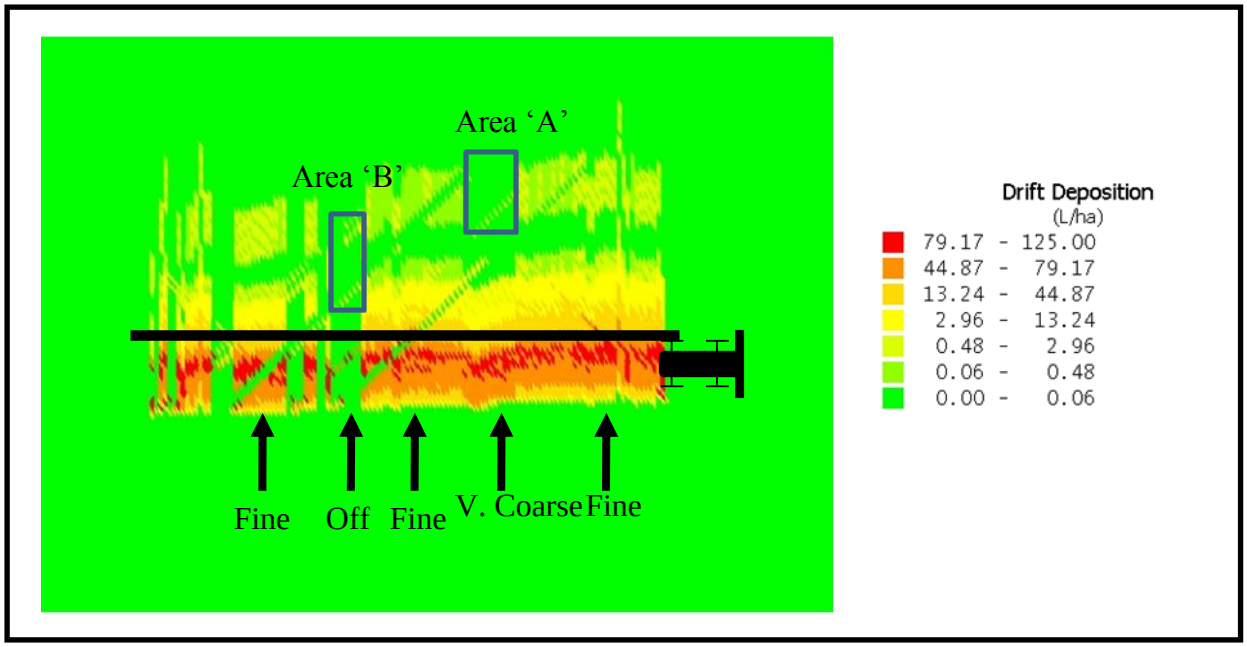

Figure 54. Proof-of-concept testing predicted depositions and nozzle selection based on protecting areas from drift

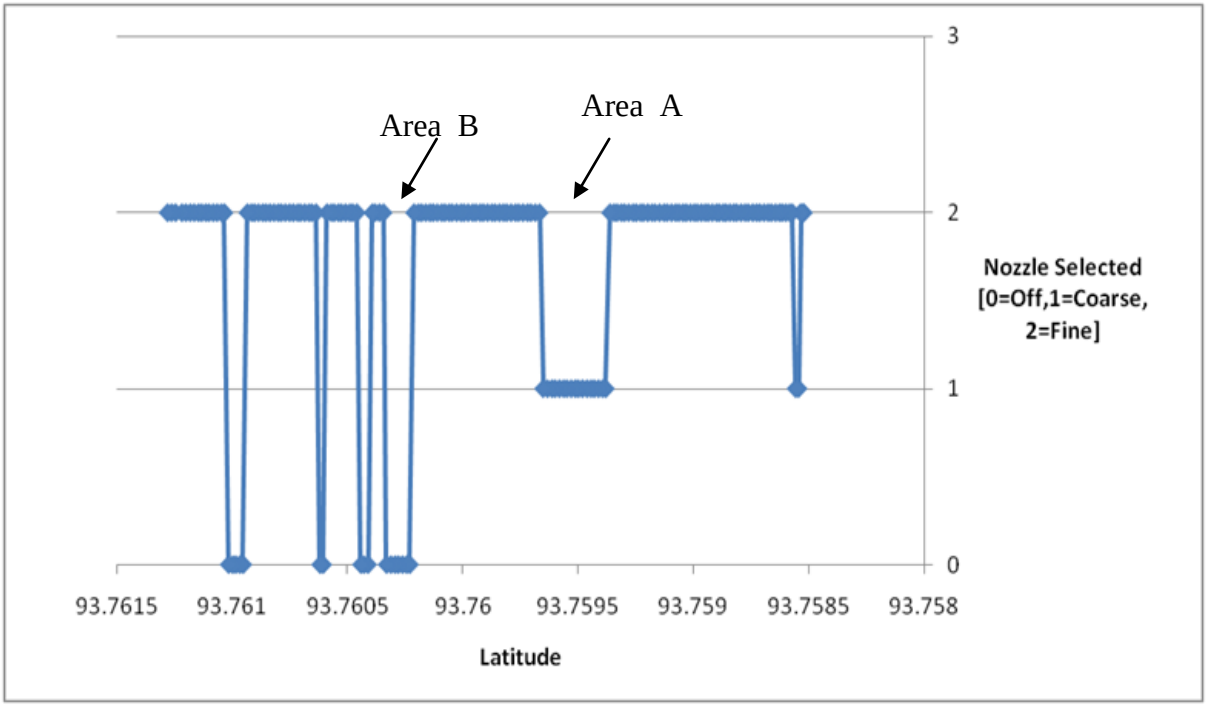

Figure 55. Selected nozzles as recorded by the controller

In Figure 54, predicted depositions can be seen within the sensitive areas which seem to violate to acceptable drift levels. These depositions are explained by the functionality of

the controller. Maintained predicted drift records precede the control process by one control iteration, through the use of the look-ahead distance (i.e. drift is predicted and stored before selecting a nozzle for application). Recorded predictions within an iteration are based on applying with the nozzle implemented during the previous iteration. With this methodology, the iteration which initializes nozzle transitioning (and thus violates the acceptable drift level) is evident within predicted drift records. In the development of the controller, it was assumed that most sensitive areas will be large relative to the grid size and distance covered over a time step, therefore recording the initial violating prediction would not cause a significant feature on the prediction map. While the controller records predicted drift based on the nozzle implemented over the previous iteration, the actual nozzle used for application over the area is selected, through the use of the look-ahead distance, to protect the sensitive area from excessive drift.

It is of note that the look-ahead procedure is not simply a look-ahead in distance but also a look-ahead in time. Protection of the sensitive areas is therefore dependent upon the assumption that weather and operating conditions, including wind direction, are those occurring at one look-ahead time step in the future. Highly fluctuating conditions, most notably wind speed and direction, can create instances where this assumption would lead to large predictive inaccuracies and thus contamination of sensitive areas.

Predicted depositions at the locations of each of the Kromekote cards placed along the border of, and within sensitive areas are shown in Figure 56. The x-axis and its origin within the figure corresponds to that shown in Figure 46. It is of note that cards from distances of 0-6 m and 24-30 m were outside the boundaries of the sensitive areas (per Figure 46). Row numbers correspond to the three rows of cards paced at varying distances perpendicular to the boom edge with row 1 closest to the boom edge.

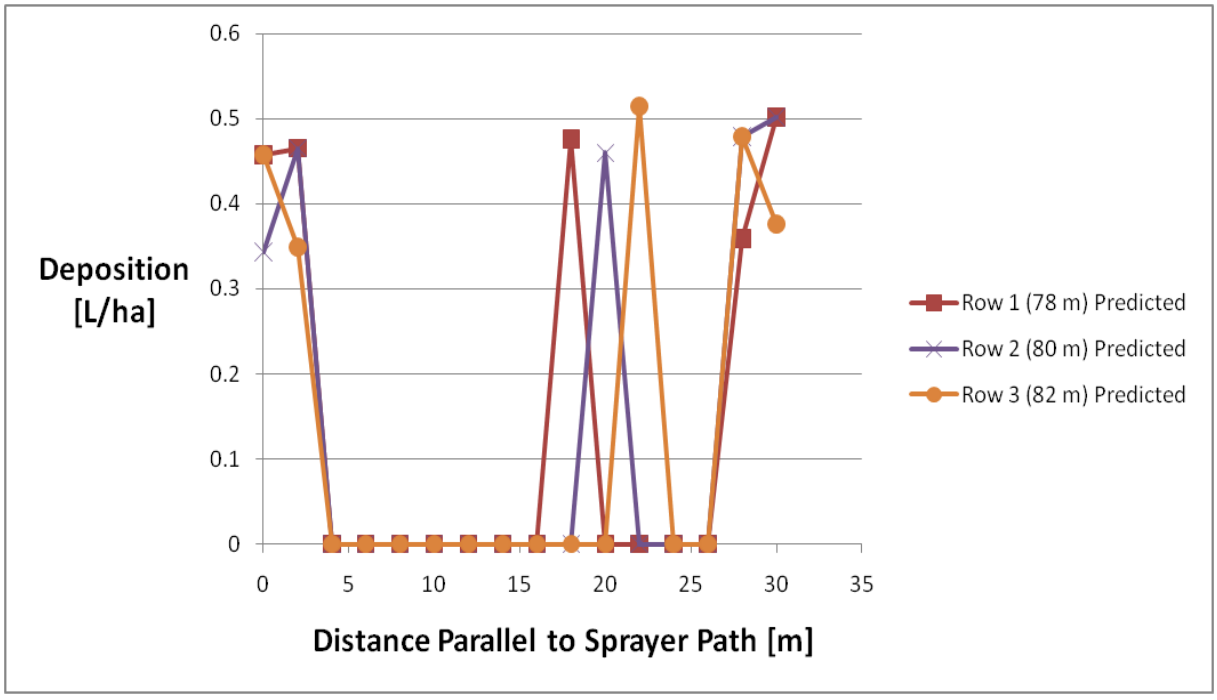

Figure 56. Predicted depositions within and around sensitive area "A"

The satisfactory theoretical ability of the controller to protect the sensitive area from drift is evident from this figure. From 15-22 m, spikes in depositions are for the "triggering" cases where wind direction shifted causing drift back onto the sensitive areas. The fast update rate of the controller is evidenced by the quick decline and return of deposition from and to 0.45 L/ha.

Figure 57 displays the experimentally measured depositions at positions corresponding to those of the predicted depositions in Figure 56.

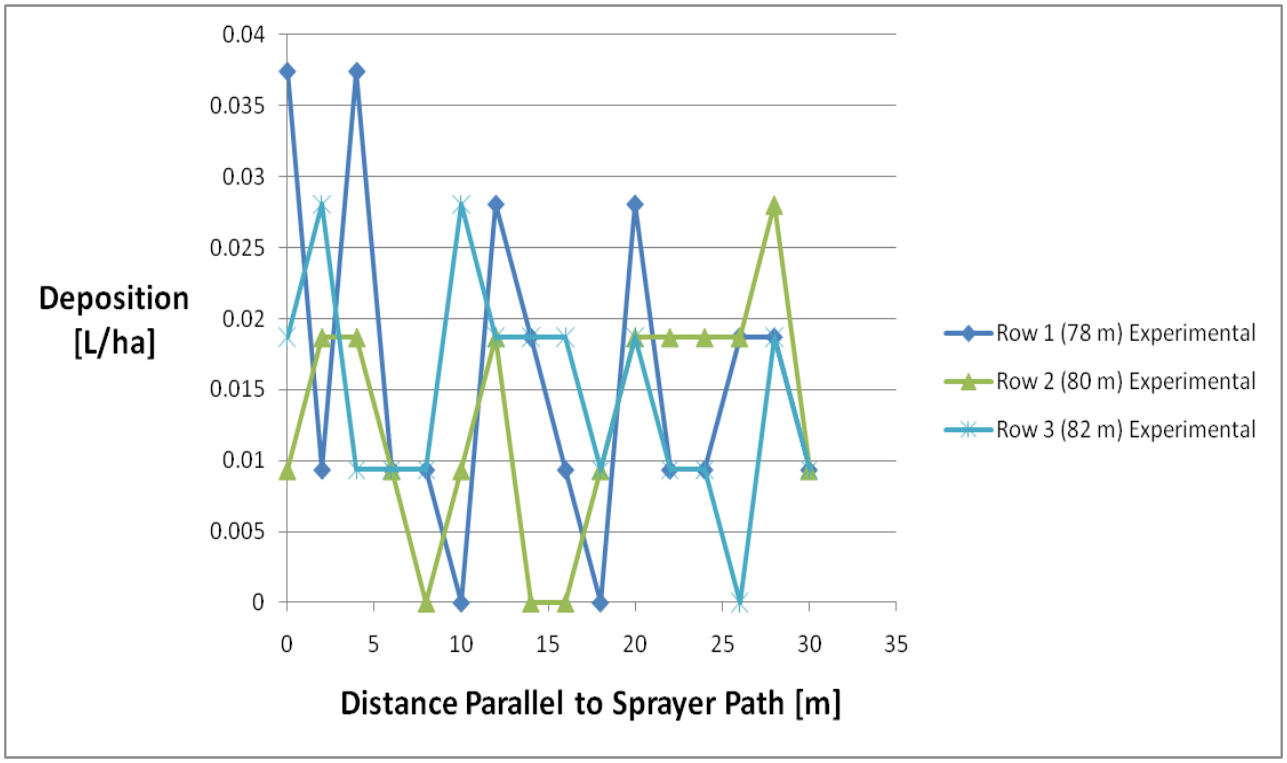

Figure 57. Experimental depositions within and around sensitive area "A"

Experimental depositions display little relation to those predicted in Figure 56. Based on the levels of deposition seen within the sensitive area, the 0.029 L/ha acceptable level would not be violated however there is not sufficient evidence to say protection is solely due to the controller's actions.

For sensitive area "B", which was closer to the boom edge, predicted deposition levels are shown in Figure 58.

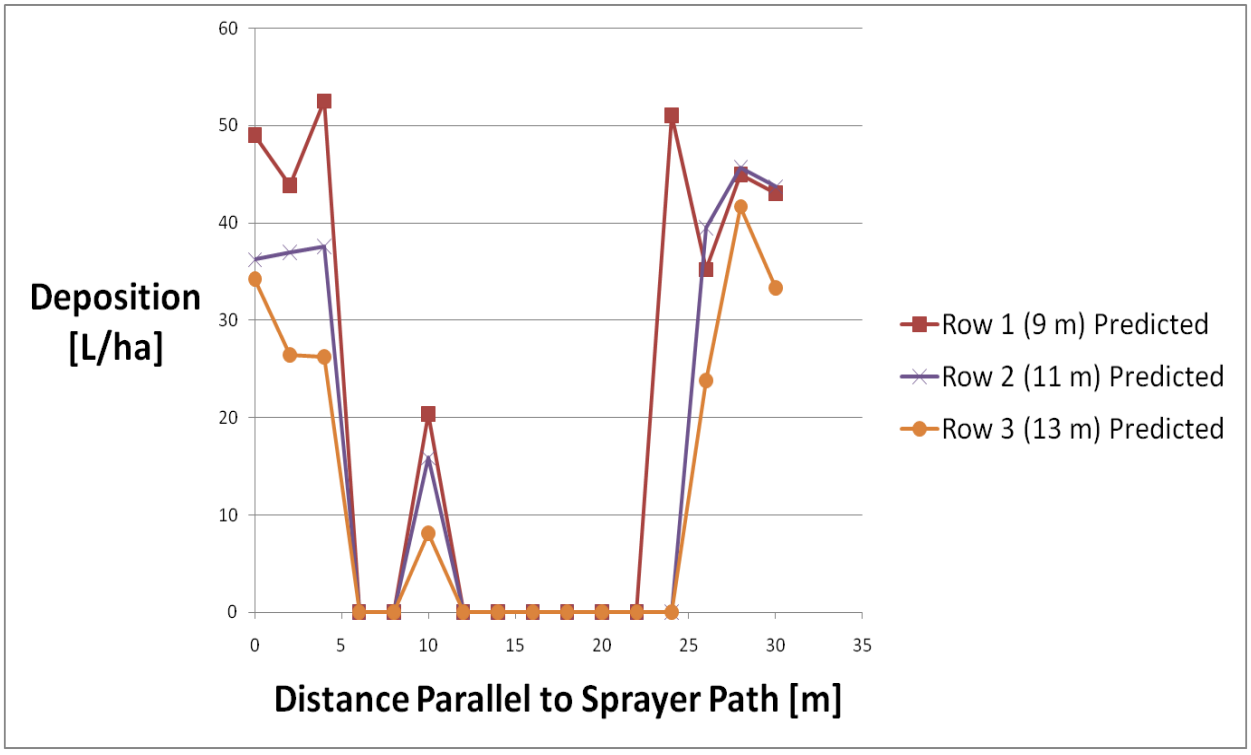

Figure 58. Predicted deposition levels for area "B"

Predicted deposition levels within the sensitive area are zero except for the trigger point seen at 10 m. The decreasing deposition with distance from the boom edge can be seen when comparing the three rows at 10 m. As was the case with area "A", large predicted depositions along the border show the controllers ability to recognize the sensitive area with high resolution and thus preserve efficacy within the swath. A plot of experimental deposition is shown in Figure 59 for comparison to these predicted values.

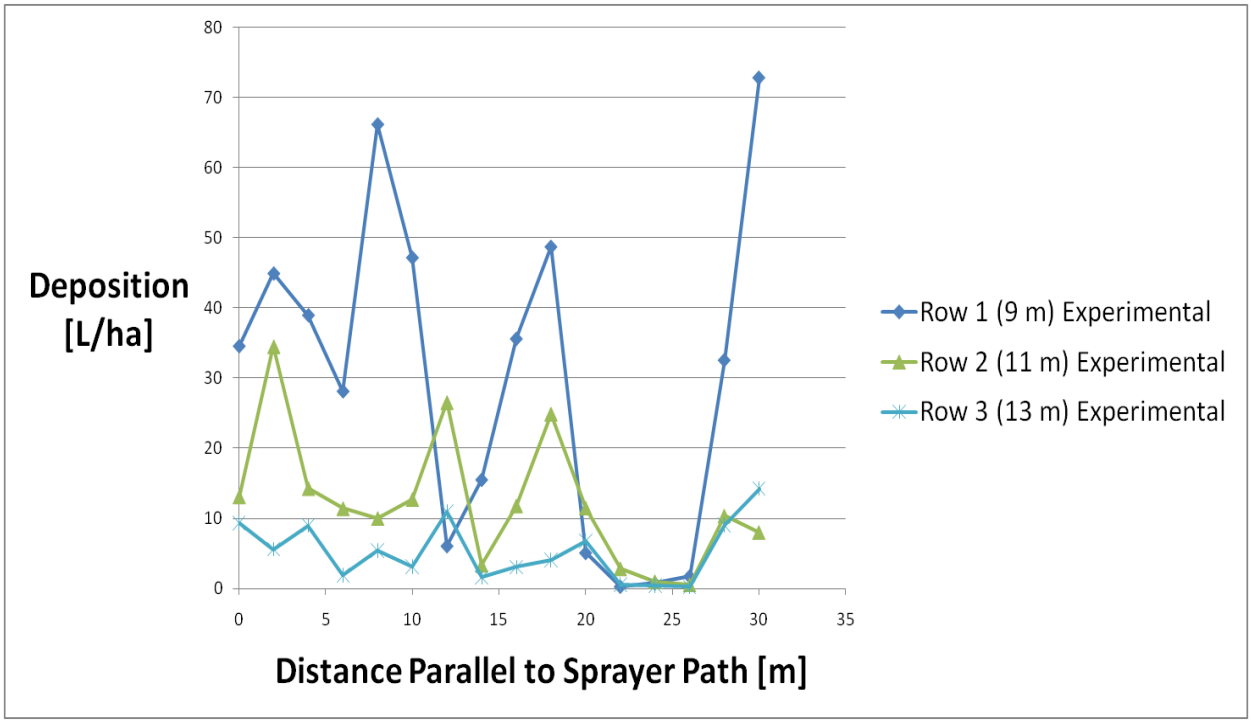

Figure 59. Experimental depositions for area "B"

As in the case of sensitive area "A", the experimental deposition levels for sensitive area "B" display little resemblance to the predicted depositions. With the closer proximity of area "B" to the boom edge, much higher actual levels of deposition are seen than for area "A". With the high sensitivity level specified, the area would be highly contaminated.

The most likely cause for discrepancies seen between the experimental and predicted depositions is an inability of the controller to accurately represent the effects of wind direction on drift. Limitations of the controller in regards to wind direction are seen in two areas, wind direction resolution and the temporal effects of wind.

The controller truncates wind directions to 45° increments in order to simplify the mapping procedure. Truncating wind direction leads to low direction resolution, particularly for areas near the boom edge, and thus an inability to accurately represent the wind impact seen in the field. With 45° increments, true wind direction can be as much as 22° from the represented value. Proof-of-concept testing was conducted on a deemed "stable" day, however over the short duration of testing wind direction was seen to vary by more than 30° from parallel to the card vector as shown in Figure 60.

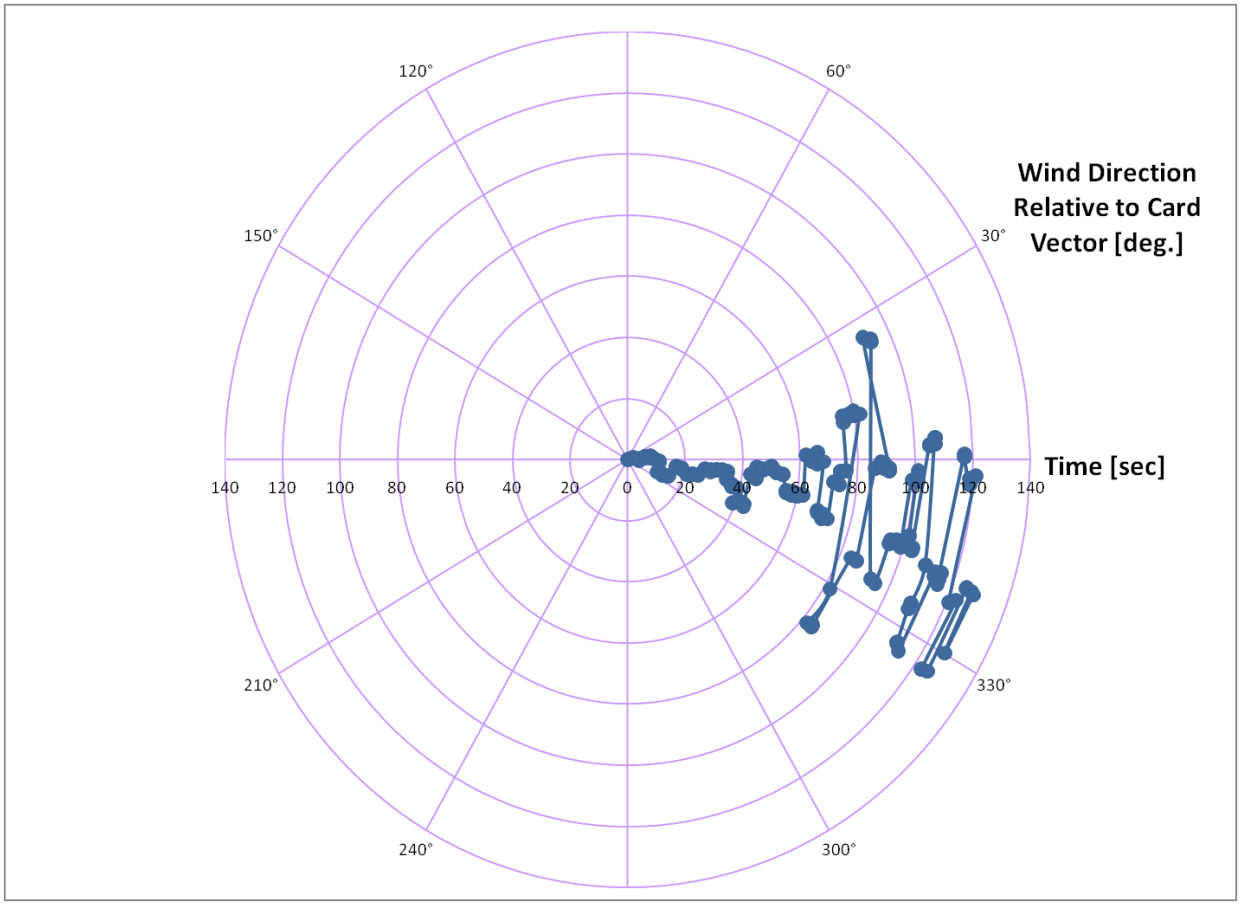

Figure 60. Wind direction variability from parallel to card vectors over proof-of-concept duration

An inability to represent the temporal effects of wind direction on drift is one of the greatest weaknesses of the controller. A single wind direction is assumed to act on each droplet from release until deposit. In reality, the variable nature of wind both in time and space leads to a constantly changing wind direction vector acting on the droplet. The controller's inability to represent the travel direction of a droplet is magnified when observing depositions at greater distances, as wind acts on the droplet for a greater duration. The use of multiple wind directions acting on a droplet is limited by two aspects of the controller. First, the use of multiple wind directions over the trajectory of the droplet would greatly add to the complexity of the prediction algorithm, thus increasing run time. Decreasing update rate has been a theme throughout development of the controller due to its impact on predictive accuracy. Second and perhaps more importantly, an inherent problem is

that the ultimate flight path of a droplet is influenced by subsequent but unknown wind shifts occurring after a droplet is released which cannot be predicted by on-board sensors. Even if the complexity of multiple wind directions could be accommodated and still maintain reasonable real-time speed, the controller cannot look into the future. When a droplet is released, the wind profile which will ultimately act on it during the duration of its flight path has yet to be established. The highly variable nature of drift limits the ability to assume what this profile will be. Based on the test data collected, assuming a wind profile could lead to greater inaccuracies than using a single instantaneously measured wind.

8.2. Predictive Accuracy Testing Results

8.2.1. Qualitative Accuracy Analysis

The five sets of in-field tests generated a large database for use in evaluating predictive accuracy. In terms of statistical properties, the experimental unit within the tests is the card vector, made up of 26 cards. Depositions on individual cards within the vectors are dependent on one another disallowing treatment as experimental units; however depositions amongst vectors are independent, as vectors were spaced so that wind direction deviations did not cause overlap. Results were therefore observed on a card vector basis.

For each of the five tests, predicted and experimental depositions seen within each of the card vectors were plotted for analysis. Figure 61 displays a single card vector representative for each of the five tests. Depositions are expressed as the logarithm of percent deposition calculated as

Equation 16. Drift deposition representation

$$Measure_{displayed} = \mathrm{Log}_{10}\left(\frac{deposition}{application\ rate} * 100\right)$$

Percent depositions were included in the analysis rather than absolute depositions to remove the impact of slight variations in application rate between the five tests and within a single test. The log transformation allows for better viewing of the ranges in deposition encountered within the vector. The lower limit of the logarithm scale was truncated to -2, the corresponding representation of the experimental deposition resolution attained using the scanner.

The model exhibits an overprediction region from around 4 m to 20 m from the boom edge which varies in magnitude between the 5 tests. This “bulging” region was most evident in the highest drift potential case, test 4, and least evident in the lowest drift potential case, test 5, however varies unpredictably for the intermediate three tests. Overprediction quickly transitions to underprediction around 20 m. The underprediction region is predominantly made up of predictions which are zero. Even in the greatest drift potential case, there are no predicted drift deposits beyond 30 m from the boom edge.

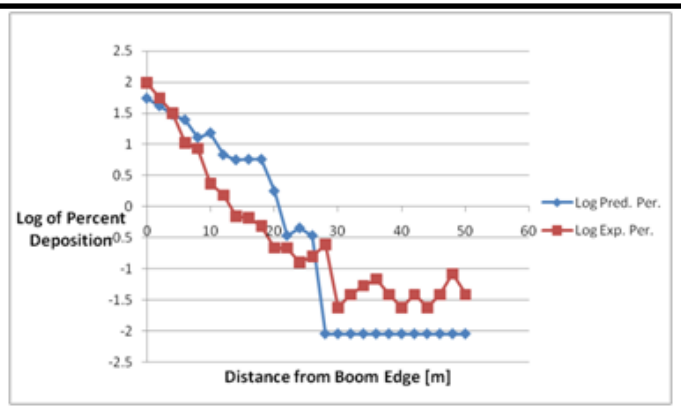

Test 1

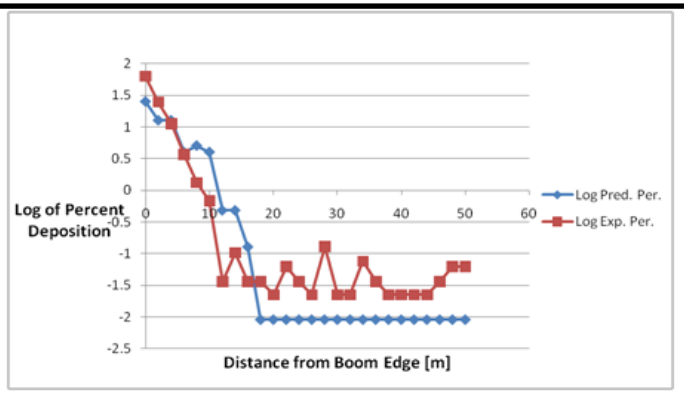

Test 2

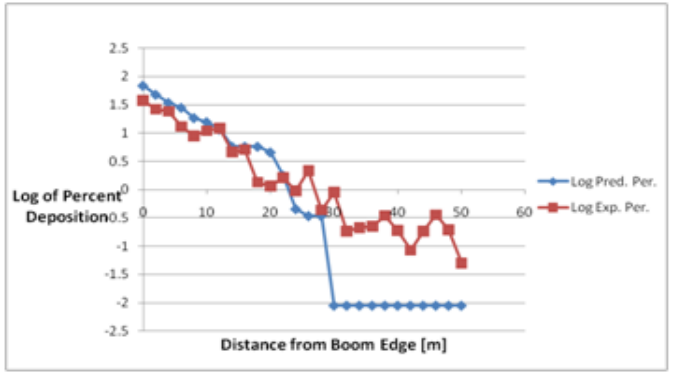

Test 3

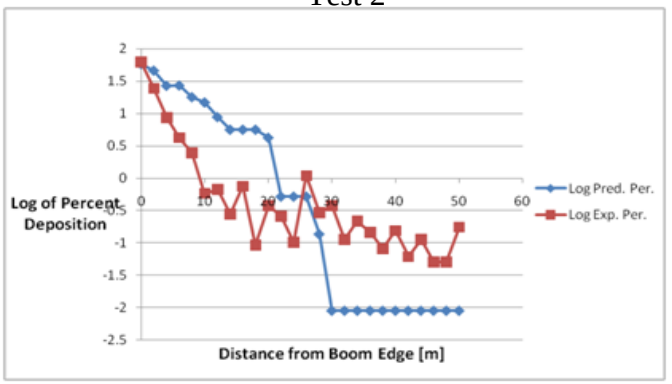

Test 4

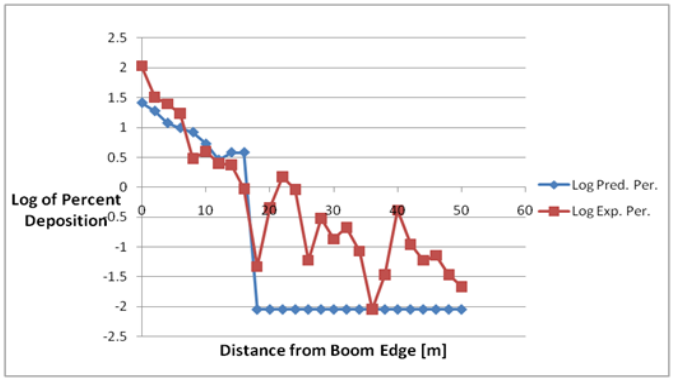

Test 5

Figure 61. Representative predicted/experimental depositions along card vectors compared for each of the five tests

Table 11 compares the average percentage of the volume lost in the form of fallout (deposited) drift for the predicted and experimental measures over each of the five tests. Test 4, the highest drift potential case, produced the maximum predicted drift, however greater experimental drift was seen in test 3. In-field collection cards only account for drift depositing within 50 m of the boom edge. Reduced measured volume in test 4 was likely due to drift which remained airborne beyond 50 m and was not measured. Low predicted and measured drift in test 5 were due to a combination of low drift potential (large droplet sizes, low wind speed, low boom height) and highly variable wind directions encountered during testing. Predicted and experimental drift volumes, and thus percent error, are biased toward representing depositions near the boom edge, as drift deposition decreases exponentially with distance from the boom edge (shown by the linear trends seen in the logarithmic plots of Figure 61). More in-depth analysis is necessary to gauge model predictive ability.

Table 11. Average percent volume lost as fallout drift for each of the five tests

	Percent of Volume Lost				
	Test				
	1	**2**	**3**	**4**	**5**
Predicted	14.44	5.63	22.67	23.00	1.71
Experimental	9.14	8.01	15.87	14.95	3.36
Percent Error	58.10	-29.73	42.85	53.82	-49.23

To determine the variability in depositions, cards from each of the card vectors were combined in distance subsets and plotted with error bars representing the 95% confidence limits at each distance of measure (Figure 62-Figure 65). Based on the method of testing, error bars are not used to draw statistical conclusions as test conditions (wind speed and/or direction) were known to change for each of the 10 card vectors thus inducing known, rather than random error. Additionally the assumption that the logarithmic representation of the depositions follows a normal distribution should be validated to justify using the normal distribution to determine 95% confidence intervals. Error bars in this instance are used to represent variability caused by changing weather conditions in the case of the predicted depositions, and changing weather conditions and random errors in the case of the experimental depositions. Variability analysis was conducted for four of the five test cases.

Test 5, performed with the coarse nozzle, experienced highly variable wind directions during testing, resulting in extremely high degrees of predictive and experimental variability thus it was excluded from the variability analysis.

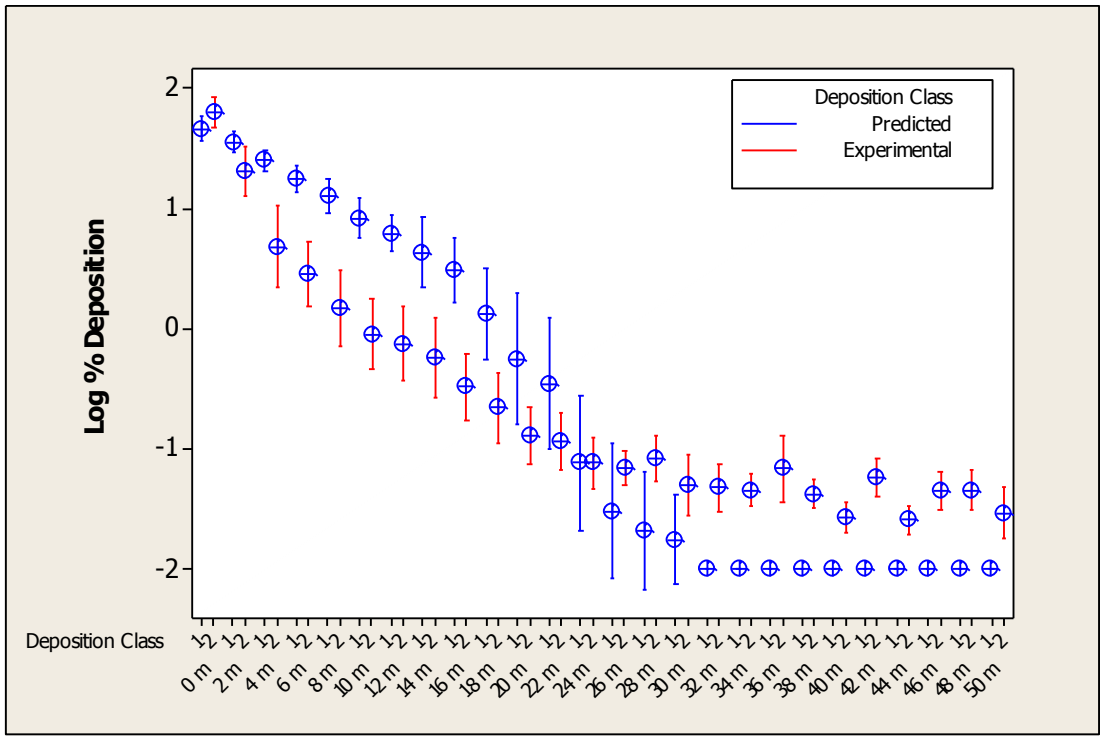

Figure 62. Predicted and experimental deposition mean and 95% confidence interval at each distance from the boom edge for test 1

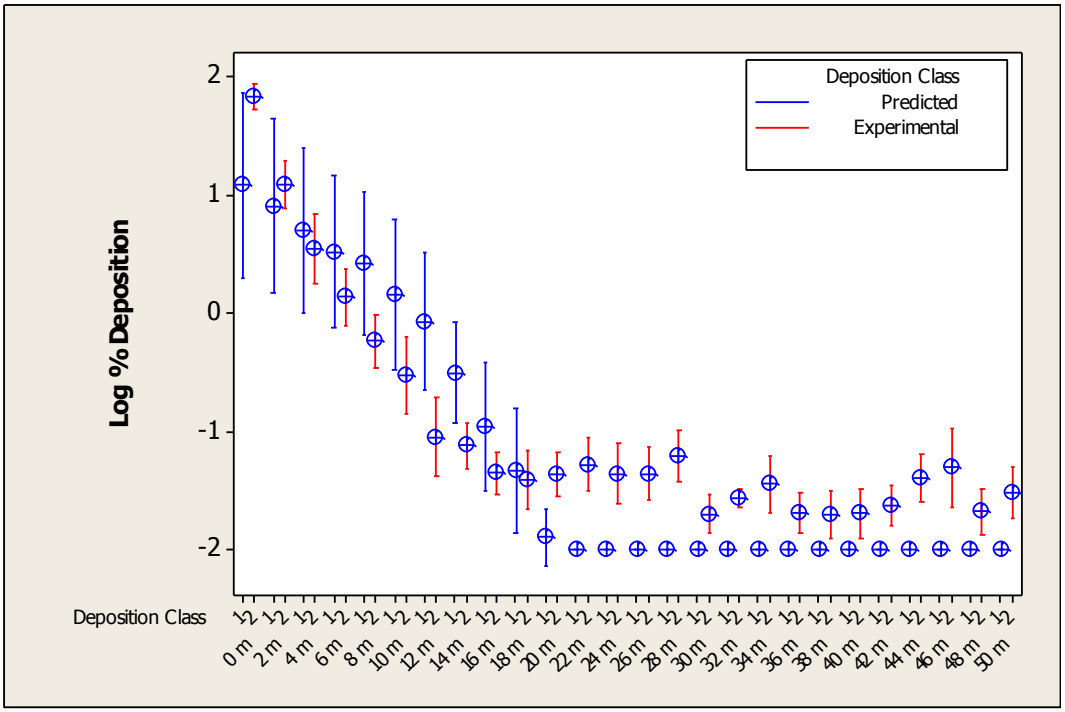

Figure 63. Predicted and experimental deposition mean and 95% confidence interval at each distance from the boom edge for test 2

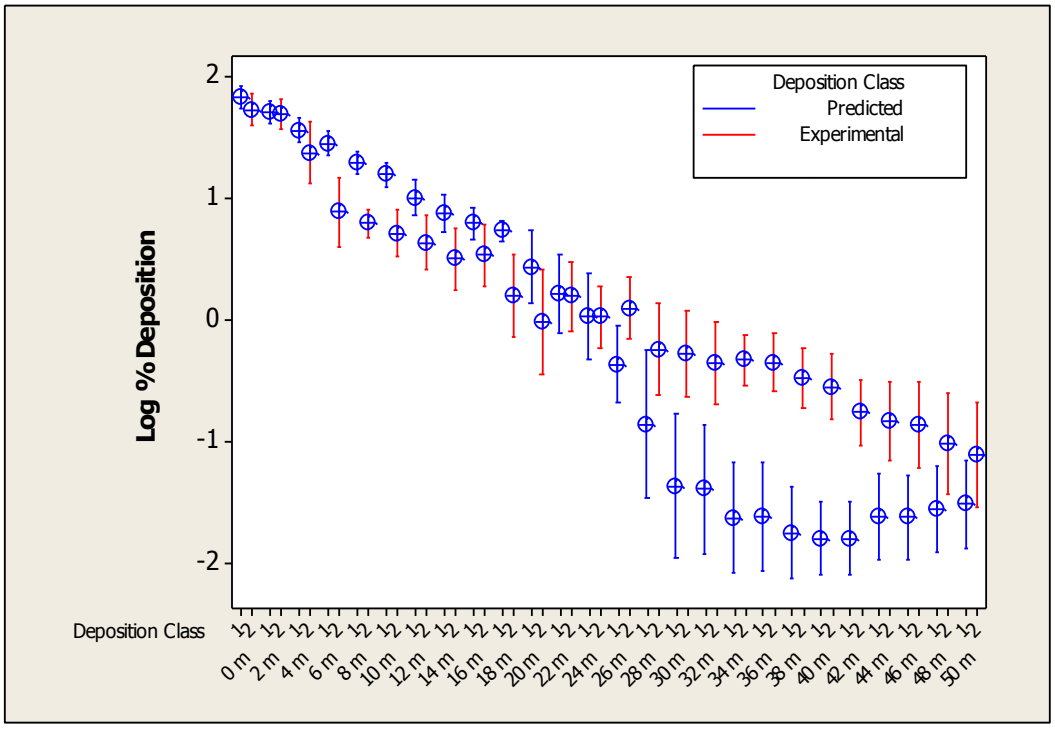

Figure 64. Predicted and experimental deposition mean and 95% confidence interval at each distance from the boom edge for test 3

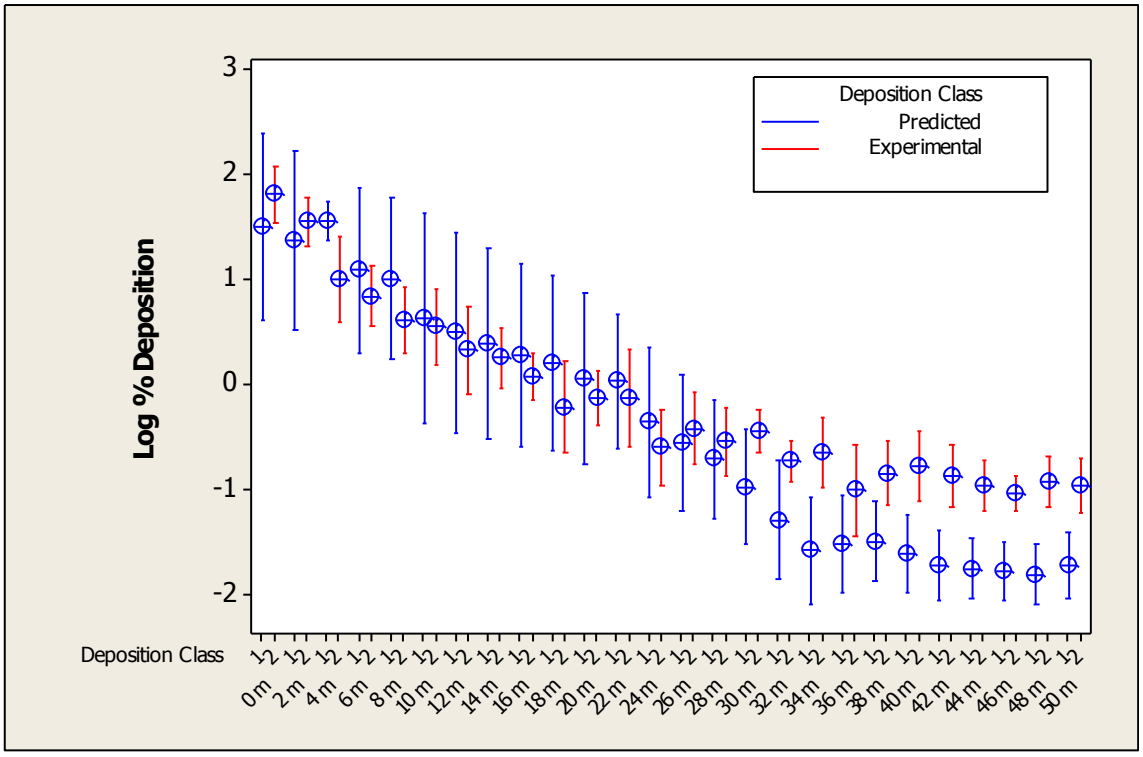

Figure 65. Predicted and experimental deposition mean and 95% confidence interval at each distance from the boom edge for test 4

Mean predicted and experimental deposition levels within the variability plots display the same patterns seen within the single card vector plots (Figure 61). The model generally displays high predictive accuracy in the region near the boom edge (<5 m), possibly as a result of assumed instantaneous wind speeds and directions being more representative of these droplets trajectories. An overprediction bulge, more evident in tests 1 and 2, occurs from 5 m to 20 m from the boom edge where the model then transitions sharply to under prediction. Of particular interest are the surprisingly high levels of variability seen within the predicted depositions. Predicted deposition variability is due entirely to changing weather conditions, most notably wind speed and wind direction, during the testing. The high degree of variability seen in deposition is thus indicative of highly variable wind speeds and directions. For test cases 2 and 4 wind direction shifts were largely responsible for the changes in predicted depositions. For cases 1 and 3 much less predicted variability is seen with the bulge region, due to more consistent wind directions.

Predicted and experimental depositions were plotted three dimensionally to visually determine if there is a direct correlation (“tracking”) between predicted and experimental depositions. The third dimension within the plots is the row number, 1-10. A visual correlation analysis was selected over a quantitative correlation analysis due to the value of spatial viewing.

Plotting the data three dimensionally and on the log scale allows for relative comparisons of deposition at each distance over the 10 rows. A direct correlation between experimental and predicted depositions is indicative of two predictive qualities. First, the predictive model contains variables which are truly representative of the drift phenomenon. Second, the *expression* of the variables within the model are representative of the drift phenomenon. A third predictive quality not evaluated when looking for a direct correlation is model bias, however bias is easier to correct and thus of less interest than the first two qualities.

As the predicted deposition varies mainly with wind speed and direction fluctuations, the direct correlation analysis specifically determines if wind speed and wind direction are good predictive variables of drift. Three dimensional predicted and experimental deposition plots are shown for test 1 (low wind speed) and test 3 (high wind speed) in Figure 66.

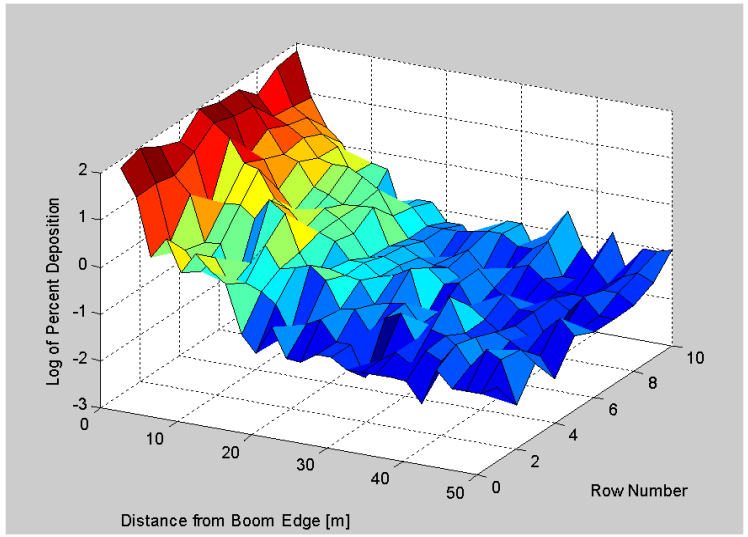

Test 1 Experimental

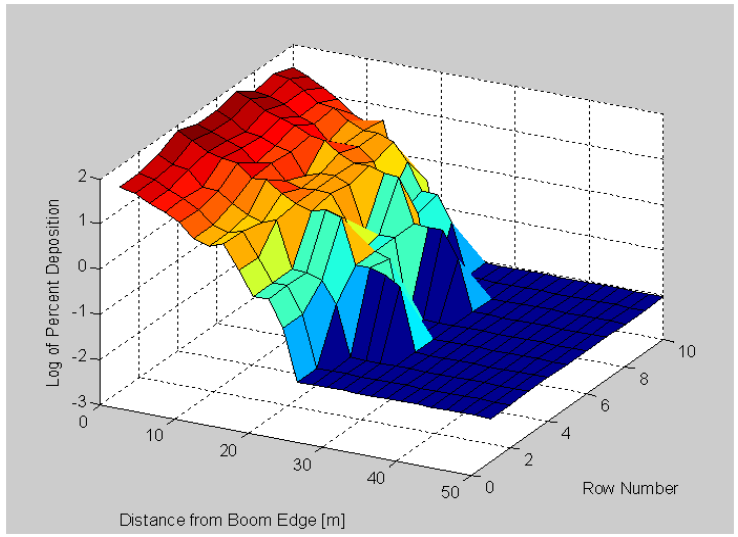

Test 1 Predicted

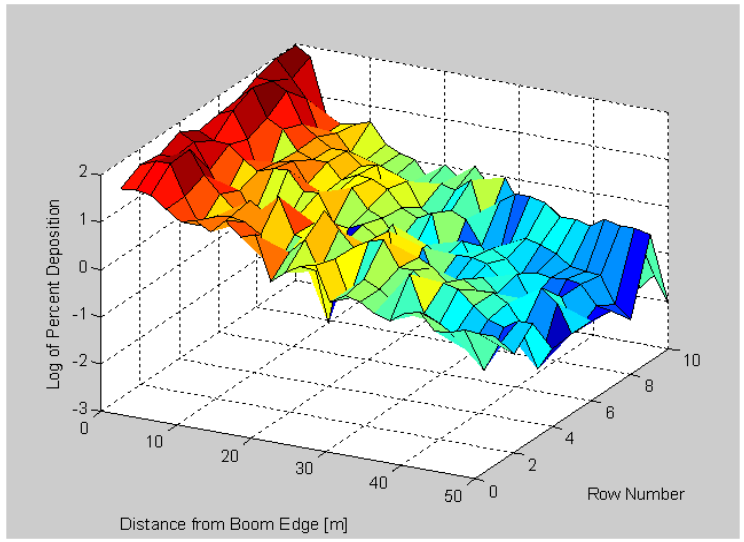

Test 3 Experimental

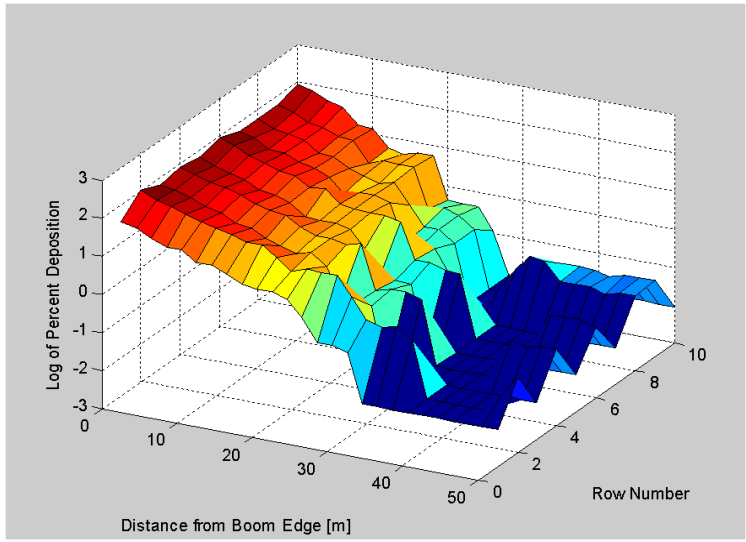

Test 3 Predicted

Figure 66. Visual 3-D correlation analysis for low (Test 1) and high (Test 3) drift potential cases

Predicted deposition for tests 1 and 3 visually were not directly correlated with the experimental depositions. Each card vector within the predicted deposition plots displays a consistent trend. High depositions, relative to the surrounding card vectors, near the boom edge correspond to high depositions at greater distances from the boom edge within the same card vector. In the same manner relatively low depositions near the boom edge translate to low depositions seen at greater distances from the boom edge. The assumed single wind vector acting on each droplet is the cause for these consistencies and rigid prediction plots. A spike in wind direction increases drift as a whole for a vector rather than just near the boom edge as the wind is assumed to act upon all droplets expelled by the nozzle at the instant in which wind speed and direction are measured.

Experimental depositions exhibit an entirely different behavior. Trends in deposition seen near the boom edge do not translate to the same trends seen at greater distances from the boom. Trends do however hold consistent over shorter distances (4-6 m) suggesting that trends seen do in fact exist, and are not due to measurement error which would cause isolated spikes and valleys. As stated earlier during the evaluation of proof-of-concept testing, the effect of wind variability within a droplet's trajectory is the likely cause of a lack in prolonged trends. Droplets which drift large distances from the boom edge are acted upon by different wind vectors than those droplets which deposit soon after release (assumedly the larger droplets). The assumption that a single and consistent wind direction acts upon all droplets is inherently flawed and based upon the data seen within Figure 66, a major contributor to diminished predictive accuracy.

8.2.2. Quantitative Accuracy Analysis

The goal of the quantitative accuracy analysis was to statistically evaluate the drift model's predictive ability. Several approaches were taken to quantify predictive accuracy including more traditional approaches and an innovative method.

8.2.2.1. Correlation

A plot of the predicted deposition versus the experimental deposition for an ideal model would present a straight line with slope of one and *y*-intercept of zero. Data from test 1-4 were combined and a plot of the logarithm of predicted percent deposition versus the log

of the experimental deposition for each card location was generated (Figure 67). As in earlier analysis, test 5 was excluded from the accuracy testing due to the high degree of wind direction and wind speed variability over the test duration.

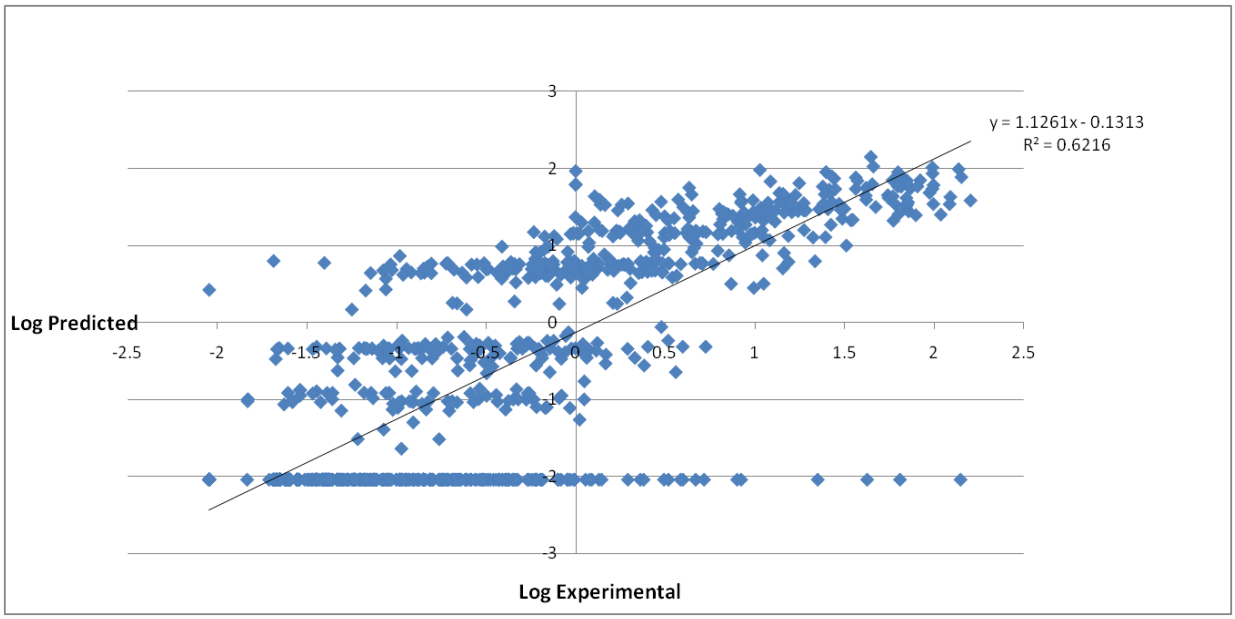

Figure 67. Log of predicted deposition versus log of experimental deposition for tests 1-4 combined with linear regression line

The plot in Figure 67 displays four distinct regions of data, termed regions 1 through 4 referenced from the top of the graph to the bottom. The four regions display horizontal or predicted deposition trends. Region 1, the top region, corresponds to high predicted depositions which occur near the edge of the boom. This region contains a high degree of variability due to the exponential decrease in predicted (and experimental) depositions as one moves downwind from the boom edge. A void area exists between regions 1 and 2 which corresponds to few predicted deposition values of 1-3% (i.e. 10^{0}-$10^{0.5}$). This void region is followed by two middle regions separated by a second void. The two middle regions correspond to predicted deposition levels of around 0.31% and 0.1%, representing predicted depositions typically seen beyond 20 m from the boom edge. According to the clustered nature of these two regions, there is little predicted variability seen in deposition from 20 m to 30 m. Region 4 in Figure 67 represents 0% (i.e. no drift) predicted depositions. As can be

seen in the earlier figures, from 30 m outward, the model generally predicts 0 L/ha deposition even at the high wind speeds seen in the test 3 and 4.

Generation of regions suggests the method of prediction is too discrete. Discrete properties of the model are derived from the use of the grid mapping scheme and ten droplet sizes to represent the nozzle spectrum. Decreasing grid sizes would lead to increased resolution and thus a more area specific representation of drift. A more continuous representation of the droplet spectrum would provide for greater variability in drift distances and thus deposition levels. Additionally, a nozzle spectrum representation which includes greater definition and resolution at the small droplet sizes is required to generate depositions at greater drift distance (>30m) and thus better compare to experimental depositions.

The regression line fit to the dataset has a slope of 1.12, *y*-intercept of -0.1313, and coefficient of determination of 0.62. Nuyttens et al. (2007) performed statistical testing on the correlation coefficient when evaluating the performance of his developed prediction model. In a similar manner for this dataset, a null hypothesis that the correlation coefficient is zero, meaning no correlation between predicted and experimental deposition, is rejected at the 0.01 significance level therefore there is significant correlation between the predicted and experimental depositions.

8.2.2.2. Paired T-test, Application at Individual Distances from the Boom

Statistical testing conducted in order to determine predictive accuracy was based on paired difference t-tests. Paired difference t-tests remove variability which is caused by a certain characteristic of each observable unit. Within the spray drift analysis, pairing experimental and predicted depositions at each location within card vectors theoretically removes variability that is seen between card vectors within a test due to changing wind speed and direction conditions.

A paired difference t-test was conducted on the predicted and experimental depositions at each downwind distance for tests 1 and 3 to determine predictive ability of the model at different distances. The observational unit within this testing is deposition on an individual card as comparisons are being made at each distance, therefore dependence on other cards within the same vector does not violate test assumptions. The null hypothesis in this testing is that the difference is zero, or the experimental and predicted samples are the

same. Failure to reject the null hypothesis however does not conclude that the predicted and experimental depositions are in fact the same, as low confidence levels due to high variability can lead to failure to reject the null hypothesis. Rejecting the null hypothesis concludes that there is a significant difference between the predicted and experimental deposition levels. A summary of the statistical testing conducted at each distance is shown in Table 12, with "x" denoting rejection of the null hypothesis at a significance level of 0.05 (two sided).

Table 12. Summary of paired-difference statistical testing performed for tests 1 and 3 at each distance of drift measure

	p-value (2-sided)		Null Hypothesis*	
Distance (m)	Test 1	Test 3	Test 1	Test 3
0	0.08	0.21		
2	0.02	0.96	x	
4	0	0.36	x	
6	0	0	x	x
8	0	0	x	x
10	0	0	x	x
12	0	0.01	x	x
14	0	0.07	x	
16	0	0.26	x	
18	0.02	0.04	x	x
20	0.07	0.01		x
22	0.11	0.99		
24	0.07	0.62		
26	0.37	0.22		
28	0.86	0.17		
30	0.42	0.11		
32	0	0.01	x	x
34	0	0.01	x	x
36	0.01	0.02	x	x
38	0	0.01	x	x
40	0	0.01	x	x
42	0	0	x	x
44	0	0.02	x	x
46	0	0.03	x	x
48	0	0.07	x	
50	0.01	0.12	x	

*Where an "x" indicates a rejection of the null hypothesis

Both tests 1 and 3 exhibit a region between 20 and 30 m from the boom edge where the null hypothesis is not rejected. The fact that there appears to be high variability within this region (as represented by log transformations in Figure 62 and Figure 64, which actually includes greater variability than that used within the test due to the paired effect) suggests that the failure to reject the null hypothesis within this region is not due to similarities in the predicted and experimental depositions but rather the high levels of variability within the data. As expected, the null hypothesis is rejected for the bulging region of overprediction and the region of underprediction from 30 m to the edge of the boom.

8.2.2.3. Paired T-test, Application at Card Vectors

Analyzing predicted and experimental depositions on a basis of the true experimental unit, card vectors, requires the derivation of a single composite measure characterizing the deposition seen within an entire vector. A measure was derived as follows

Equation 17. Unbiased summation observational unit

$$Observational\ unit = \sum_{i=1}^{26} \frac{Deposition_i}{Average\ Experimental\ Deposition_i}$$

where

$Deposition_i$ = the predicted or experimental percent deposition (depending on the subset of conversion) at card *i* within the card vector.

$Averge\ Experimental\ Deposition_i$ = the average percent deposition at each card *i* distance within the specific test, calculated based on the 10 cards at card *i* position

The derived observational unit provides an unbiased summation of all the depositions within the card vector. Dividing the deposition at each distance by the average experimental deposition at each distance creates a normalized or relative measure of deposition thereby generating the unbiased unit. The average experimental deposition is derived from the in-field test dataset, however in application it can be viewed as an independent scaling factor.

In order to determine the predictive accuracy of the model for tests as a whole, rather than at certain distances, a paired difference t-test was conducted using the differences

between the predicted and experimental derived observational units as objects of testing. The ten card vectors within each test provided ten repetitions with the local variability removed using the pairing method. The null hypothesis within this testing is that that the difference between predicted and experimental observational units is zero. A summary of the results of this analysis is shown in Table 13.

Table 13. Summary of predictive accuracies for each test

	Test 1	Test 2	Test 3	Test 4	Test 5
p-value (2-sided)	0.012	0.004	0.001	0.006	< 0.001
Null Hypothesis	x	x	x	x	x

For each of the 5 cases, the null hypothesis was rejected (as denoted by "x") at the 0.05 significance level. Test 5 had the most significant rejection level, as there was much disagreement between the predicted and experimental depositions caused by high variability within the wind direction throughout the test.

8.2.2.4. Comparison with other Predictive Models

While the predicted depositions were shown to be significantly different than the experimental depositions for each of the 5 tests, such a measure of absolute accuracy does not fully evaluate the usefulness of the predictive model for nozzle control. A relative comparison to other available prediction models is also necessary to determine if an alternative model is available which better matches the in-field collected data. As in the absolute evaluation, both qualitative and quantitative techniques were explored in this analysis.

A single representative card vector was selected from test 1 for use within the qualitative assessment. Predicted deposition at each distance within the vector was calculated using prediction models by Smith et al. (2000b), Nuyttens et al. (2007), Ganzelmeier et al. (1995), Wolf et al. (2001), and Teske et al. (2001). Figure 68 displays a comparison of drift as predicted by each of the models to both the experimental (in-field measurements) depositions as well as the nozzle selection controller prediction model.

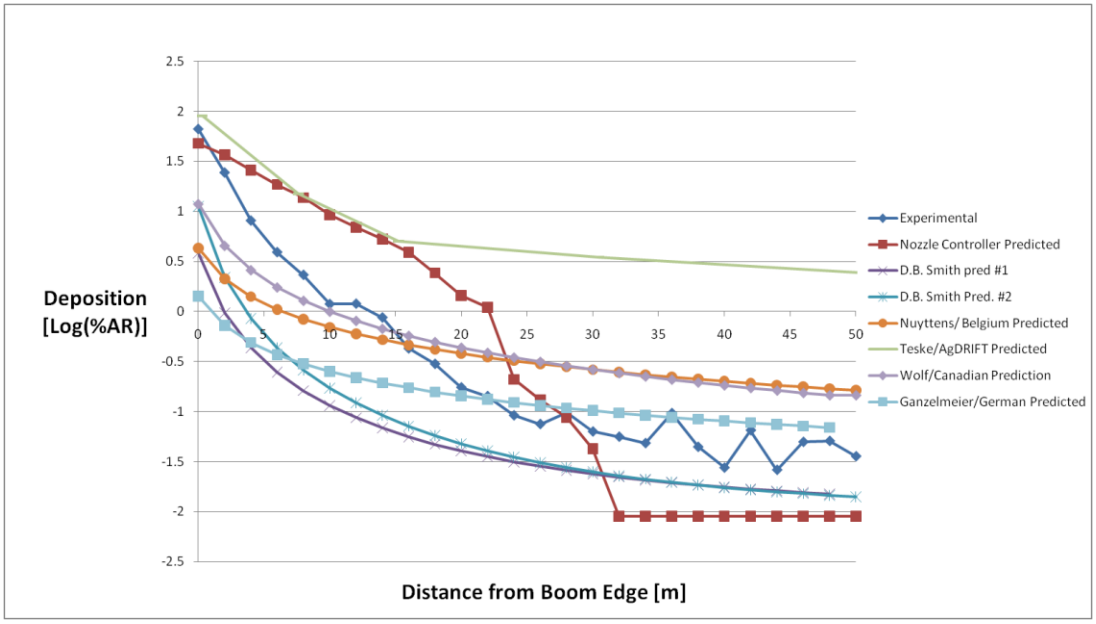

Figure 68. Comparison of alternative drift models to nozzle controller predicted depositions and in-field measurements

The model described by Teske et al. (2001) is that which is used within AgDRIFT®. This model strongly overpredicts drift for the entire card vector. Smith et al.'s two regression models underpredict drift for the entire vector however are relatively good matches to the experimental measures at distances greater than 30 m. The German (Ganzelmeier et al.), Belgium (Nuyttens et al.), and Canadian (Wolf et al.) prediction models exhibit similar behavior, underpredicting depositions near the boom edge then overpredicting at distances greater than 15 m. The German model does a very good job of predicting drift greater than 30 m downwind. The bulge described earlier in the nozzle selection controller's prediction model is clearly evident, and noticeably absent in each of the other prediction models. Overall the Canadian prediction model appears to best match the experimental deposition.

The weather and operation conditions over the duration of test 1 were appropriately applied to each of the alternative prediction models to derive deposition levels within each of the ten card vectors. In the models by Smith et al. and Nuyttens et al., drift depositions are a function of specific operating conditions, therefore unique deposition levels were derived for each of the card vectors. Models by Wolf et al., Ganzelmeier et al., and Teske et al. predict drift for a general set of conditions, resulting in identical depositions in each of the ten card

vectors. For this reason, among this last set of models only Wolf et al.'s was considered in further analysis. Two additional models not included within the qualitative assessment were added to the quantitative assessment. The first model is DRIFTSIM which was used to develop the single prediction equation expressed within the nozzle selection controller. The second model is an extension of the current nozzle controller prediction method. Termed the Static Hybrid prediction model, this alternative predicts drift based on an averaged set of operating conditions over the duration of test 1, resulting in an consistent representation of drift for each of the ten card vectors (similar to Wolf et al.'s model in calculating a constant set of values for each card vector).

Paired difference t-testing was applied to each combination of the nozzle controller's model with alternative models. The goal of such testing was to determine which, if any, of the alternatives are significantly more accurate than the nozzle selection controller current prediction model. Accuracy was defined as the magnitude of predicted error. Predictive error for each model was calculated by taking the absolute value of the predicted measure minus the experimental measure, where the measure is that shown in Equation 17. Paired difference tests were conducted by comparing the predictive error for each of the alternative models to the nozzle controller's model.

The null hypothesis in the predictive error testing was that the predictive error of the nozzle selection controller prediction model is equal to the predictive error of the alternative model. Two alternative hypotheses (the difference between predicted errors is greater than zero, and the difference between predicted error is less than zero) were included to determine which of the predictive models was more accurate. A significance level of 0.05 was required for rejecting the null hypothesis in each of the cases.

Table 14 displays the results of the error testing. A conclusion was drawn for each of the five tests individually and for all tests combined. When a significant difference was encountered between two prediction models, the more accurate of the two models is listed. Failure to reject the null hypothesis is represented by a "-".

Table 14. Statistical comparison of predictive accuracy between alternative models and nozzle controller model NCM=nozzle controller model, NA=not applicable

	Test 1	Test 2	Test 3	Test 4	Test 5	Combined
NCM/DRIFTSIM	DRIFTSIM	-	-	-	-	DRIFTSIM
NCM/Static Hybrid	Static	Static	-	-	-	Static
NCM/Wolf	-	NA	NA	NA	NA	NA
NCM/Nuyttens	-	NCM	-	Nuyttens	-	NCM
NCM/Smith #2	Smith	Smith	NCM	-	-	Smith

Wolf et al.'s prediction model was only compared to the controller for test 1 as the model was not applicable to wind speeds encountered in the other four tests. The prediction model used within the nozzle selection controller was only significantly more accurate than Nuyttens et al.'s prediction model. DRIFTSIM, the Static Hybrid model, and Smith et al.'s prediction methods were all significantly more accurate than the nozzle selection controller prediction method.

Smith et al.'s model accounts for temperature, wind direction, pressure at the nozzles, and application rate in predicting drift. This model was developed from a regression analysis based on limited in-field testing. The model performs surprisingly well considering droplet size, wind speed, and boom height (the three most influential drift variables) are not included within the model.

The Static Hybrid model provided significantly greater accuracy re-enforces earlier conclusions that the nozzle selection controller's predictive model is not able to track in-field changes. Attempting to track the real-time changes, in fact, reduces the controller's accuracy.

Developing the prediction equation from DRIFTSIM data significantly reduced predictive accuracy. Reduced accuracy was evident in earlier development of the regression equation, however it was deemed a necessary tradeoff for increased computing time. A comparative plot of predicted depositions using DRIFTSIM and the nozzle selection controller along with the experimental deposition is shown in Figure 69. Depositions at each distance are an average of the 10 cases from test 1 resulting from the application of each respective method (DRIFTSIM predicted, controller equation predicted, and experimental). The most characteristic discrepancy between the controller's prediction model and the

experimental data, the overprediction "bulge" between 5 and 20 m, is a product of the equation development and was not inherited from DRIFTSIM.

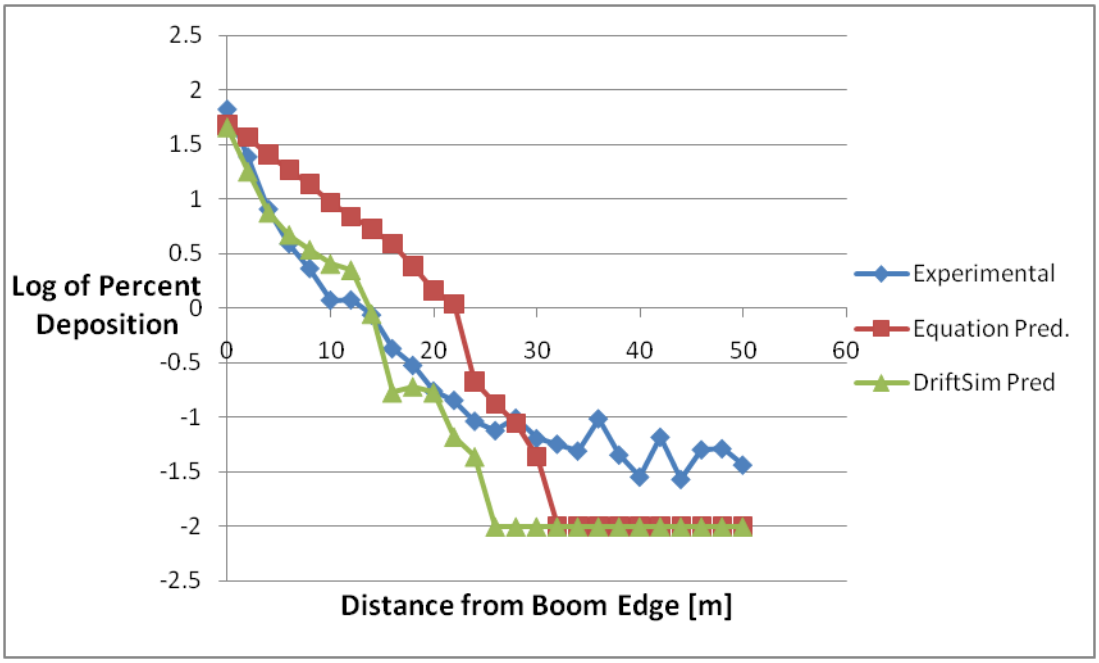

Figure 69. Graphical comparison of DRIFTSIM and controller's predicted deposition at each distance from the boom edge to in-field measurements

DRIFTSIM exhibits high predictive accuracy up to 20 m from the boom edge. DRIFTSIM'S predictions were generated by modifying the prediction algorithm within the nozzle controller to revert back to the "look-up" table method to determine drift distance. The discrepancies in predicting drift at greater distances (>25m) are inherited from the limited definition of the nozzle spectrum, as seen in the regression predictions.

An alternative approach to "looking-up" drift distances was explored to utilize the predictive accuracy of DRIFTSIM seen in Figure 69, while still maintaining a fast run time. Rather than referencing a .txt file for each predictive iteration, DRIFTSIM's lookup tables were read into the program in their entirety upon startup and stored within a large array. Rather than looking at an exterior source, which increases required program executions, predictions are made by referencing the internal array. Computing times observed when implementing this method were nearly identical to the regression method of prediction, however a two minute load time upon startup is required to read in the 28 Mb lookup tables

in their entirety. While this method reduces computing time, the increased RAM and hard drive requirements limits implementation on current field controllers. It is also of note that the direct use of DRIFTSIM data does not alleviate the "tracking" errors outlined in Figure 66, which are inherited by the regression equation from DRIFTSIM, rather than derived from the regression process.

8.3. Error Budget

8.3.1. Controller Errors

The first step in improving the nozzle selection controller is determining sources of error. In answering the question "Is predicted drift greater than acceptable drift", the controller relies on predicted drift levels and established levels of acceptable deposition. Errors are induced to the system through both predicted and acceptable values.

The selected approach to determining levels of acceptable deposition is reliant on toxicity studies of pesticides. As these are cause and effect determined levels with an overall high degree of conservativeness, description within the controller is their most significant avenue of error induction. Increasing the specificity of acceptable drift to sensitive areas would increase overall ability to protect sensitive areas (as opposed to the chosen general approach).

Predicting drift is the fundamental function of the controller. Sources of error in the prediction process are as follows:

- Error of inputs
- Modeling error
- Placement error

Prediction is based on sensor measured, drift influential variables. A 100% accurate prediction model can still be rendered in-effective if the sensors do not provide accurate measures of in-field conditions. An inclusive list of sensors and their approximate accuracies is shown in Table 15.

Table 15. Accuracies of sensors implemented on the test machine

Variable	Error
Wind Speed	± 2%
Wind Direction	± 3°
Temperature	± 1°C
Humidity	± 5%
Boom Height	5%
Pressure	± 0.5%
Flow Rate	± 0.5%
Sprayer position	3 cm

Errors within the wind speed, temperature, humidity, boom height, and pressure values result in errors seen in predicted drift distances. Droplet size, although not measured real-time, misrepresentation can also lead to overall drift distance errors. Nozzle spectrums for the Varitarget nozzles were measured through the use of DropletScan™. A similar imaging software, DepositScan, exhibited up to 33% errors in measuring small droplets (Zhu et al., 2011). Wind direction, flow rate, and sprayer position error reduce accurate representations of both the magnitude and placement of predicted depositions. Wind direction and sprayer position sensor errors are less than positioning resolution thus, within the context of the controller, are low contributors to overall error.

Applying the maximum errors of each of the sensors leads to overall drift distance prediction errors as high as 19%. The high impact of droplet size on drift combined with its high degree of uncertainty places a premium on the incorporation of state-of-the-art methods for droplet size measurement into defining nozzle spectrums.

Modeling errors are derived from two fundamental sources:

- The independent variables used to predict drift are not truly indicative of the drift process.
- The relationship between the chosen independent variables is not indicative of the drift process.

While extensive research has been conducted to determine which variables influence drift, there remains much uncertainty concerning what variable set best characterizes the drift

phenomenon. The interaction of wind and particle motion spatially and temporally is not agreed upon by researchers. Reduced accuracy due to the simplistic handling of wind speed and direction in the controller testing is indicative of an insufficient representation of each of these variables.

The bulge induced by the prediction model, which is noticeably absent within the DRIFTSIM data, is representative of in-exact relationships between the independent variables and drift distance. In this instance, the regression model insufficiently described the variability seen within the DRIFTSIM data, therefore numerical relationship deficiencies were to blame. While developing a more complex regression model would possibly increase predictive accuracy, there are two properties of the deriving dataset which limit the attainable predictive accuracy. First, developing a regression model for a wide range in operating conditions results in a very general representation of drift. The more general the dataset, the more variably the model must account for, thereby reducing accuracy at a specific set of operating conditions. Second, the deriving dataset inherits a degree of "randomness" from the random-walk model, generating contradictions within the deriving dataset. Regardless of the complexity of the regression model, contradictions in data cannot be accounted for and will reduce overall predictive accuracy. In addition to errors induced from the derived regression model, in-exact representation of relationships in the Fluent model employed to develop the dataset are also a source of error.

Placement errors are related to assumptions and simplifications within the mapping algorithm. A list of crucial assumptions which reduce predictive accuracy is as follows:

- A single wind direction at the time of release of each droplet is responsible for the droplets travel path.
- Wind direction increments in 45° intervals.
- A single deposition occurs over an entire grid cell.
- Droplet spectrum is sufficiently defined by ten droplet size classes.

8.3.2. Experimental Data Errors

In the comparison of predicted depositions to experimental depositions, the experimental depositions were considered to be known (i.e. true measure of the drift

phenomenon). In reality errors are made in field measurements which are both random and systematic. Systematic error is of greater concern as its effect is consistent across the entire dataset and can lead to inaccurate statistical conclusions.

DropletScan™ had been verified previously by several researchers for quantifying deposition on Kromekote cards. Confidence in the accuracy of this method has been called into question with the recent study of the accuracy of a related scanning software, DepositScan, in determining sizes of small droplets. Due to the high driftability of small droplets, the majority of droplets analyzed on collection cards within the study are considered "very fine" therefore accuracy in measuring the size of small droplets is critical to the validity of the experimental study. A comparison of the average depositions measured for test 1 to data collected by Wolf and Caldwell (2001) under similar conditions is shown in Figure 70. In Wolf's testing, concentrations of dyes measured within petri dishes were used to quantify drift. Wolf data displays similar characteristics to that evaluated using the DropletScan™ increasing confidence in experimental accuracy.

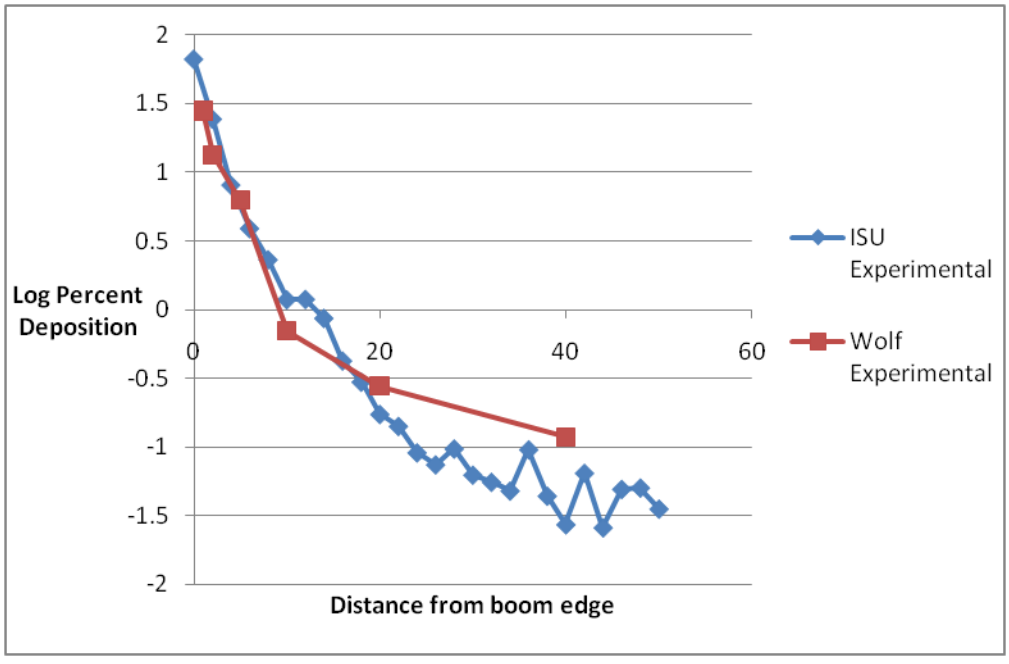

Figure 70. Comparison of experimental depositions obtained from test 1 to in-field measurements by Wolf and Caldwell (2001).

8.4. Methods for Improvement

One of the most challenging aspects of drift prediction is handling the effects of wind speed and wind direction. Wind speed generates a drag force on the droplets propelling them in the direction specified by the wind direction vector. Within the nozzle selection controller, it was assumed that initial or release wind speed and direction acted on each droplet for the duration of its trajectory. The inability of the nozzle selection controller to consistently agree with trends of field measured deposition suggests that this method of representing the effects of wind on the droplets is invalid. Additionally the static prediction model was significantly more accurate than the dynamic model, therefore accuracy of the system was decreased using an approach of relatively faster real-time wind updates for prediction.

An analysis of the response of in-field measured deposition to changing wind speed and direction was performed in order to gain a better understanding of how temporal and spatial wind speed and direction measurements impact deposition. Specifically, alternative methods to representing wind speed and direction influences over time as well as the time durations for which wind speeds and directions act on a single droplet were analyzed.

Depositions at 2 m ("near-field drift") and 20 m ("far-field drift") from the boom edge were selected as focal points for the experimental deposition analysis. As previously mentioned, trends in deposition were not consistent throughout a card vector, as seen in Figure 66, due to different wind profiles acting on droplets deposited at each distance. Division into a near-field and far-field case allows for more distance-specific analysis.

The drift controller's prediction method neglects the influence of wind speed and direction vectors acting on a droplet after release. An inability of the prediction model to track with experimental depositions suggests that representations of both wind speed and direction occurring after the droplet's release are necessary for truly predicting the drift distance of a droplet. A *wind speed effect* and *wind direction effect* variable were defined to provide a simplistic temporal representation of wind speed and direction respectively as follows:

Equation 18. Wind speed effect

$$wind\ speed\ effect_t = \frac{\sum_{i=0}^{N} wind\ speed_{t+i\Delta t}}{N+1}$$

Equation 19. Wind direction effect

$$wind\ direction\ effect_t = \frac{\sum_{i=0}^{N} wind\ direction_{t-i\Delta t} - \sum_{i=0}^{N} wind\ direction_{t+i\Delta t}}{2(N+1)}$$

where:

t=instance in time

Δ*t*=inverse of the system update rate, i.e. 2 seconds

N=interval of consideration

$Wind\ speed\ effect_t$=the wind speed effect measured at an instance in time (e.g. units, m/sec)

$Wind\ speed_{t+i\Delta t}$ =the wind speed *i* time steps after an instance in time

$Wind\ direction\ effect_t$ = the wind effect at sampling time *t* (e.g. units, degrees)

$Wind\ direction_{t-i\Delta t}$ = the non-truncated wind direction *i* time steps before sampling time *t*

$Wind\ direction_{t+i\Delta t}$ = the non-truncated wind direction *i* time steps after sampling time *t* measured

The *wind speed effect* is simply an average of the wind speeds from *t* to $t+N\Delta t$, thus generating a composite representation of future, relative to a droplet released at *t*, wind speeds which act on a droplet. Based on its definition, it is hypothesized that *wind speed effect* is directly related to the drift distance of a single droplet as well as experimental deposition at time *t* (where *t* maintains both spatial and temporal implications).

The *wind direction effect* variable attempts to represent the cumulating or concentrating nature of wind direction. In regards to drift, it is hypothesized that *wind direction effect* would be directly related to experimental deposition caused by the wind carrying droplets from other locations within the field to the position of measure. Both past (t-$i\Delta t$) and future ($t+i\Delta t$) consideration of wind directions are required to capture this cumulating effect of wind direction. It is of note that the *wind direction effect* does not directly represent variable wind directions which act on a *single* droplet released at time *t*, but

rather variable wind directions acting on *multiple* droplets released from time $t\text{-}N\Delta t$ to $t+N\Delta t$. This method of representing the wind direction effects at an instant in time t, removes the spatial transformations which are otherwise generated if observing the influence of variable wind directions acting on a single droplet. The *wind direction effect* variable however is an indirect measure of this phenomenon, and was assumed within the following analysis to be a suitable representation of the varying wind directions acting on a single droplet. A visual representation of the functionality of the *wind direction effect* variable, in context to the methods of experimental measurement, is shown in Figure 71.

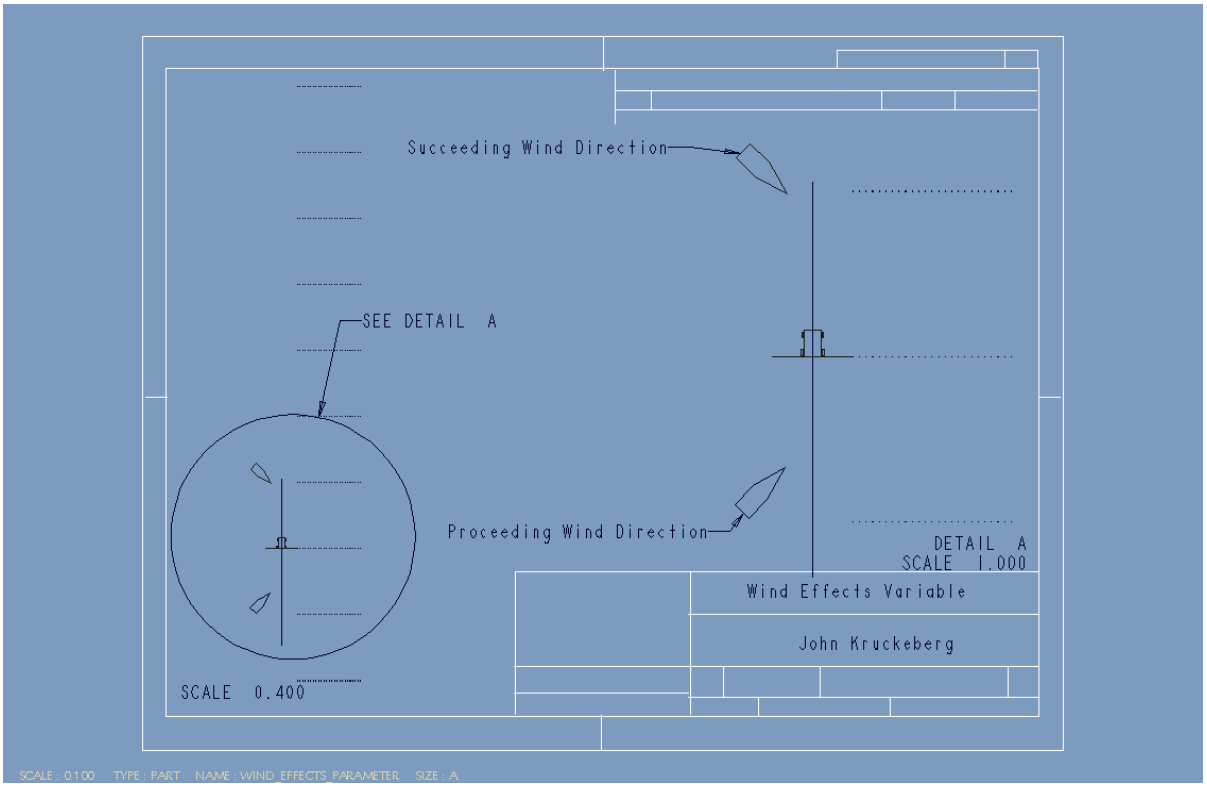

Figure 71. High magnitude wind direction effect example

The case shown in Figure 71 would result in a high magnitude *wind direction effect* value and a hypothesized high level of experimental deposition at the card vector perpendicular to the shown sprayer position (at time t). Proceeding wind directions (at $t\text{-}i\Delta t$) would have positive values and thus have a net positive effect on the *wind direction effect* variable, while succeeding wind directions ($t+i\Delta t$) would have negative wind directions

however due to subtraction would also have a net positive effect on the *wind direction effect* variable

Droplets which deposit near the boom edge (2 m) remain suspended in the air for relatively little time when compared to those which drift to long distances (20 m). Based on the terminal velocity analysis summarized in Figure 8, a 50 µm diameter droplet (a medial droplet size classified as highly driftable) would require four seconds to travel the vertical distance equal to the boom height established during in-field testing. The *wind speed effect* was calculated at each sampling instance based on a time duration (defined as $N\Delta t$ in Equation 18) of four seconds and is shown plotted with the experimental deposition at 2 m from the boom edge in Figure 72 for tests 1-4.

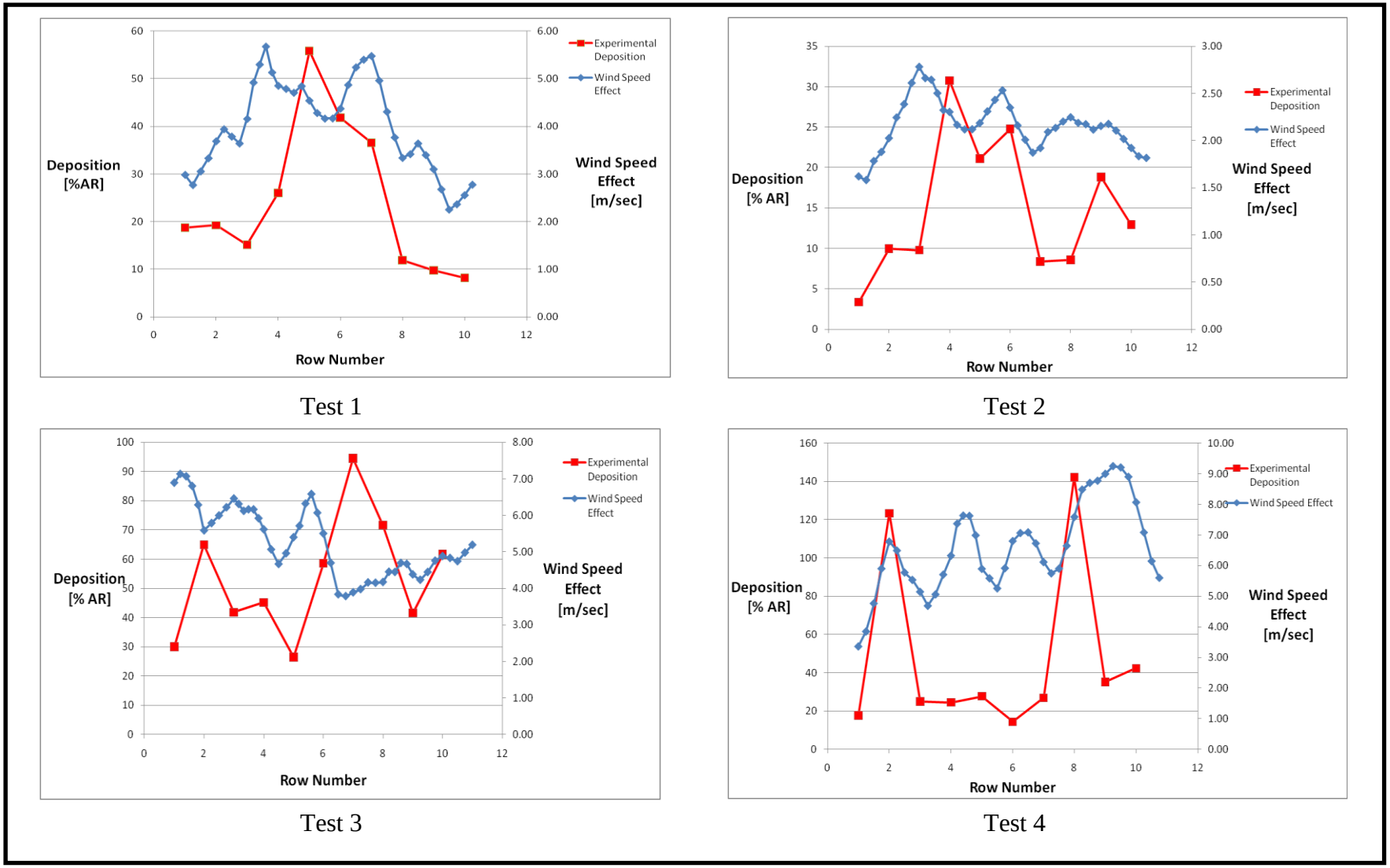

Figure 72. Graphical correlation between experimental deposition at 2 m from the boom edge and the wind speed effect calculated based on a duration of 4 seconds

Tests 1 and 2 suggest relationships between the *wind speed effect* and the experimental depositions, however these same trends are not existent in tests 3 and 4. Additional time durations were applied to the *wind speed effect* variable and plotted with experimental deposition however none of the alternatives explored provided a significant visual upgrade in trending with the experimental deposition.

In a similar manner, time durations were applied to the *wind direction effect* variable and plotted with experimental deposition located at 2 m. The most significant visual trending between the *wind direction effect* and experimental deposition occurred when a duration of 4 seconds was applied (as in the *wind speed effect* case). Plots of the *wind direction effect* and experimental deposition are shown in Figure 73 for tests 1-4.

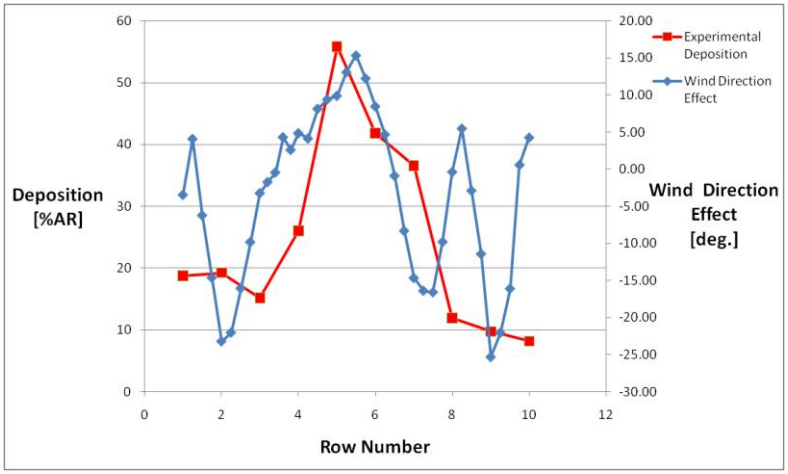

Test 1

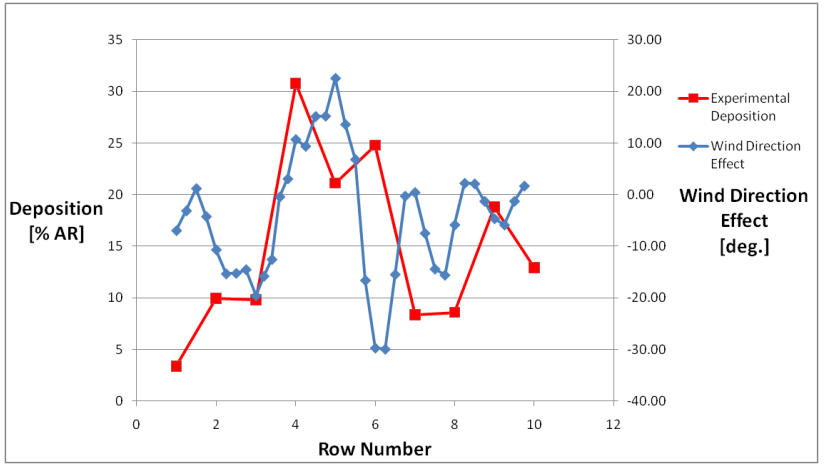

Test 2

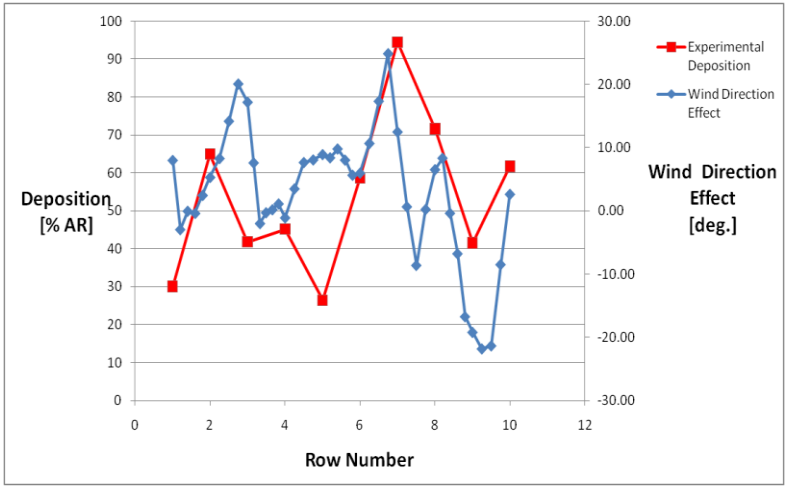

Test 3

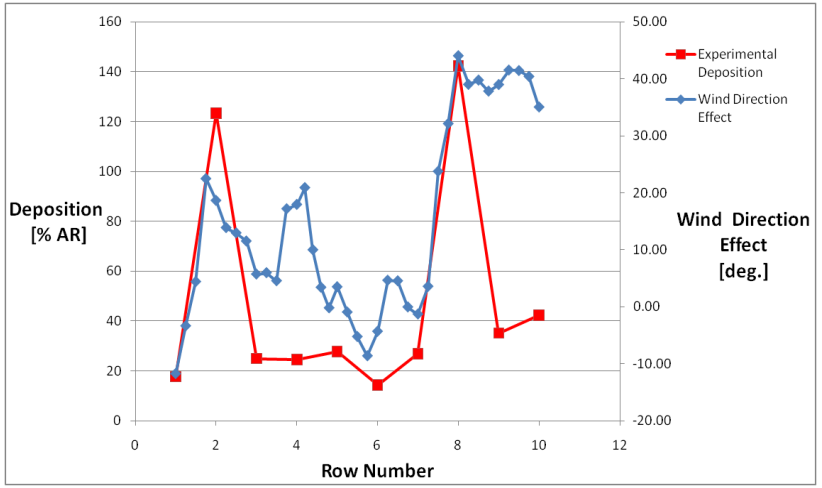

Test 4

Figure 73. Graphical correlation between experimental deposition at 2 m from the boom edge and the wind direction effect calculated based on a duration of 4 seconds

The trends within each of the four tests suggest a direct relationship between the *wind direction effect* and experimental deposition. It is important to consider the limited resolution in the experimental deposition when analyzing the datasets as there were only ten rows of card vectors thus only ten measures. Random or systematic error within the experimental dataset can lead to false conclusions being drawn with a limited resolution. In spite of this limitation, the observed relationships are worthy of note. Trends seen in each of the four tests show potential increased predictive accuracy if the temporal effects of wind direction are incorporated within the model.

Spearman's correlation coefficients for *wind speed effect*/experimental deposition at 2 m, *wind speed effect*/experimental deposition at 20 m, *wind direction effect*/experimental deposition at 2 m, and *wind direction effect*/experimental deposition at 20 m pairings were calculated for a range in time durations considered for both the *wind speed effect* and *wind direction effect* variables. The dataset for which this analysis was conducted was composed of weather conditions and experimental depositions from tests 1-4 combined. Varying time durations represent different time periods for which wind speed and direction are considered to be acting on a single droplet. Spearman's correlation coefficient is a measure of the degree to which either the *wind speed effect* or *wind direction effect,* calculated based on each respective time duration, explains the experimental deposition. Specifically, Spearman's correlation coefficient characterizes the degree to which the relationship between the respective variable and experimental deposition is explained by a monotonic (maintaining a given order) function. A summary plot of the correlation coefficients versus the time duration considered for each pairing is shown in Figure 74.

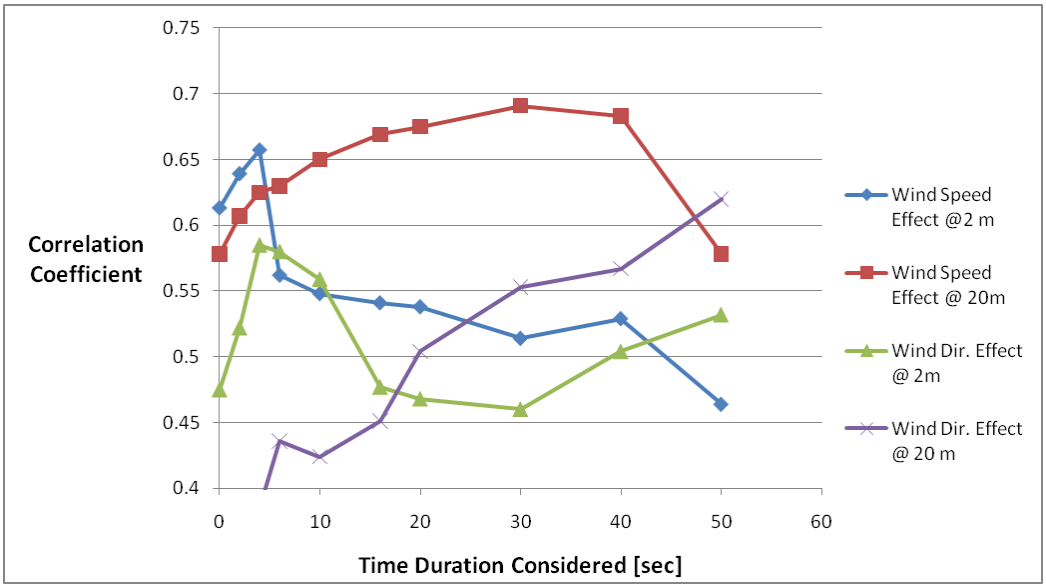

Figure 74. Correlation coefficients versus time duration for pairings of wind speed effect and wind direction effect with experimental deposition at two different locations from the boom edge

Correlation coefficients for the *wind speed effect* and *wind direction effect* coupled with deposition at 2 m were maximized at a four second duration (as was seen in the visual correlation analysis). Correlation with the deposition at 2 m decreased for both increasing and decreasing durations around 4 seconds signifying the optimal ability of the four second duration to capture the impacts of wind speed and direction on drift at short distances. This result is consistent with the earlier hypothesis that droplets which deposit near the boom edge are acted on by wind speeds and directions for relatively short time durations. At far-field distances (20 m), the correlation coefficient for the *wind speed effect* and deposition reached a maximum at a 30 second time duration. The decrease in the correlation coefficient for increasing durations (beyond 30 seconds) considered suggests that wind speeds occurring greater than 30 seconds after release do not have an impact on the drift distance of a droplet released at an instance in time. The *wind direction effect* correlation to deposition displays continued increasing trends even at 50 seconds of duration. Limited recorded weather conditions before and after test runs restricts the ability to consider greater durations.

Figure 74 is indicative of the extensive time durations which must be considered to truly determine the deposition at any point within the field. Additionally, depositions at

different distances from the boom edge require varying durations of considered wind speed and direction. In the context of a drift controller, information concerning wind speed and direction up to 30 seconds (and possibly greater for wind direction) after an instance time are required to make prudent decisions concerning which nozzle should be used for application. In its current form, the nozzle controller's method of describing drift is a modeling approach based on conditions encountered at the release time of a droplet. The results summarized in Figure 74 indicate that true representation of the drift phenomenon requires both modeling and predictive capabilities which describe future weather conditions. Further research is necessary to develop these predictive capabilities.

8.5. Conclusions

The following conclusions were drawn based on the proof-of-concept and accuracy testing results:

- The nozzle controller theoretically protects sensitive areas from excessive amounts of drift by correctly transitioning nozzles based on predicted drift deposition levels. Oversimplified and under-characterized wind interactions within the predictive model however limit the controller's ability to protect sensitive areas in practice.
- For the tested weather conditions and sprayer application setup, the developed prediction model within the nozzle controller is significantly different than the drift phenomenon occurring in the field.
- Significant biasing error is generated within the controller's prediction algorithm by the development of a regression equation from the DRIFTSIM data. When implemented using the appropriate techniques, direct use of the lookup tables offers improved predictive accuracy with identical run times when compared the regression equation method.
- A low resolution representation of a nozzle's droplet spectrum (i.e. 10 droplet size classes) generates systematic predictive errors. As very fine droplets are responsible for far-field drift, a high resolution expression of droplets less than 150 μm is critical for predicting drift which deposits greater than 20 m from the boom edge.

- Attempting to account for real-time operating conditions with a single release wind speed and direction characterizing the air drag effects on a droplet significantly reduces the controller's predictive accuracy. Prediction based on generalized weather conditions held constant over testing as well as a more simplistic model by Smith et al. (200b), which does not attempt to capture the highly variable nature of wind speed, produced significantly greater predictive accuracies than that of the nozzle controller in its current form.
- In order to accurately represent drift on a real-time basis, knowledge of wind speed and direction profiles up to 30 seconds after a droplet is released are required. In the context of the nozzle control process, a truly predictive approach to evaluating drift is necessary rather than the current controller's drift modeling method.

Chapter 9. Conclusions

Increasing spray drift regulations in the United States and abroad have placed a focal point on implementing best management principles when spraying to reduce drift. Spraying with a large droplet size has been shown to be the most effective measure in limiting the amount of off-target drift. The use of large droplet sizes however does not come without a cost, as large droplets can reduce efficacy, costing farmers and applicators both time and money. In order to balance drift and efficacy, state-of-the-art drift reduction technologies inform applicators of the real-time magnitude and potential effects of drift, allowing for the selection of droplet sizes on an as-needed basis. The principal component of these controllers is a drift prediction model which provides real-time drift potential.

With the decision making process and mode of action controlled solely by the applicator, nozzle selection is both subjective and inefficient. Establishing a scientific, objective basis for nozzle selection is a critical step for the future development of automated nozzle selection controllers which fully optimize the balance between drift and efficacy.

Information requirements for automated real-time nozzle selection were reviewed, developed, and packaged for use within a nozzle selection controller. An exemplary controller was designed, implemented, and tested to evaluate feasibility and quantify performance.

9.1. Results

Further development of existing drift prediction models was the first step in generating a basis for real-time nozzle selection control. Current drift prediction methods, including those in state-of-the-art real-time prediction settings, do not possess the run-time or mapping capabilities required for real-time nozzle control. A prediction equation and mapping algorithm were developed for use in nozzle control, and testing was conducted in the lab to evaluate the impact of highly influential drift variables and overall performance.

Large impacts of boom height, wind speed, selected nozzle, and wind direction were observed in the lab tests. A GPS simulator was linked to the controller and the combined system performed as an effective tool in simulating in-field spraying events. Test files recorded by the program displayed the ability of a nozzle selection controller to be used for both educational and regulatory purposes.

Decision making for real-time nozzle selection control is a specialized risk assessment process. EPA's current risk assessment methods were reviewed and integrated into the controller. The basis for protection of sensitive areas is derived from toxicity studies. A simplified approach was developed for nozzle selection, as a tier 1 example for future development of more sophisticated models. Generalized high, medium, and low sensitivity categories were establish for common pesticide/sensitive area combinations. It is anticipated that as the EPA continues to develop more specific regulatory measures, possibly for direct use by decision making controllers, a more inclusive dataset of acceptable drift to sensitive areas would be established. Such a dataset could be easily incorporated into the controller for a more inclusive and specific approach to the protection of sensitive areas.

A range in droplet sizes where efficacy of pesticides is maintained was derived from a literature review. Contrary to popular belief, multiple studies showed medium droplet sizes of fungicides and insecticides optimize the balance between droplet energy for canopy penetration and leaf coverage thereby maximizing efficacy. The relationship between droplet size and efficacy is dependent on the mode-of-action of the pesticide, however conflicting studies suggest that to truly optimize efficacy, one needs to equally consider the specific active ingredient of each pesticide. Within the nozzle selection controller, an assumed "smaller is better" methodology was implemented such that when drift is not a concern, fine droplets may be selected for application. The prototype controller was implemented with a default nozzle selector for applicator entry of an override to the highest efficacy nozzle.

A controller was developed and implemented on a self-propelled sprayer in the form of a prototype automated nozzle controller. In-field testing was conducted in order to display proof-of-concept and evaluate the controller's predictive accuracy. The controller was found to theoretically protect sensitive areas based on predicted drift, however overly simplistic and unrepresentative characterizations of the drift phenomenon limits the ability of the controller, in its current state, to maintain acceptable levels of deposition within sensitive areas.

The use of release wind speed and direction to represent full trajectory wind influences was identified as a major source of error within the controller predictions. Real-time updated weather condition inputs to the model significantly reduced predictive accuracy, as release wind speeds and directions are limited indicators of trajectory-duration

wind conditions. Developed wind speed and direction effects variables which account for the changing wind conditions after a droplet's release were shown to be more explanatory and directly related to experimental depositions.

The following specific conclusions can be made from this work:

- In evaluating drift in a discrete domain, a high resolution description of the nozzle spectrum is critical toward achieving overall high predictive accuracy. A high fidelity representation of the spectrum for very fine droplets (<150 μm) is of particular importance as smaller droplets are the predominant subjects of long distance spray drift.
- Representing the spray drift phenomenon in the form of a single regression equation based on a broad scoped dataset is a challenging, multifaceted endeavor. Limitations in generating a highly specific model while accounting for the complex, even random nature of drift, suggest alternative methods of describing spray drift are necessary. While initially perceived as being an inefficient method of prediction, lookup tables (the raw form of the regression models) generated from previous, in-depth drift analysis are one possible alternative.
- Accurately representing drift on a micro-scale (every few seconds and for high spatial resolutions) for control processes requires true drift *prediction* rather than merely *modeling.* Modeling describes mechanistic phenomenon, while prediction attempts to represent future occurrences. As the trajectory of spray droplets are influenced by highly variable weather conditions (most notably wind speed and direction) occurring after release, the prediction scope should include a representation of these future variables.
- For droplets drifting long distances from the boom edge (>20 m), test data suggests that droplets are influenced by wind speed and direction for durations of 30 seconds or more after release. Characterizing conditions for such long durations is a major hurdle which must be overcome prior to implementing a nozzle controller on a micro scale.

9.2. Recommendations for Future Research

Research into the following areas would generate valuable understanding for the further development and improvement of the automated nozzle selection control process:

- Investigate the impact of increased controller resolutions, both mapping and nozzle spectrum description, on predictive accuracy.
- Determine the effects of turbulent activity near the boom on drift. Turbulence generated by the sprayer chassis and boom leads to complex droplet trajectories. Research conducted to better understand the impacts of turbulence on drift is necessary to further develop drift modeling techniques.
- Development of alternative methods for representing the impacts of multiple wind speeds and directions on droplets throughout their trajectory while maintaining nozzle control capabilities. Additionally identify and investigate methods to predict future wind speeds and directions which act on droplets, in the context of real time drift prediction.
- Determine the suitability of the nozzle controller's modeling approach to nozzle control on a macro-scale. A macro scale would encompass large sensitive areas (>50 m along the characteristic length) and generalized weather conditions implemented for prediction and nozzle control over durations greater than those used during testing (0.5 Hz). Macro scale prediction and control would be dependent on representing gradually changing conditions rather than the highly variable (second-to-second) changes in wind speed and direction.
- Implementation of nozzle selection control on a sprayer section basis and potentially on a nozzle by nozzle basis for improved optimization of drift and efficacy.

References

AAPCO. 1999. Pesticide Drift Enforcement Survey. Available at: http://aapco.ceris.purdue.edu/doc/surveys/drift99.html. Accessed 5 February 2011.

Anon, 1983. *Risk assessment in the federal government: managing the process*. National research council, committee of the institutional means for assessment of risk to public health. Washington, DC.: National Academy Press.

ASABE S572.1. 2009. Spray nozzle classification by droplet spectra. American Society of Agricultural Engineers, St. Joseph, MI.: ASAE.

ASABE S561.1. 2009. Procedure for Measuring Drift Deposits from Ground, Orchard, and Aerial Sprayers. American Society of Agricultural and Biological Engineers, St. Joseph, MI.

Baetens, K., D. Nuyttens, P. Verboven, M. De Schampheleire, B. Nicolai, and H. Ramon. 2007. Predicting drift from field spraying by means of a 3D computational fluid dynamics model. *Computers and Electronics in Agriculture* 56:161-173.

Barry, J.W., R.B.Ekblad, G.P. Markin, and G.C. Trostle. 1978. Methods for sampling and assessing deposits of insecticidal sprays over forests. United States Department of Agriculture Technical Bulletin. 1596: 1-155.

Bilanin, A.J., M.E. Teske, J.W. Barry, and R.B. Ekblad. 1989. AGDISP: The aircraft spray dispersion model, code development and experimental validation. *Transactions of the ASAE. 32(1): 327-334.*

Bird, R.B., W.E. Stewart, and E.N. Lightfoot. 1966. *Transport Phenomena*. Wiley International Edition. New York. John Wiley and Sons, Inc.

Bohn, D. A. 1988. Environmental effects on the speed of sound, J. *AudioEng. Soc.,* 36(4), 223– 231.

Bode L.E., B.J. Butler, and C.E. Goering. 1976. Spray Drift and Recovery as affected by spray thickener, nozzle type, and nozzle pressure. *Transactions of the ASAE* 19(2): 213-218.

Bosanquet, C.H. and J.L. Pearson. 1936. The spread of smoke and gases from chimneys, *Trans. Faraday Soc*., 32: 1249.

Bretthauer, S.M., T.A. Mueller, R.C. Derksen, H. Zhu, and L.E. Bode, 2008. The effects of spray application rate and droplet size on applications to control soybean rust. Presented at the 2008 ASABE Annual International Meeting. Paper No: 084219. ASABE, Rhode Island Convention Center, Providence, RI.

Bui, Q.D. 2005 A new nozzle with variable flow rate and droplet optimization. Presented at the 2005 ASAE Annual International Meeting. Paper No: 051125. Tampa Convention Center. Tampa, Florida.

Center for Disease Control. 2010. *Pesticide Illness and Injury Surveillance*. September 16, 2010. Available at: http://www.cdc.gov/niosh/topics/pesticides/. Accessed 20 Jan. 2011.

Cochran, B.C. 2002. The influence of atmospheric turbulence on the kinetic energy available during small wind turbine power performance testing. IEA Expert Meeting on: Power Performance of Small Wind Turbines Not Connected to the Grid. Soria, Spain.

Collins, J. 2005. FIFRA-Federal Pesticide Law. Southern Regional Water Program. Available at: http://srwqis.tamu.edu/. Accessed 20 Jan. 2011.

Cooper, J. and H. Dobson. 2007. The benefits of pesticides to mankind and the environment. *Crop Protection* 26(2007): 1337-1398.

Daniels, R. and J.G. Jones. 1970. Discrete-step model of low-altitude atmospheric turbulence based on a Marcov chain. *RAE.Tech. Rep. 70010.*

DEFRA. 2001. Local environment risk assessment for pesticides: horizontal boom sprayers. Department for Environment, Food, and Rural Affairs. London, England.

Delaplane, K.S., 1996. Pesticide usage in the United States: history, benefits, risks, and trends. The University of Georgia Cooperative Extension Service. Project 93-EPIX-1-145. Athens, Georgia.

Derksen, R.C., H.E. Ozkan, R.D. Fox, and R.D. Brazee. 1999. Droplet spectra and wind tunnel evaluation of venturi and pre-orifice nozzles. Transactions of the ASAE 42(6):1573-1580.

Derksen, R.C., S.A.Miller, H.E. Ozkan, and R.D. Fox. 2001. Spray deposition characteristics on tomatoes and disease management as influenced by droplet size, spray volume,

and air assistance. Presented at the 2001 ASABE International Meeting Paper No: 01-1120. Sacramento Convention Center, Sacramento, California.

Douglas, G. 1968. Influence of size spray droplets on the herbicidal activity of diquat and paraquat. *Weed Res.* 8: 205-212.

Duggupati, N.P. 2007. Assessment of the Varitarget nozzle for variable rate application of liquid crop protection products. MS Thesis. Manhattan, Kansas: Kansas State University, Department of Biological and Agricultural Engineering.

Elliott, J.G., and B.J. Wilson. 1983. The influence of weather on the efficiency and safety of pesticide application---The drift of herbicides. Occasional Publication No. 3, British Crop Protection Council, Croydon, UK.

Ellis, C.B., and P.B. Miller. 2010. A spray drift model for assessment of ground deposits from boom sprayers. ASABE Annual International Meeting Paper No: 1009781. David L. Lawrence Convention Center, Pittsburgh, Pennsylvania.

EPA. 1999. United States Prevention, Pesticides: For Your Information. California Department of Pesticide Regulation. Available at: http://www.cdpr.ca.gov/docs/dept/factshts/epadoc.htm. Accessed 10 January 2011.

EPA. 2009a. Pesticide registration (PR) notice 2009-X draft: pesticide drift labeling. Washington DC. Available at: http://www.regulations.gov/#!documentDetail;D=EPA-HQ-OPP-2009-0628-0002. Accessed 1 December 2010.

EPA. 2009b. Draft notice 2009-X: additional information and questions for commenters. Washington DC. Available at: http://www.regulations.gov/#!documentDetail;D=EPA-HQ-OPP-2009-0628-0004. Accessed 1 December 2010.

Feng, P.C., T. Chiu, R.D. Sammons, and J.S. Ryerse, 2003. Droplet size affects glyphosate retention, absorption, and translocation in corn. *Weed Science* 51(3): 443-448.

Ganzelmeier, H., D. Rautmann, R. Spangenberg, M. Streloke, M. Herrmann, H.J. Wenzelburger and H.F. Walter. 1995. Studies on the Spray Drift of Plant Protection Products: Results of a Test Program Carried out Throughout the Federal Republic of Germany, Blackwell Wissenschafts, Verlag GmbH, Berlin.

Grover, R., J. Maybank, B.C. Caldwell, and T.M. Wolf. 1997. Airborne off-target losses and deposition characteristics from a self-propelled, high speed and high clearance ground sprayer. *Canadian Journal of Plant Science* 77(3): 493-500.

Hall, C.D. 1975. The simulation of particle motion in the atmosphere by a numerical random-walk model. *Quart. J. R. Met. Soc.* 101:235-244.

Hanna, H. M., A. Robertson, W. M. Carlton, and R. E. Wolf. 2006. Effects of nozzle type and carrier application on the control of leaf spot diseases of soybean. Presented at the 2006 ASABE Annual International Meeting. Paper No: 061162. ASABE, Oregon Convention Center, Portland, OR.

Hewitt, A.J., J. Maber, and J.P. Praat. 2002. Drift management using modeling and GIS systems. *Proceeding of the World Congress of Computers in Agriculture and Natural Resources* 290-296.

Hipkins, P., R. Grisso, B. Wolf, and T. Reed. 2009. Droplet chart/selection guide. Virginia Cooperative Extension Publication No:442031.

Hoffmann, W.C., and A. J. Hewitt. 2004. Comparison of three imaging systems for water sensitive papers. Presented at Joint ASAE/CSAE Annual International Meeting, Paper No. 041030. St. Joseph, MI.

Holterman, H.J., J.C. Van de Zande. H.A. Proskamp, and J.M. Michielsen. 1997. Modelling spray drift from boom sprayers. *Computers and Electronics in Agriculture* 19: 1-22.

Jones, E.J., J. E. Hanks, and G. D. Willis. 2002. Effect of different nozzle types on drift and efficacy of Roundup Ultra. Mississippi Agricultural and Forestry Experiment Station Bulletin 1119.

Knutson, R.D. 1999. Economic impacts of reduced pesticide use in the United States: measurement of costs and benefits. Texas A&M Agricultural Extension Service. AFPC Policy Issues Paper 99-2.

Kuchnicki, T.C., D.L. Francois, J.D. Whall, and T.M. Wolf. 2004. Canadian regulatory goals and proposed approach to buffer zones. *In Proc. 2004 International Conference on Pesticide Application for Drift Management*. Waikoloa, Hawaii.

Lafferty, C.L. and L.F. Tian. 2001. The impacts of pre-orifice and air-inlet design features on nozzle performance. Presented at the 2001 ASAE Annual International Meeting Paper No. 01-1079. Sacramento Convention Center. Sacramento, California.

Lebeau, F., A. Verstaete, B. Schiffers, and M.F. Destain. 2009. Evaluation of a real-time spray drift using TRDrift Gaussian advection-diffusion model. *Commun. Agric. Biol. Sci.* 74(1):11-24.

Leung, D.Y.C. and C.H, Liu. 1995. Improved estimators for the standard deviations of horizontal wind fluctuations. *Atmospheric Environment* 30(14): 2457-2461.

McKinlay, K.S., S.A. Brandt, P. Morse, and R. Ashford, 1972. Droplet size and phytotoxicity of herbicides. *Weed Science Society of America* 20(5):450-452.

McKinlay, K.S., R. Ashford, and R. J. Ford, 1974. Effects of droplet size, spray volume, and dosage on paraquat toxicity. *Weed Science Society of America* 22(1): 31-34.

Miller P.C.H, and D.J. Hadfield. 1989. A simulation model of the spray drift from hydraulic nozzles. *Journal of Agriculture Engineering Research* 42:135-147.

Maksymiuk, B. and A.D Moore. 1962. Spread Factor variation for oil-base, aerial sprays. *Journal of Economic Entomology.* 55(5): 695-699.

Nuyttens D., M. DeSchampheleire, K. Baetens, and B. Sonck. 2007. The influence of operator controlled variables on spray drift from field crop sprayers. *Transactions of the ASABE* 50(4): 1129-1140.

Office of Pesticide Programs (OPP). 2004. Overview of the ecological risk assessment process in the office of pesticide programs. US Environmental Protection Agency. Washington D.C.

Ozkan, H.E., D.L. Reichard, H. Zhu, and A.S. Babeir. 1995. Drift retardant chemical effects on spray droplet size pattern and drift. *Agricultural Sci.* 2: 131-140.

Ozkan, E. H., H. Zhu, and R. C. Derksen. 2006. Evaluation of spraying equipment for effective application of fungicides to control Asian soybean rust. Presented at the 2006 ASABE Annual International Meeting. Paper No: 061161. ASABE, Oregon Convention Center, Portland, OR.

Pimentel, D., H. Acquy, M. Biltonen, P. Ric, M. Silva, J. Nelson, V. Lipner, S. Giordano, A. Horowitz, and M. D'Amore, 1992. Environmental and economic costs of pesticide use. *Bioscience* 42,750–760.

PMRA. 2005. Agricultural buffer zone strategy proposal. Regulatory Proposal PRO2005-06. Health Canada. Ottawa, Ontario.

Prasad, R., and L. Beresford. 1992. Influence of droplet size and density on phytotoxicity of three herbicides. *Weed Technology* 6(2): 415-423.

Prokop, M., and K. Veverka, 2003. Influence of droplet spectra on the efficiency of contact and systemic herbicides. *Plant Soil Environ*. 49(2):75-80.

Prokop M., and K. Veverka, 2006. Influence of droplet spectra on the efficiency of contact fungicides and mixtures of contact and systemic fungicides. *Plant Protection Sci.* 42: 26-33.

Rautmann, D. 2003. Drift reducing sprayers—testing and listing in Germany. Presented at the 2003 ASAE Annual International Meeting Paper No. 031095. Riviera Hotel and Convention Center. Las Vegas, Nevada.

Reichard, D.L., H. Zhu, R.D. Fox, and R.D. Brazee. 1992. Wind tunnel evaluation of a computer program to model spray drift. *Transactions of the ASAE* 35(3):755-758.

Risk Assessment Forum. 1998. Guidelines for ecological risk assessment. EPA/630/R-95/002F. Washington DC.

SAS. 2004. *SAS User's Guide: Statistics*. Ver. 9.2. Cary, N.C.: SAS Institute, Inc.

SDTF, 1997. A Summary of Ground Application Studies, Stewart Agricultural Research Services, Inc. Macon, MO.

Shaw, B. 1996. Minimizing Spray Drift. Agricultural Chemical Safety Presentation of the Texas Agricultural Extension Service. Texas A&M University. College Station, Texas. Available at: http://agsafety.tamu.edu/Educational%20Material/Index.html. Accessed 10 January 2011.

Shaw, D.R., W.H. Morris, E.P. Webster, and D.B. Smith. 2000. Effects of spray volume and droplet size on herbicide deposition and common cocklebur control. *Weed Technology* 14(2): 321-325.

Smith D.B., F.D. Harris, and C.E. Goering. 1982. Variables affecting drift from ground boom sprayers. *Transactions of the ASAE* 25(6): 1499-1523.

Smith, D.B., W.H. Morris, E.P. Webster, and D.R. Shaw. 2000a. Droplet size and leaf morphology effects on spray deposition. *Transactions of the ASABE* 43(2):255-259.

Smith, D.B., L.E. Bode, and P.D. Gerard. 2000b. Predicting ground boom spray drift. *Transactions of the ASAE* 43(3): 547-553.

Spray Drift Workgroup. 2007. Spray drift workgroup-final report to PPDC.

Stone, D. 2008. History of pesticide use and regulation. Oregon State Extension. Available at: http://people.oregonstate.edu/~muirp/pesthist.htm. Accessed 13 March 2011.

Storozynsky, B. 1997. Airborne spray drift results. Alberta Farm Machinery Research Center. Lethbridge, Alberta.

Sullivan, P.J. 1971. Longitudinal dispersion within a two-dimensional turbulent shear flow. *Journal of Fluid Mechanics* 49: 551-576.

Sumner, P. E., P. M. Roberts, and R. P. Edwards. 2007. Comparison of low-drift nozzles for canopy penetration in cotton. Presented at the 2007 ASABE Annual International Meeting. Paper No: 071152. ASABE, Minneapolis Convention Center, Minneapolis, MN.

Taylor, W. E., A. R. Womac, P. C. H. Miller, and B. P. Taylor. 2004. An attempt to relate drop size to drift risk. *In Pro. 2004 International Conference on Pesticide Application for Drift Management*, Oct 27-29, Waikoloa, Hawaii.

Teske, M.E., D.L. Valcore, and A.J. Hewitt. 2001. An analytical ground sprayer model. Presented at the 2001 ASAE Annual International Meeting. Paper No:011051. Sacramento Convention Center, Sacramento, California.

Teske, M.E., N.B.Birchfield, and S.L. Bird. 2004. Development and validation of a mechanistic ground sprayer model. Presented at the 2004 ASAE/CSAE Annual International Meeting. Paper No. 041036. Fairmont Chateau Laurier. Ottawa, Ontario.

Thompson N., and A.J. Ley. 1983. Estimating spray drift using a random-walk model of evaporating drops. *Journal of Agriculture Engineering Research* 28: 419-435.

Threadgill E.D., and D.B. Smith. 1975. Effects of physical and meteorological parameters on the drift of controlled-size droplets. *Transactions of the ASAE* 18:51-56.

USDA. 2006 Agricultural Chemical Usage: 2005. Field Crops Summary. Available at: http://usda.mannlib.cornell.edu/MannUsda/homepage.do. Accessed 22 May 2009.

White, T. 2006. ARS software increases spray accuracy. Farm Progress Prairie Farmer. January 2006. pp. 22.

Wolf, R., 2003. Assessing the Ability of DropletScan™ to Analyze Spray Droplets From a Ground Operated Sprayer. *Technical Note: Applied Engineering in Agriculture* 19(5).

Wolf, T.M., B.C. Caldwell, G.I. McIntyre, and A.I. Hsiao, 1992. Effect of droplet size and herbicide concentration on absorption and translocation of C-2,4-D in oriental mustard (*Sisymbrium orientale*). *Weed Science Society of America* 40(4): 568-575.

Wolf. T.M., R. Grover, K. Wallace, S.R. Shewchuk, and J. Maybank. 1993. Effect of protective shields on drift and deposition characteristics of field sprayers. *Canadian Journal of Plant Science* 73: 1261-1273.

Wolf, T.M. 2000. Low drift nozzle efficacy with respect to herbicide mode of action. *Aspects of Applied Biology* 57: 29-34.

Wolf, T.M. and B.C. Caldwell. 2001. Development of a Canadian spray drift model for the determination of buffer zone distances. In *Expert Committee on Weeds - Comité d'expertsen malherbologie (ECW-CEM). Proceedings of the 2001 National Meeting, Québec City. Sainte-Anne-de-Bellevue, Québec: ECW-CEM*. Eds. D Bernier, D R A Campbell and D Cloutier. p. 60.

Woodward, S.J., R.J. Connell. J.A. Zabkiewicz. K.D. Steele, and J.P. Pratt. 2008. Evaluation of the AgDISP ground boom spray drift model. *New Zealand Plant Protection* (61):164-168.

Yates, W. E., R. E. Cowden, and N. B. Akesson. 1985. Drop size spectra from nozzles in high-speed airstream. *Transactions of the ASAE* 28(2): 405-410.

Zhu, H., D.L. Reichard, R.D. Fox, H.E.Ozkan, and R.D. Brazee. 1995. DRIFTSIM, a program to estimate drift distance of spray droplets. *Applied Engineering in Agriculture* 11(3): 365-369.

Zhu, H., R.W. Dexter, R.D. Fox, D.L. Reichard, R.D Brazee, and H.E. Ozkan. 1997. Effects of polymer composition and viscosity on droplet size of re-circulated spray solutions. *Journal of Agric. Engineering Res.* 67: 35-45.

Zhu, H., M. Salyani, and R.D. Fox. 2011. A portable scanning system for evaluation of spray deposit distribution. *Computers and Electronics in Agriculture* (2011).